TECHNISCHE
UNIVERSITÄT
WIEN
Vienna University of Technology

DIPLOMARBEIT

IMPLICATION OF URBAN HEAT ISLANDS FOR ARCHITECTURE

ausgeführt zum Zwecke der Erlangung des akademischen Grades einer
Diplom-Ingenieurin

unter der Leitung von
Univ. Prof. Dipl.-Ing. Dr. techn. A. Mahdavi
E 259-3 Abteilung für Bauphysik und Bauökologie
Institut für Architekturwissenschaften

eingereicht an der
Technischen Universität Wien
Fakultät für Architektur und Raumplanung

von
Elke Krätschmer

Matrikelnr. 0030595
Friedlgasse 25/27, 1190 Wien

Wien, am

ABSTRACT

This work intends to give an overview of the topic of urban heat islands with a focus on facts important to architects and urban planners. Furthermore, a study of a local heat island in Vienna, Austria was conducted using mobile traverses to collect data. A general explanation of heat islands is given and methods and tools to measure and model them are explained. The focus then lies on mitigation measures that can be implemented by planners. Results of the study are presented, and the correlation between urban heat islands and the local environment is discussed.

ACKNOWLEDGMENTS

1 INTRODUCTION

1.1 Objective

Urban heat islands (UHIs) are a well-known phenomenon all over the world and are studied with renewed interest in the context of a changing climate. This diploma thesis deals with their implication for architecture. The goal of the present work is to give an overview of the theme and a summary of important studies done in this field until today. The main focus lies on aspects that are interesting for architects and urban planners, especially on mitigation measures that they can implement. Furthermore, a study of different situations in Vienna has been started and will be described in this thesis. First results will be analyzed and discussed.

1.2 Motivation

UHIs are well-known and much researched among meteorologists, but little information do architects and urban planners have, who could contribute essentially to their mitigation.

Climate change is finally accepted to be happening and considered as a threat to health by the European Commission, which makes the subject of heat islands even more up to date. Heat waves are expected to happen more often and to be even stronger in the future. They do not only influence the quality of life, but also increase morbidity and mortality among the people concerned. The heat waves of 2003 and 2006 are responsible for thousands of deaths in Europe. In 2007 a heat wave did great damage in Southern Europe (EC 2010). Difficulties arise especially in cities that have to deal with even higher temperatures due to heat islands. UHI mitigation can help reduce emissions responsible for climate change and adapting cities to the expected warmer summers in the future climate.

Apart from influencing the quality of life and health, UHIs also cost money. Mills & Kalkstein (2009) invented a monetized value of excessive heat event mortality in the USA to allow estimates on heat related health costs. Higher energy demands for cooling, leading to increased energy bills, are another aspect of rising temperatures. In Europe air-conditioning increased about 100% from 2000 to 2007 (Karlessi et al.

2009). Energy savings as a result of UHI mitigation measures therefore save money and also reduce emissions for the production of energy, which in return has a positive effect on climate. Buildings represent 40% of the global use of primary energy (WBCSD 2010) and therefore show an outstanding potential for reduction. Figure 1.1 shows the energy consumption of different sectors and their projected trends to the year 2050 following business as usual or different pathways suggested by WBCSD (2010).
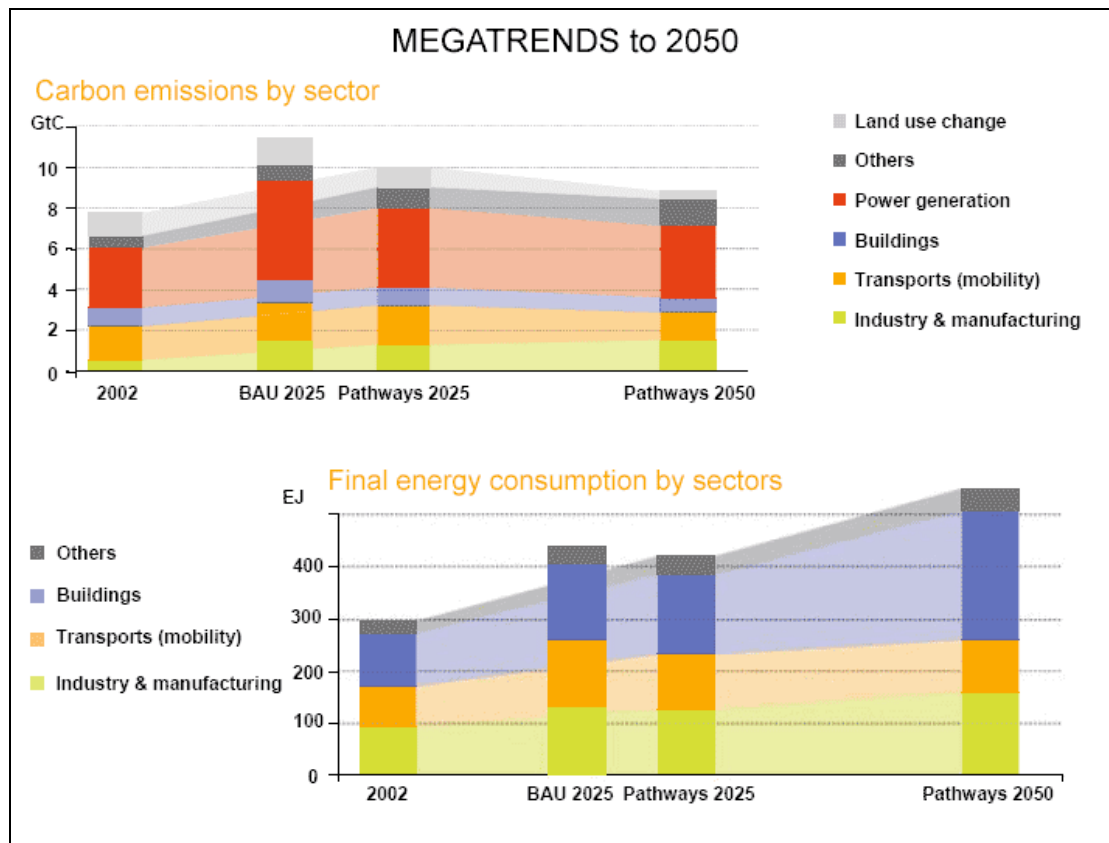
Figure 1.1: Megatrends to 2050 (BAU... Business as usual, WBCSD 2010)

Research on mitigation measures is very important as urbanization will continue and worsen the situation in cities. Areas with greatest development and least vegetation, usually the city center, tend to be hottest. UHIs are connected to the size and density of a city; the larger and denser a city, the higher the intensity. The 2009 Revision of the World Urbanization Prospects by the United Nations names the percentage of world population residing in urban areas with 50.46% for 2010 and estimates that by 2050 68.7% will live in urban areas (UN WUP 2009). Heat islands tend to get more intense as cities grow.

To sum up, UHI mitigation means less energy costs as well as better quality of life, health and comfort for users through improved indoor and outdoor climate conditions. Therefore, mitigation measures should be in the repertoire of every architect and urban planner.

1.3 Structure

As few sources of comprehensive information about UHIs and their mitigation exist for architects and urban planners, this work intends to provide a summary of that theme. It is mainly based on literature and provides an overview of possible actions. Chapter 2 summarizes the status quo of knowledge. It starts with a general explanation of UHIs and then focuses on factors that can be changed to mitigate heat and on studies done in that field so far. Methods to measure and model UHIs and mitigation measures are also presented briefly.

To practically study a local heat island in Vienna, Austria, measurements were taken with the help of a mobile weather station mounted on a bike trailer. Its build-up, equipment and the measurements will be described in chapter 3. Results are shown in chapter 4 and discussed in chapter 5. Conclusions are drawn in chapter 6.

2 LITERATURE REVIEW

2.1 Urban Heat Islands

2.1.1 Definition

The atmosphere in cities is modified in comparison to rural areas, a phenomenon which is called urban climate. It leads to the so-called urban heat islands, meaning that the air and surface temperatures in urban and suburban areas are higher than in surrounding rural areas. This does not naturally mean that there is one single island, but there are different more or less connected overheated areas in the city. Figure 2.1 shows a typical profile of an urban heat island and its air and surface temperature changes over the city depending on the environment. The UHI usually reaches its peak in the city center and is lower in areas with more vegetation.
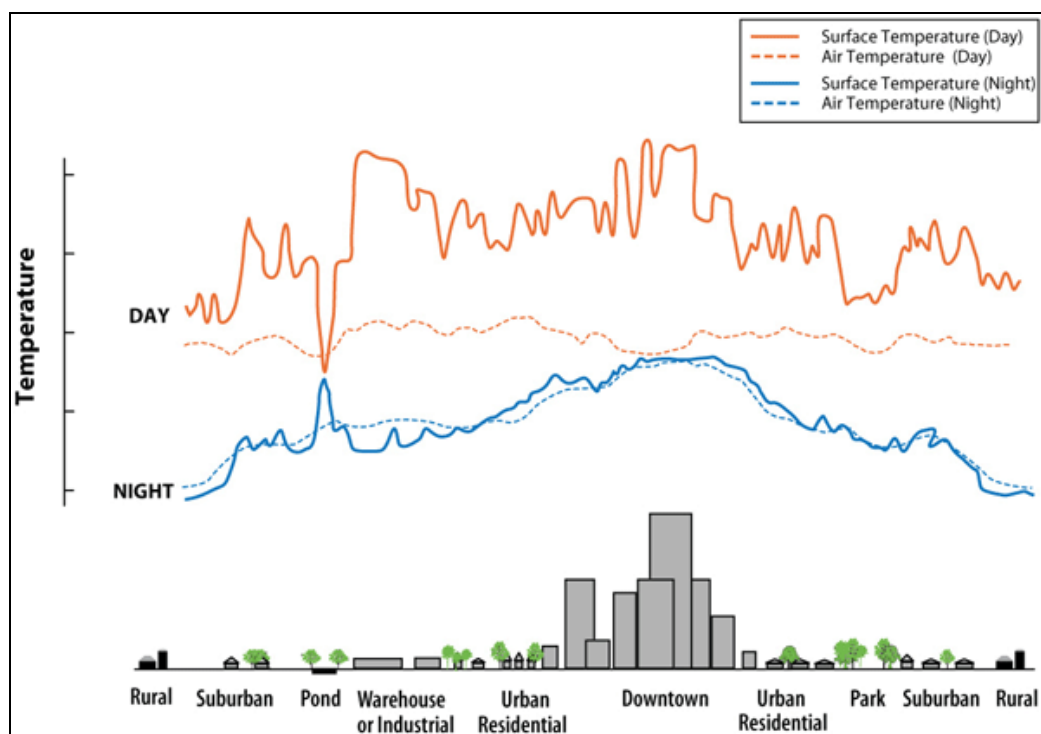

Figure 2.1: Sketch of an UHI profile (US EPA 2010)

Also so-called cool islands exist, which are city areas that are at least sometimes during the day cooler than the rural surroundings. This happens especially in cold

northern climates, where the low summer sun casts long shadows, and in some desert climates (Gartland 2008).

Furthermore, there are also non-urban heat islands. Hogan and Ferrick (1998) observed non-urban heat islands during winter and found a local heat island of 4°C along Connecticut river caused by the release of latent heat of the growing ice cover.

2.1.2 Structure of the Urban Atmosphere

The lowest layer of the Earth's atmosphere, the troposphere, is influenced by the Earth's surface. Most impacts take place at the planetary boundary layer (PBL) also known as atmospheric boundary layer (ABL), where heat and drag from the surface create turbulence. Above the PBL is the free atmosphere (FA).

"*Scientists have found significant differences in the boundary layers over rural and urban areas. [...] Warmer urban surfaces create a thicker boundary layer, above which the temperature reverts to that of the rest of the troposphere. The temperature inside the boundary layer is approximately constant because turbulent eddies keep the air well mixed. [...] In rural areas at night, the surface is cooler than the air above it, creating a stable layer of cooler air below warmer air. At night in urban areas, slowly cooling urban surfaces cause heated air to form an inversion above the canopy layer* (Gartland 2008, pp.32-34)."

Typical temperature profiles for the atmosphere over rural and urban environments are shown in figure 2.2 for daytime and figure 2.3 for nighttime.
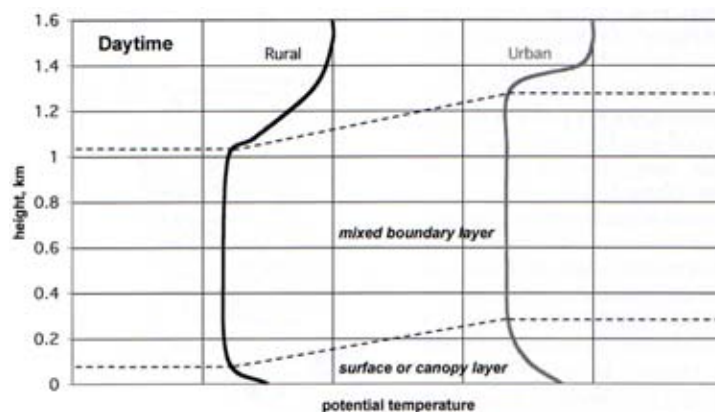
Figure 2.2: Typical daytime potential temperature profiles (Gartland 2008)
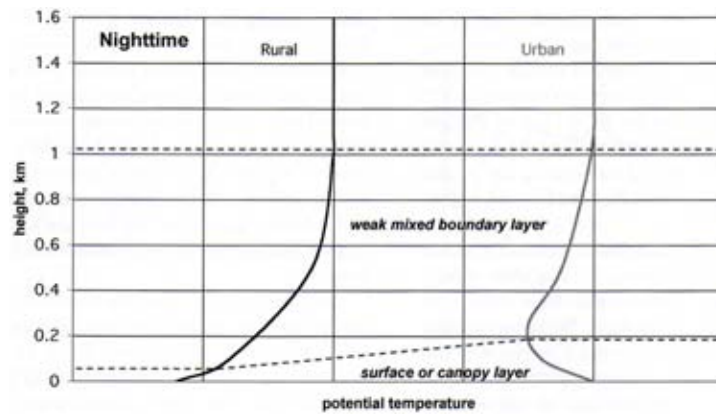
Figure 2.3: Typical nighttime potential temperature profiles (Gartland 2008)

While the rural boundary layer is simply divided into the Surface Layer (SL) and the Mixing Layer (ML), the Urban Boundary Layer (UBL) is more complex and its influence reaches further up, as is shown in figure 2.4. It consists of the Urban Canopy Layer (UCL), which reaches from the ground to the average roof level, followed by the Urban Roughness Sublayer (URS) and the Urban Mixing Layer (UML).
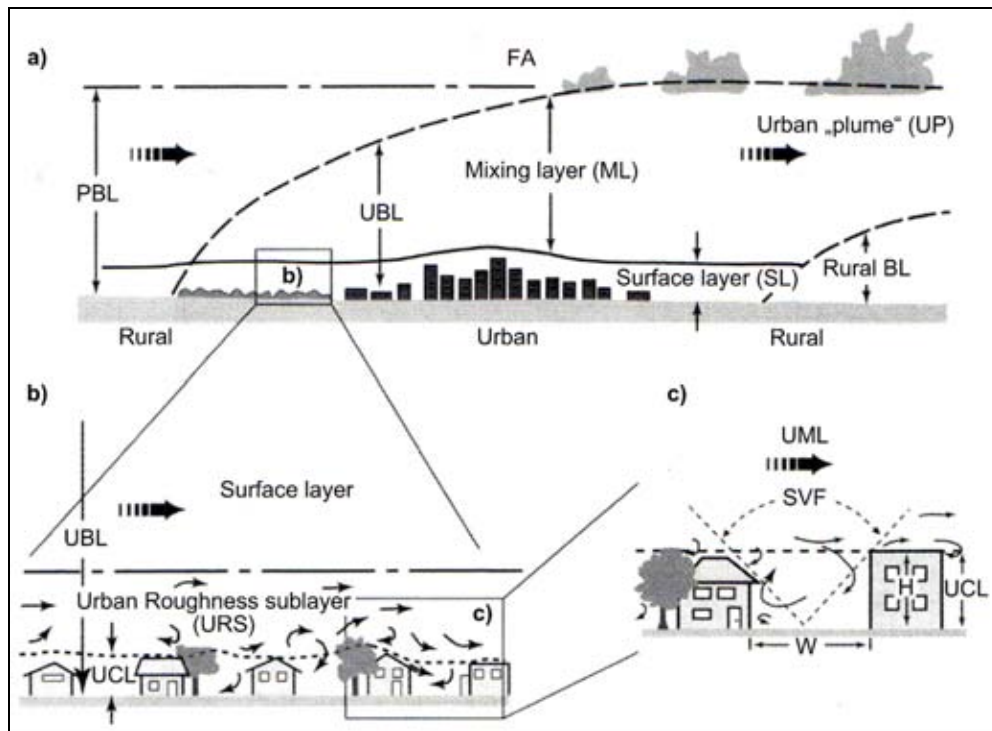
Figure 2.4: Modification of the PBL by cities (Kuttler 2009)

During windy weather the layers are almost not formed. Ideal conditions to observe UHIs are during calm and clear periods. The urban plume can sometimes lead to urban conditions in rural surroundings.

2.1.3 The UHI Effect

The effect of heat islands is different in every city, depending on local factors. Heating of surfaces leads to higher air temperatures, which usually cause negative effects such as discomfort, health problems and higher mortality. The urban overheating is a problem especially during summer. The habitability of cities decreases, while the energy consumption increases and leads to higher costs and more pollution. Mitigation measures can help solving these problems.

In some cases the UHI effects may even be positive. In colder cities the higher ambient air temperature can be beneficial for heating energy demands in winter. Another advantage of the higher temperatures, which anticipate cooling in the evening, are the benefits for visitors of open air events. Big events can create their own climate that makes the stay outside at night more comfortable (e.g. Jahrmarkt Pützchen bei Bonn, Brandt 2005).

2.1.4 The UHI Intensity

The heat island intensity is used to measure the heat island effect. It is calculated from the difference between the temperatures (Kuttler 2009):

$$\varDelta T = T_{urban} - T_{rural} \tag{2.1}$$

In case of a cool island the intensity would be negative. The intensity varies over time, it has its lowest point in the morning and usually reaches its peak at night because urban materials continue to release heat while rural areas cool down. The exact time of the peaks depends on the materials used on site, as wood for example releases heat faster than concrete (Gartland 2008).

2.1.5 Factors That Influence the Formation of an UHI

The formation of an urban heat island is very complex and influenced by a combination of many interacting reasons. According to Gartland (2008), the five most important factors are higher net radiation, increased heat storage, reduced evaporation, lower convection and more anthropogenic heat.

An important criterion of urban areas are the on-site materials. Common building materials are impermeable and have high surface temperatures as they absorb and retain more heat than natural materials. Their surface temperature influences the ambient air temperature through radiation and convection. Rain hitting the impermeable surfaces is drained off through canal systems and therefore not available for dissipating heat through evaporation. Dark colors and street canyons especially trap the heat. Dark dry surfaces can reach temperatures up to 88°C in direct sunlight, while surfaces with vegetation and moist soil only reach around 18°C (Gartland 2008). The most important characteristics of materials are solar reflectance or surface albedo and thermal emittance, which both are usually low for common building materials.

Emissivity is the thermal radiation from a body. Its importance concerning UHIs depends on the geometry of the urban structure and the sky view factor. A low sky view factor slows down cooling at night. Urban geometry, especially the ratio of building height to building width (H/W), is also important for the formation of UHIs. It determines how much street area is exposed to direct sunlight, how easily wind can access the area and if the heat is trapped in a street canyon.

The amount of vegetation on site also is of great influence. The less vegetation, the more the surfaces and the air can heat up because there are more heat-storing materials. Less vegetation also means less cooling shadows and reduced evapotranspiration by the plants, which use heat when evaporating water.

Another important factor influencing heat islands is the wind. Buildings act as windbreaks and their surface roughness slows down wind velocity, which results in less heat convection and increased UHI intensities. On the other hand, buildings can also create turbulences and local wind peaks. Due to temperature and pressure differences, urban heat islands sometimes create their own breezes (e.g. sea breezes in coastal cities), which can also contribute to their mitigation. Winds and their effects are very complex, vary greatly and are hard to predict.

Heat generated by people, their activities, buildings, industry and traffic in cities as well as the resulting air pollution also have an impact on the formation of UHIs. To enable the comparison of different cities, the energy use of a region – as a sign of anthropogenic heat – is divided by the relevant area. In general, the energy use is increasing, which leads to more anthropogenic heat and extra pollution in producing

the energy. The energy demand usually is bigger in winter due to heating, but the need of cooling in summer is increasing (Gartland 2008).

A study under controlled conditions by Kolokotroni & Giridharan (2008) focuses on the impact of physical characteristics on the UHI intensity in London. The on-site variables studied are aspect ratio, plan density ratio, green density ratio, fabric density ratio, surface albedo and thermal mass. Measurements from 80 locations are used for a daytime and nighttime trend analysis of the heat island pattern. The data is then used in a regression analysis to determine the impact of the variables. The most critical variable turned out to be the surface albedo, which is usually low for common building materials meaning that they absorb more solar energy.

The influence of local meteorological conditions is analyzed for the case study of Hania, Crete, by Kolokotsa et al. (2009). Outdoor comfort conditions where measured for nine urban and three rural stations. As expected, the highest temperature values where measured in the city center and the highest humidity values at the coastal stations. The lowest humidity was found in the city center, which indicates that the penetration of humidity to the city center is limited. The temperature and relative humidity data was used to calculate the Discomfort Index (DI), which was found to follow the UHI intensity closely. The predominant wind directions are north and west. While the northern winds were found to not remarkably change the UHI intensity, western winds were able to reduce the temperature differences. A reason for this is the orientation of the main streets of Hania, which allows the western winds to reach the hot spots of the city. The influence of wind is particularly a local matter. Rainfall was found to have a balancing effect and to minimize the urban heat island.

2.2 Measuring and Modeling UHIs

2.2.1 Overview

To gather useful information about the complex heat island of a city, extensive measurements are needed. UHIs can vary to a great extend from one place in the city to another. Modeling is used to further understand UHIs and to estimate the effects of mitigation measures. In the following section, techniques and tools for measuring and modeling heat islands are presented.

2.2.2 Measuring UHIs

For architects and urban planners, measuring heat islands as such is not as interesting as modeling the effects of mitigation measures. Measured values however may serve as a basis for simulation studies, therefore a short overview of methods is presented here. Of course these methods can also be used to evaluate the effects of mitigation measures already applied. Gartland (2008) names the following five commonly used approaches: fixed stations, mobile traverses, remote sensing, vertical sensing and energy balances.

2.2.2.1 Fixed Stations

The most common UHI evaluation method is to simply compare existing weather data from meteorological stations, which exist in most cities all over the world. Weather services, but also companies and universities like the Vienna University of Technology (Vienna UT 2010) collect weather data, which usually can be easily accessed for little or no cost. An obvious advantage of this method is that comparing data over the years allows seeing tendencies, trends and long-term changes of the UHI intensity. A disadvantage might be that not always the same set of data is collected. Also the weather stations instrumentation, location or environment may have changed over time, which distorts the results. In Austria, the meteorological institution ZAMG therefore created an online database with corrected values of their data (HISTALP 2010). For comparison of only two stations, the locations have to be chosen wisely. They should have the same altitude, terrain and general climate, which is not always possible.

"*In general, for heat islands the ideal place to measure air temperature is in the 'canopy layer'. [...] Standard measurements of canopy layer temperatures are made at a standing person's chest height, usually at a height of 1.5 metres (5 feet) above the ground* (Gartland 2008, p.28)."

Urban weather stations are often located on top of buildings (e.g. Vienna UT), also due to security reasons, while rural stations are often situated at airports, which do not represent typical rural conditions. Thus, these analyses are not always the best representation of the UHI, but they still give a descriptive image of UHI trends and tendencies as Figure 2.5 shows. It displays the difference in daily temperatures of the central business district and the airport of Melbourne, Australia, in summer and winter.
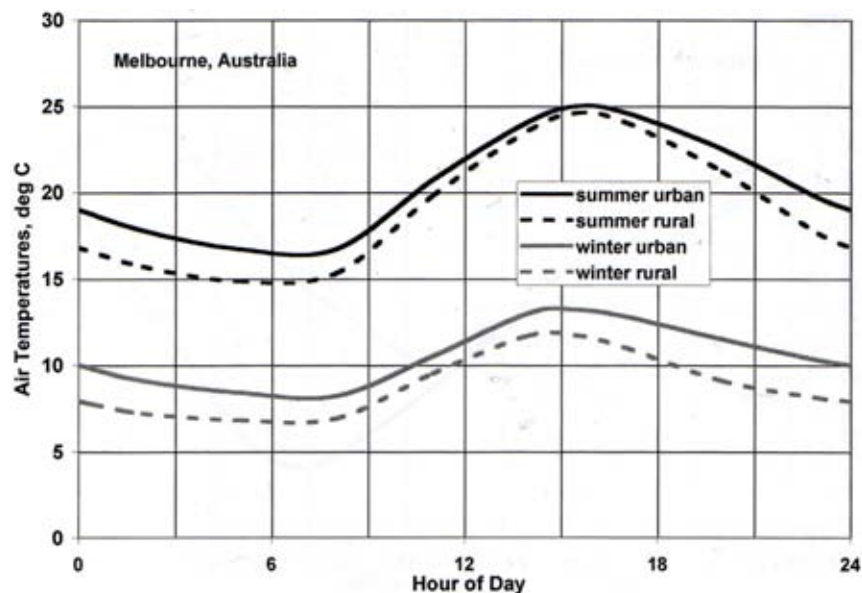

Figure 2.5: Summer and winter UHI trends in Melbourne, Australia (Gartland 2008)

If there are enough stations available in the area, it is possible to generate two-dimensional contour maps of the city's temperatures as shown in Figure 2.6 for the city of Minneapolis, Minnesota.
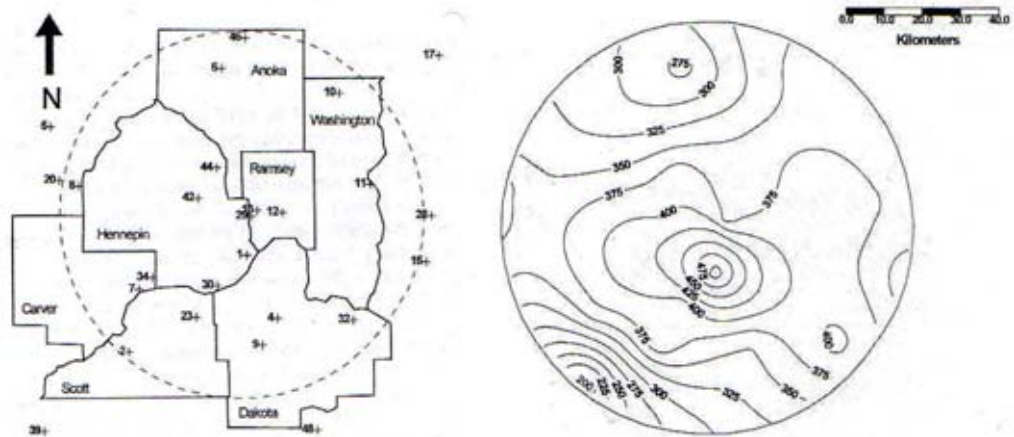
Figure 2.6: Temperature contour map of Minneapolis, Minnesota (Gartland 2008)

To gather additional data, e.g. for closing gaps in a temperature contour map, extra stations can be fixed temporarily. A station should at least include instruments to measure temperature, humidity, wind speed and wind direction. A pyranometer to measure solar radiation levels can also be useful. Additional fixed stations can be expensive and difficult to set up, an economic alternative are the mobile traverses explained in the following section.

2.2.2.2   Mobile Traverses

With a set of weather instruments, measurements are taken at representative stops on a predetermined path. The travel can be done by foot, bicycle, car, public transport or even railway at any time of day or night, sometimes depending on traffic conditions. "*Most studies perform traverses at night during calm, clear weather in order to measure maximum heat island intensities* (Gartland 2008, p.29)."

A disadvantage of this method is, that the measurements are not recorded simultaneously. Although mobile traverses can be completed in short time, conditions can vary significantly. If the higher costs do not matter, it is of course possible to use more than one set of travelling equipment at the same time. It is also important to keep away the instruments from sources of heat while travelling and to give them enough time to reach equilibrium with their surroundings before taking readings. The measurement points should be chosen wisely to avoid disturbing influences.

Nakao et al. (2009) performed moving measurements with a car. For their continuous moving measurement method they developed an estimation system that deals with the measurement errors due to the sensor lag, the GPS time delay and the speed of the vehicle and were able to at least decrease them.

2.2.2.3 Remote Sensing

While the above-mentioned methods focus on air temperatures, remote sensing is used to study surface temperatures and other characteristics of surfaces by measuring their reflected and emitted energy. Satellites or airplanes take pictures of the visible and invisible energy radiating from surfaces. Satellites usually pass over an area twice a day, which enables the study of daytime and nighttime thermal characteristics as well as seasonal variations. For the analysis, days with clear weather must be chosen. Airplane flights can be done at any time of the day to capture daily patterns, but they are very expensive and often need special permissions to fly at lower altitudes. Figure 2.7 shows a thermal image of Vienna, Austria, taken in the morning hours of August 16, 2001. The difference between the hot areas of the city (yellow, orange and red) and the cooler surroundings (green and blue) is clearly visible, but inside the urban area temperatures also vary greatly depending on the underlying surfaces.
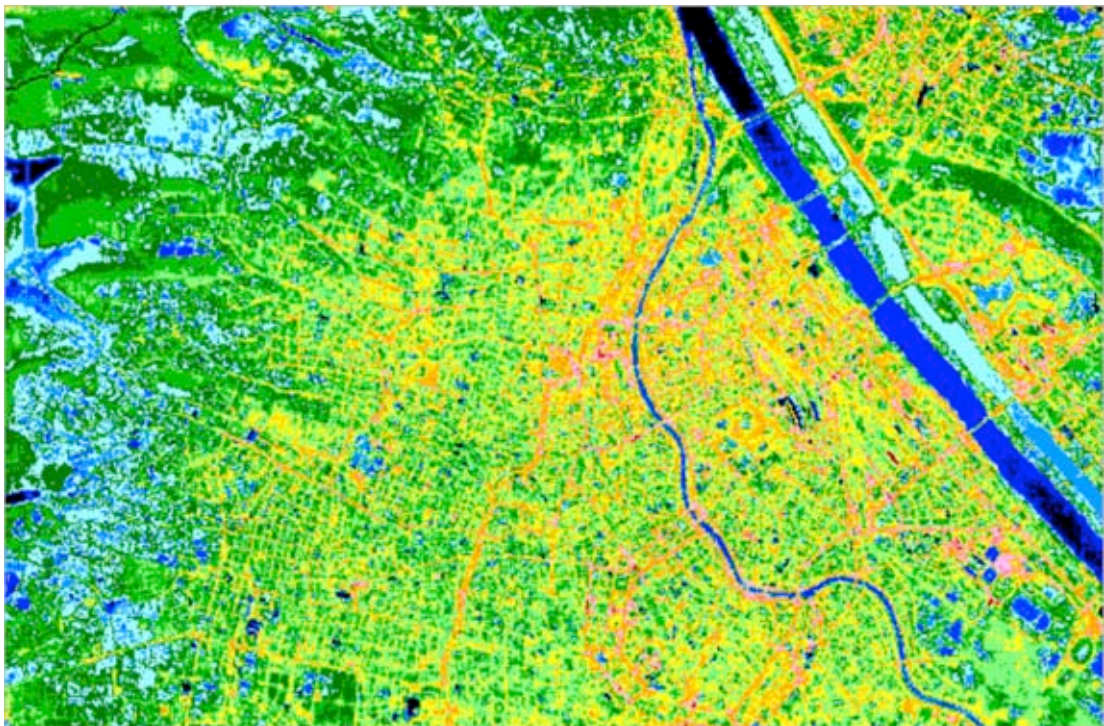

Figure 2.7: Thermal image of Vienna ranging from hot (red) to cool (blue) (MA22, 2003)

The thermal pictures do not show temperatures of walls and under trees, which are also important for UHIs, but allow visualizing temperatures over large areas. Medium resolution images are used to study the relationship between land use or land cover (e.g. vegetation) and UHI, while high-resolution images allow research in a smaller scale by studying the precise underlying surface. For sensible urban planning, each type of surface should be kept at a reasonable percentage.

2.2.2.4 Vertical Sensing

Through measurements with balloons, monitoring equipment on radio towers or through flying at different altitudes with a helicopter or airplane a vertical temperature profile can be created. It provides better understanding of the UHI effect on the local climate.

2.2.2.5 Energy Balances

Another way of measuring heat islands is measuring energy flows in and out of surfaces and using the energy balance equation (Gartland 2008):

Convection + Evaporation + Heat storage = Anthropogenic heat + Net radiation (2.2)

To obtain the net radiation, incoming and reflected solar radiation is measured with a pyranometer or albedometer, the atmospheric radiation is measured with a radiometer and the surface radiation with a pyrgeometer. Equation 2.3 is then used to calculate the net radiation (Gartland 2008):

Net radiation =
Incoming solar – Reflected solar + Atmospheric radiation – Surface radiation (2.3)

The net radiation can also be measured directly with a net radiometer. Convection is detected by an eddy covariance system with a sonic anemometer and fine wire thermocouples, and evaporation using an eddy covariance system with a sonic anemometer and hygrometer. To measure heat storage a heat flux meter is used. Sometimes not every variable is obtained through measurements, but calculated from the energy balance equation to reduce equipment costs. Local weather variables such as air temperature, humidity and wind speed should also be recorded in order to compare data from different sites and times.

2.2.2.6 Urban Climatic Maps

Urban climatic maps derived from measurements provide a basis for urban planning and allow the definition of critical zones, where UHI mitigation measures should be applied first.

2.2.3 Modeling UHIs

Modeling heat islands is not only useful for understanding them, but also enables the estimation of effects and effectiveness of mitigation measures, which is of special interest for architects and urban planners. The models allow taking a look at single buildings, the neighborhood or an entire urban region. In the following section, a list of modeling tools and calculators can be found, which does not claim to be complete. Different models and particularities of their data handling are also discussed by Mirzaei & Haghighat (2010).

2.2.3.1 Building Energy Models

Building energy models predict the heating and cooling energy demands of a building. They are usually used to evaluate energy efficiency measures. In UHI research they are also used to estimate the effects of mitigation measures such as cool roofs, shading from trees or cool pavement around a building.

Gartland (2008) names **DOE-2**, a program developed by the US Department of Energy (US DOE), as the most commonly used tool, although it was superseded in 2001 by the more advanced **EnergyPlus** program. DOE-2 was widely used for the simulation of heat island mitigation measures even though it has some known limitations. It can underestimate the savings from cool roofs by up to 50%, but still many studies are based on it.

The most up to date DOE-2 Software is **eQuest** (Quick Energy Simulation Tool), which can be downloaded from the Internet for free (eQuest 2010). It claims to be a tool designed for users of any kind, as no extensive experience should be needed to handle it. It includes wizards for building creation and energy efficiency measures, which guide you through the single steps, as well as a graphical reporting tool. It is not necessary to complete all the information, as the program gets missing data through an "intelligent default" process. The results include hourly simulations of

heating and cooling loads and the energy consumption of various technical equipment (e.g. heating, cooling, lightning, ventilation) for a one-year period.

DesignBuilder, a program based on EnergyPlus, but with a comprehensive user interface, has a free fully functional 30-day trial version available on the Internet (DesignBuilder 2010). Models for the simulation can be assembled without limitations on form or surface shape or imported from CAD-Software. The program provides data templates for common building constructions, activities, HVAC (Heating, Ventilating and Air Conditioning) and lightning systems, but it is also possible to add own values. Heating and cooling loads are calculated using the ASHRAE (American Society of Heating, Refrigerating and Air Conditioning Engineers) approved ´Heat Balance´ method. The program can calculate photovoltaic systems and has an integrated CFD (Computational Fluid Dynamics) function. The user is able to control the level of detail. Global changes can be applied to the model at building, block or zone level at time steps of less than an hour. Furthermore, the CO_2 generation can be calculated. For simulation, ASHRAE worldwide design weather data and locations are included and over 2100 EnergyPlus hourly weather files are available for free. It is also possible to simulate naturally ventilated buildings. Besides the calculation of the thermal performance of a building, DesignBuilder can also create rendered images or movies including the effect of site shading for any day of the year.

The building modeling and simulation program **Tas** (EDSL 2010) enables the simulation of heating and cooling loads with the corresponding annual energy demand, natural ventilation and passive design. The software features 150 international weather sites in its own database and can also import other climate data by converting TMY2 files. This allows the use of full year, hourly-based weather data from over 2500 sites worldwide. If the desired location is not available, the program can generate the data through interpolation of the nearest 3 or 4 weather sites. Tas was used in Vienna for the thermal optimization of "Haus der Forschung" (Mascha 2006).

Ecotect Analysis (Autodesk 2010) is another program to calculate the thermal performance and analyze the energy use and carbon emissions of a building. Furthermore, it is able to visualize solar radiation on surfaces and windows and calculate day lightning, shadows and reflections. It can also estimate the water usage and its costs. The web-based application **Green Building Studio** (based on

DOE-2) allows Ecotect users to quickly evaluate energy efficiency and carbon neutrality of their design.

The Sustainable Buildings Industry Council (SBIC) recommends **Energy-10** for small commercial and residential buildings with one or two thermal zones (SBIC 2010). For those buildings, hourly energy simulations show the energy and cost savings of different design strategies such as passive solar heating and cooling, natural ventilation, improved building insulation and more. The program can also simulate the performance of a photovoltaic system. It features the ASHRAE library of constructions. Results are shown in the form of graphs. Energy-10 was designed to help obtaining energy credits under the US Leadership in Energy and Environmental Design (LEED) program.

TRNSYS, short for TraNsient Systems Simulation, is a program developed by the University of Wisconsin (TRNSYS 2010). It is used to simulate low energy buildings, technical equipment and machines such as solar thermal and photovoltaic systems, HVAC systems and more. Due to its modular structure, it is very flexible. The results, e.g. room temperature, heating, cooling and energy demands, are shown graphically and in ASCII format.

White & Holmes (2009) describe the development of new versions of another building simulation program called **ROOM**. OutdoorROOM was created to model the influence of surface materials and building masses on heat fluxes to and from the urban surface and on urban heat islands. StadiumROOM can model empty or occupied stadiums with an optional comfort cooling system consisting of air supply through jets under the seats. The roof can also be opened during simulation. Solar Tower is a modified version of the façade version of ROOM developed to investigate the potential for large-scale solar power generators. The models are currently being validated and are a good example of the potential that lies in the adaptation of building energy models for UHI research.

2.2.3.2 Roof Energy Calculators

For the US market, some web-based tools exist, which allow a quick estimation of energy and cost savings when implementing the mitigation measure of cool roof systems.

The **DOE cool roof calculator for low-slope roofs** developed by the Oak Ridge National Laboratory (ORNL) comes in two versions (ORNL 2010). Version 1.2 estimates heating and cooling savings for flat roofs with non-black surfaces for small and medium-sized facilities, while version 2.0 estimates energy and peak demand savings for large facilities that have a demand charge based on a peak monthly load. The results are estimates in comparison to a black roof. The calculators work with only a handful of variables, so the results depend greatly on good input values. To compare two non-black roofs, two separate estimates are needed and the differences in savings have to be calculated manually.

The **DOE steep-slope calculator** is also developed by ORNL and estimates cooling and heating savings for residential roofs with non-black surfaces. It is about the same as the calculators for low-slope roofs, with only a handful of input values to enter, but the user interface is different and blinking all the time, which makes it quite hard to use the tool. The same problem occurs with a **Solar Reflectance Index (SRI) calculator** ORNL also offers on its homepage. The SRI calculates solar reflectance and thermal emittance of cool roofs in one single value.

The ORNL / LBNL (Lawrence Berkeley National Laboratory) **Roof Savings Calculator** (RSC) is based on DOE-2 and simulates hourly values of heating and cooling loads for a year for commercial and residential buildings based on the weather data of the selected location. A drawback is that only US locations are available. From these values it calculates the energy savings compared to a base case. At the moment this calculator is still being validated (RSC 2010).

Green Roofs for Healthy Cities North America (GRHC) offers the **GreenSave Calculator**, which makes it possible to compare the life-cycle costs of green roofs with conventional roofing systems. However, this tool is only available for GRHC members (GRHC 2010).

2.2.3.3 Microscale Models

Microscale models, such as urban canyon models, enable researchers to study a configuration of buildings surrounding a street. They are based on energy balance equations and take into account the geometry of the canyon, wind, solar radiation and shading. These models are used to clarify the mechanisms of UHIs and help to evaluate the effects of urban geometry on urban climate, and of urban climate on the

energy use of buildings. They are useful for estimating the effects of cooling surfaces or adding vegetation. An example for urban canyon models is the software tool **Solene** (Miguet & Groleau 2008).

ENVI-Met is a freeware program available on the Internet in the recent version V3.1 Beta III for Microsoft Windows (ENVI-Met 2010). A Linux version is planned for the next version 4.0. It is a three-dimensional microclimate model that simulates the surface-plant-air interactions in urban environment. For the simulation of these interactions, it combines the calculation of fluid dynamics parameters with the thermodynamics processes taking place at the ground surface, at walls and roofs or at plants. It includes the simulation of turbulence, the flow around and between buildings, exchange processes of heat and vapor at the ground surface, walls and vegetation, vegetation parameters, bioclimatology and particle dispersion. The program uses a resolution of 0.5 to 10 meters in space and 10 seconds in time and can even simulate complicated geometric forms such as balconies. Additional software ranges from editors to graphical visualization tools for the results. As ENVI-Met is a microscale model, it is necessary to force it with external data from other models to simulate specific meteorological conditions.

Comfort models evaluate the human comfort under different conditions. They are based on similar equations as the canyon models. The model **OUTCOMES** for example "*calculates an energy balance for a human being based on the weather and the characteristics of the surroundings. OUTCOMES has been used to see how human comfort is improved by shade trees* (Gartland 2008, p.38)."

2.2.3.4 Mesoscale Models

Mesoscale models are used to evaluate the effects of UHI mitigation on regional air temperatures and air pollution. Heat island effects are modeled using a combination of meteorological and photochemical models.

MM5 (Mesoscale Meteorological Model 5) was developed for meteorological modeling by the Pennsylvania State University and the National Center for Atmospheric Research (MM5 2010). It is commonly used to simulate the climate and weather of mesoscale regions. MM5 consists of different modules and can be used together with the Comprehensive Air quality Model with extensions (**CAMx**), which can simulate the air quality of a region, to evaluate heat island effects on larger

regions. To evaluate the effects of mitigation measures the input for these models must be extensively manipulated. This makes modeling of mitigation measures very difficult and time-consuming, but it is nevertheless very useful. Temperature, energy use, emissions and smog formation are very interdependent, thus the models have to be run iteratively. As there already exists the next-generation model **WRF** (Weather Research and Forecasting Model), MM5 is not developed further.

Another meteorological model is the Regional Atmospheric Modeling System **RAMS** (ATMET 2010). It is used for numerical simulations of atmospheric meteorology and other environmental phenomena on scales from meters to hundreds of kilometers. It can provide the boundary conditions for other models.

The **Mitigation Impact Screening Tool** (MIST 2010) is a simple web-based tool to predict the regional impacts of UHI mitigation measures in US cities. Based on detailed modeling of 20 cities it estimates the reduction of temperature, smog and electricity consumption as a result of increased solar reflectance and / or vegetation for about 200 locations.

2.2.3.5 Multiscale Modeling

As it is not computationally traceable to handle all scales of building-urban interactions in a single climate model, researchers in Switzerland are developing multiscale modeling of urban climate (Rasheed & Robinson 2009, EPFL 2010). A mesoscale atmospheric model is extended for easier and more accurate urban climate predictions. The results from a global atmospheric model serve as input and the mesoscale model is coupled with an urban canopy model. The resulting model is calibrated to the city of Basel and used to study UHI mitigation through urban planning interventions at building and urban scale. The aim is to produce new urban planning guidelines. The model will also be used for future simulation of pedestrian comfort.

2.2.3.6 Ecosystem Models

Ecosystem models help to take a look at the impacts of vegetation in cities.

CITYgreen, developed by American Forests, is a GIS-based model that evaluates the impact of trees and vegetation on stormwater run-off, air quality and energy use

of a region. Beyond that, the model calculates the storage of carbon by the plants. The program is used to assess the economic benefits of urban vegetation. Since July 15, 2010 it is temporarily unavailable, because it is not compatible to the new version of ArcGIS 10 (CITYgreen 2010).

i-Tree, from the US Department of Agriculture Forest Service, is a tool for the analysis of urban forests and the assessment of its benefits. Its two main components are UFORE and STRATUM. The first serves to estimate the environmental effects of trees, such as air quality improvement, CO_2 reduction and stormwater control, while the latter calculates tree costs and benefits. The freely accessible package was initially designed to help urban foresters with their work (i-Tree 2010).

The **Tree Benefits Estimator** is a simple web-based tool to estimate the benefits of planting trees based on the experience of SMUD's Shade Tree program (SMUD 2010). It is designed for US climate. The tool makes broad assumptions of a tree's impact on direct shading benefits, evapotranspiration effect, heating penalty in winter months, tree growth rates and tree survival rates. The resulting energy savings as well as carbon and CO_2 sequestration from mature trees of the specified species are calculated.

2.2.3.7 Modeling the Effects of Global Warming

One of the seven research themes in the EU Project MEIGEVille focuses on modeling the effect of global warming on indoor temperature peaks and cooling systems consumption. Dénes-Béjat et al. (2009) conducted a simulation study on an office building in France. Results show that within one hundred years the energy consumption of buildings due to cooling could be three times more important than today. Research on cooling urban areas through UHI mitigation measures is therefore important.

Crawley (2007) developed a set of 525 weather files representing the four scenarios of climate change from the Intergovernmental Panel of Climate Change (IPCC 2010) and two UHI scenarios for 25 locations. They are used in subsequent work to simulate the impacts of climate change and UHIs on office buildings.

The effects of the use of different weather data on modeling indoor climate is discussed by Leinich (2008).

2.2.3.8 SUNtool

"*Project SUNtool (Sustainable Urban Neighbourhood Modeling tool) represents a new approach for an integrated architectural design and environmental simulation tool* (SUNtool 2010)."

SUNtool is a three-year research project developed under the EC's Fifth Framework Programme "Energy, Environment and Sustainable Development". It was due for completion in 2006. Partners from Czech Republic, Finland, France, Greece, Switzerland and the United Kingdom were involved.

The modeling tool intends to be a sustainable masterplanning tool with a holistic view of community. It enables behavioral modeling and modeling the resource flows in an integrated and urban-sensitive way to optimize net resource flow profiles. It predicts the performance and environmental influences of masterplan alternatives (energy consumption and power demand, waste production, water consumption and overall community conditions) and allows studying couplings, e.g. to use energy from waste or residual heat for preheating. The results allow optimizing the site configuration and the sustainability of masterplanning proposals. The goal is to model resource flows in human behavior and urban context for the resource efficient development of sustainable communities.

The form of the neighborhood is sketched with a 3D sketching tool. Based on descriptions such as use and age of a building, default constructional and operational attributes are associated (basic definition stage). It is then possible to simulate microclimate, energy, water and waste flows or to define further details. SUNtool enables parametric studies and provides graphical results analysis facilities.

To train and inform the users on effective resource use and incorporation of sustainable technologies, an additional multimedia educational tool provides an overview of sustainable masterplanning with particular attention to the process of sustainable urban community planning. It covers design guidelines, community participation, performance prediction and measurement. Case studies from the participating countries and tutorials for using the modeling tool are also provided.

2.3 Mitigating Heat in Urban Areas

A lot of research has been done around the world to detect measures to mitigate UHIs, evaluate them, and determine the impacts of different factors. The following section provides a summary of possible mitigation measures and recent studies. First, potential modifications of buildings are presented, and then vegetation and urban planning measures are discussed.

2.3.1 Design of Buildings

Measures that can be taken in, on or around buildings are most important for architects. The easier to apply and the cheaper the measures are, the more likely they are going to be accepted not only by the architects, but also by the building owners.

2.3.1.1 Building Form

Okeil (2010) proposes a special building form called Residential Solar Block (RSB), as shown in Figure 2.8. The buildings are optimized with the specially developed program City Shadows by cutting solar profiles in the form, so that the resulting shadows almost exactly fit in the open spaces between the buildings at midday in winter. This ensures increased winter solar radiation and shading in summer. The form is also meant to increase airflows between the buildings. Furthermore, Okeil promotes green roofs to support UHI mitigation.
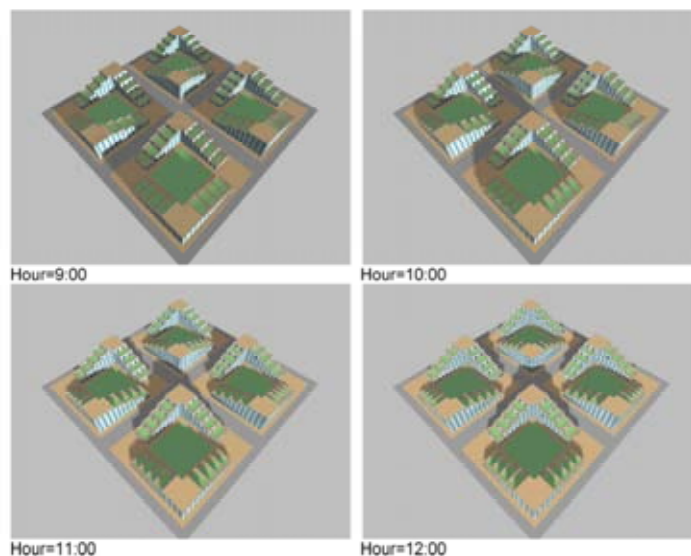
Figure 2.8: Shadows for a RSB optimized for latitude 48.00 in December (Okeil 2010)

2.3.1.2 Low Energy Techniques

Low energy techniques with low initial cost and early amortization are most likely to be accepted and can be applied to a large number of (existing) buildings. Low energy techniques like for example improved building insulation are already quite common.

Chai et al. (2009) simulated the application of three low energy techniques on one building of an existing block of six office buildings in Shanghai, China. The building was going to be refurbished because of its high cooling costs and served as a demonstration example of relatively new measures in China. The building had some roof insulation, but no wall insulation as it featured a full height single glazed curtain wall. The energy demands were simulated with Tas for a base case of the original building with all openings closed. A second case was simulated with natural ventilation, which means the windows were assumed to be open whenever possible. For case 3, the walls were insulated with low energy double-glazing and shading was simulated through a fixed overhang, the windows remained closed. Case 4 simulates a combination of insulation, shading and ventilation. A life cycle cost model compares the initial costs, operation costs, electricity consumption, maintenance, repair and replacement costs over an assumed length of life cycle of 50 years to the total electricity cost of the original building for 50 years. The advantage of a refurbishment is clearly visible from the results. Benefits include less cooling loads in the south and west zones, and less heating loads in the north zone. The biggest savings can be made during the summer cooling season, savings in heating are not significant in comparison. The overall electricity savings are more than 24%. Natural ventilation could save over 40% in spring, 25% in autumn and 8% in summer night cooling. Over the whole year smart ventilation could save over 12% electricity, together with solar shading it would be about 39% although there is extra electricity needed to operate the shading device. This is equal to minus 32 kg CO_2 / m^2. Tas cannot simulate retraceable blinds, which would further lower running costs. It also simulates cooling when the windows are open and temperature is higher than 26°C, which implies a waste of energy.

Capon & Hacker (2009) modeled simple climate change adaptation measures to reduce overheating in existing buildings. The modeled building types are a house, a flat and a block of flats, respectively. The modeled measures include solar control, natural ventilation, improved insulation, better reflectivity of external walls and

improved glazing. The measures were modeled individually and in different combinations. Results show that even simple measures such as natural ventilation at night or internal blinds have a beneficial effect, but are not sufficient regarding the effects of climate change. Especially in higher-level flats, overheating cannot be eliminated without making adaptations to the external fabric of the building. When the combination of all measures is adapted on the whole building, the CIBSE (Chartered Institution of Building Services Engineers) overheating temperature (28°C) is never exceeded for the current climate and only exceeded very little for a future CIBSE weather year of 2050. Furthermore the number of cooling degree hours above the CIBSE comfort temperature (25°C for the living room and 23°C for the bedroom) is decreased by over 90% in all cases.

2.3.1.3 *Evaporative Cooling Techniques*

Narumi et al. (2009) experimented with evaporative cooling techniques to mitigate heat in buildings. They tested rooftop spraying, veranda spraying and spraying to the outdoor unit of a room air conditioner at different times of the day on an existing but uninhabited apartment house in Osaka. The spraying units for the roof can be seen in Figure 2.9, the veranda spraying in Figure 2.10 and the spraying to the air conditioning (AC) unit is shown in Figure 2.11. Numerical simulations were also conducted in the study, assuming the building to be inhabited. For the simulation, the sidewalls were also sprayed. The results were compared to the results from non-cooled parts. The method leads to reduced surface temperatures and AC usage times as well as an improved air-conditioning efficiency, resulting in an up to 80% reduced energy consumption for cooling. Figure 2.12 shows a thermal image of the rooftop, where the cooler surface temperatures can be seen clearly. Besides the clearly beneficial effect, this method is not environmentally friendly, because a high amount of water is needed every day for the spraying.

Figure 2.9 (left): Rooftop spraying (Narumi et al. 2009)
Figure 2.10 (right): Veranda spraying (Narumi et al. 2009)
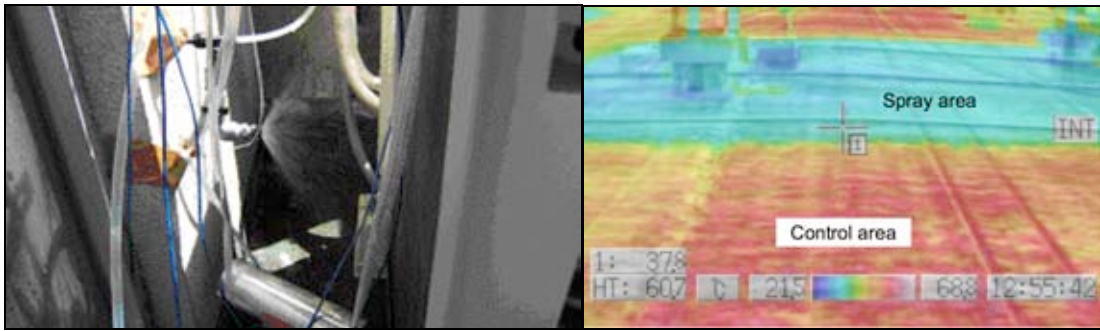
Figure 2.11 (left): Spraying to the AC unit (Narumi et al. 2009)

Figure 2.12 (right): Thermal image of the rooftop (Narumi et al. 2009)

2.3.1.4 Construction Material

Another possibility to mitigate heat in buildings is to use different construction materials.

Kandya et al. (2009) suggest using bamboo, which is the fastest naturally growing renewable material and has light weight but high strength. With its adaptability to different climate conditions, it offers good opportunities for CO_2 mitigation to prevent higher UHI intensities due to climate change. To test its structural behaviour, a bamboo arch was build and put under weight. The results qualify the material to be used as a load bearing element. Its thermal behaviour was studied with three not ventilated cubicles. The results show that bamboo has the potential to act as a "cool" material. Experiments to harvest solar energy from half split bamboo panels, with water or air as heat transfer agent, were also conducted successfully. Nonetheless, the material needs to be studied further to get the maximum benefits of its advantages as a green and cool construction material.

2.3.1.5 Reflective Materials / Cool Roofs

Roofs cover large parts of the city and are usually the hottest feature in thermal images. Common roofing materials with a solar reflectivity of about 5 to 25% absorb 75 to 95% of the sun's energy and can heat up to temperatures from 65 to 90°C. Bare metal has a higher solar reflectivity of 20 to 60%, but with its low thermal emittance values it still heats up to temperatures from 50 to 70°C (Gartland 2008). Cool materials store and release less heat to the air and help reducing the UHI. The building comfort is improved and energy for cooling can be saved which also means

less pollution from power plants. Furthermore, the lifespan of the material is increased.

Materials count as "cool", when their surface temperature generally stays below 50°C even in the summer sun, with peak temperatures of only 40 to 60°C (Gartland 2008). The two important physical characteristics are high solar reflectivity – also called albedo – and high thermal emittance, which together affect the surface temperature of materials as shown in Figure 2.13. High thermal emittance enables the material to radiate away the heat it absorbed. Of importance is only the uppermost surface, which makes it possible to use cool coatings on common materials. According to Gartland (2008) cool materials should have emittance values higher than 80%.
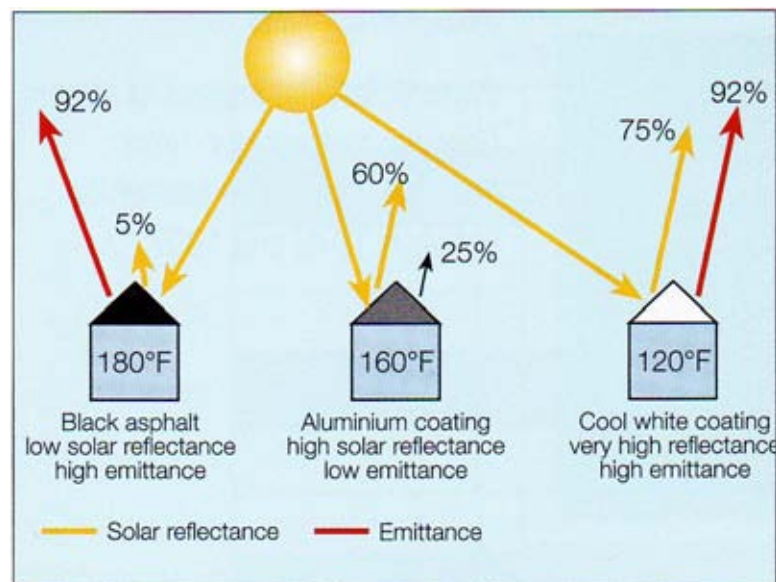
Figure 2.13: Effects of solar reflectance and thermal emittance (Gartland 2008)

Materials can reflect energy of different wavelengths differently. Cool materials can be either light-colored or even white with high solar reflectance due to titanium dioxide (TiO_2) or "cool colored" materials with high near infrared (NIR) reflectivity. While white roofs should have a solar reflectivity higher than 70%, the reflectance of cool materials can vary from 30 to 60% depending on the type of pigment and the darkness of the color (Gartland 2008). The reflectance of some materials is compared in Figure 2.14.
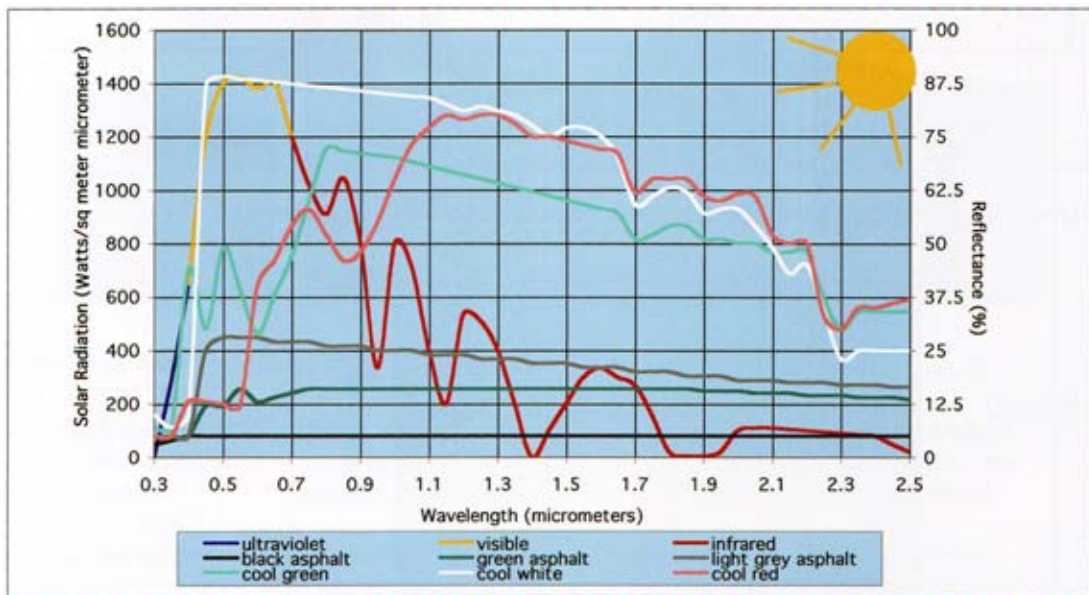
Figure 2.14: Solar reflectance of roof materials (Gartland 2008)

There exist different solutions for low-slope roofs and steep-slope roofs, with the low-slope roof market being more progressive.

The first option for low-slope roofs are cool coatings – surface treatments with the consistency of thick paint – which come in two types: cementitious coatings and elastomeric coatings. The latter have better adhesion qualities, which is in general the biggest challenge of this solution. Mixed coatings with cementitious and elastomeric ingredients are also possible. Coatings have to be applied (sprayed or rolled) to roofs in good condition, they are not meant to repair leaks. Most cool coatings are bright white, but there also exist some colored versions. To keep the good reflectance values, the surface needs to be cleaned, e.g. by pressure washing every year. Unfortunately coatings do not work for shingles on steep-slope roofs, as they can block drainage channels and the contraction and expansion of the shingles (Gartland 2008).

Another option are cool single-ply materials such as polyvinyl chloride (PVC) and thermoplastic polyolefin (TPO). They are usually bright white with a solar reflectance higher than 70%. These membranes are glued or fastened in one layer; the seams must be sealed.

For steep-slope roofs, only a few solutions for cool roofing exist. Here the color is more important as the roof is visible and contributes to the aesthetics of the building. Also glare could be a serious problem. There exist some cool tiles and cool coated metal roofing for steep-slope roofs (Gartland 2008). Examples for cool colored tiles

and their solar reflectance are shown in Figure 2.15. Figure 2.16 pictures the same for cool metal roof coatings.
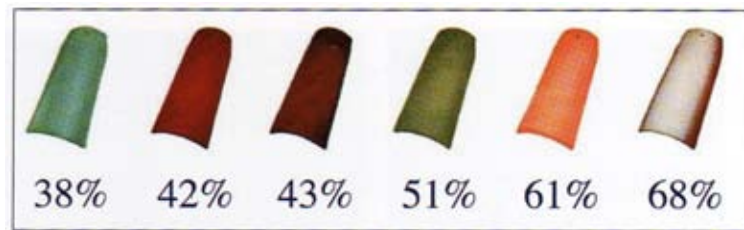
Figure 2.15: Cool colored clay tiles (Gartland 2008)
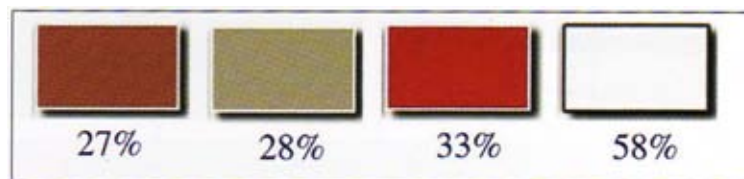
Figure 2.16: Cool colored metal roof coatings (Gartland 2008)

More research needs to be done in this field, especially concerning cool colored shingles. Levinson et al. (2009) suggest concrete tiles and asphalt shingles with a two-layer spray coating that should provide easy production and higher solar reflectance. They prepared 24 prototype tiles and 24 prototype shingles with a white base coat followed by colored topcoats. Further research is still needed, also concerning the effects of different thicknesses of the layers.

In the USA, cool roofs are part of the energy code in many states. The US EPA features a list of Energy Star certified products and the Cool Roofs Rating Council (CRRC) has a database of approved materials, but those lists should be considered carefully, as they do not apply the same standards. To promote the US knowledge and technology of Cool Roofs in the European Union, a Cool Roofs Project supported by the European Union has been founded. It is controlled by the EU – Cool Roofs Council (EU-CRC) and among other tasks provides a database of cool roof materials on its website (EU-CRC 2010).

2.3.1.6 Retroreflective Materials

In densely build areas, the heat reflected from one building would be absorbed by an other. Therefore highly reflective paints as used for cool roofs cannot be used on walls. Glare could also be a serious problem. Retroreflective materials on the other

hand, which reflect the incident light with only a small spread, could be used. As the applicable area is larger than for highly reflective paints, the effect is larger too. Materials with retroreflective attributes are widely used as road markings and signs to enhance nighttime visibility, but their heat transfer characteristics were unknown. Sakai et al. (2009) therefore made experiments and for the first time tried to measure the reflectance of retroreflective materials. The results of the experiments show, that retroreflective materials can reduce the heat generated by reflected sunlight. Figure 2.17 shows the principle of highly reflective and retroreflective materials in comparison.
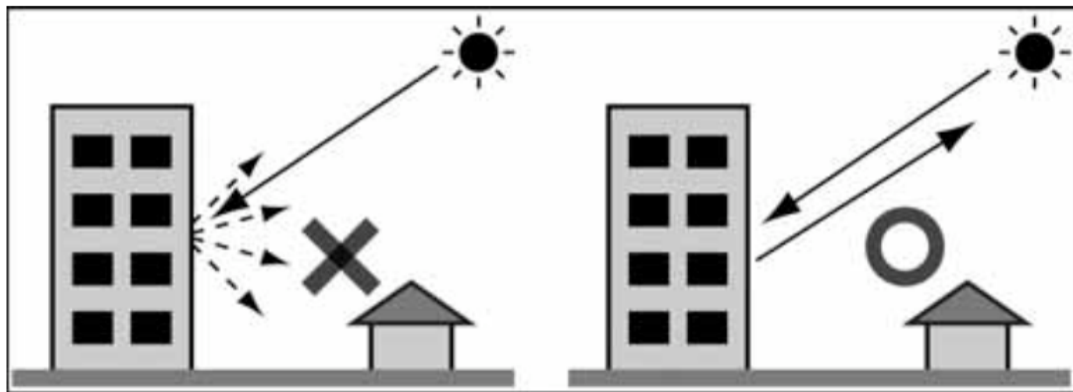
Figure 2.17: Highly reflective (left) vs. retroreflective materials (right) (Sakai et al. 2009)

2.3.1.7 Thermochromic Coatings

Karlessi et al. (2009) research on the development and comparative testing of thermochromic coatings for buildings and urban structures. The colors of the coatings consist of thermocromic pigments in the same binder systems that are used for the matching cool and common colors. Their unique characteristic is that they change their color to transparent or translucent at a transition temperature of 30°C. This is achieved by a thermally reversible transformation of the molecular structure. Measurements of eleven coatings on white concrete tiles showed that the colors turned almost white after 20 minutes. The samples stayed cooler than the same common and cool colors. Colored and colorless states of the coatings are highly reflective in the NIR spectrum, higher than cool and common colors. Thermocromic coatings can absorb solar energy at lower temperatures in winter and reduce absorption at higher temperatures in summer and thus function as energy saving systems with a potential for the reduction of heating and cooling loads. Further research is still needed concerning the aging of the coatings. Figure 2.18 shows the

daily temperature profile of a black thermocromic coating compared to those of cool and common black coatings.
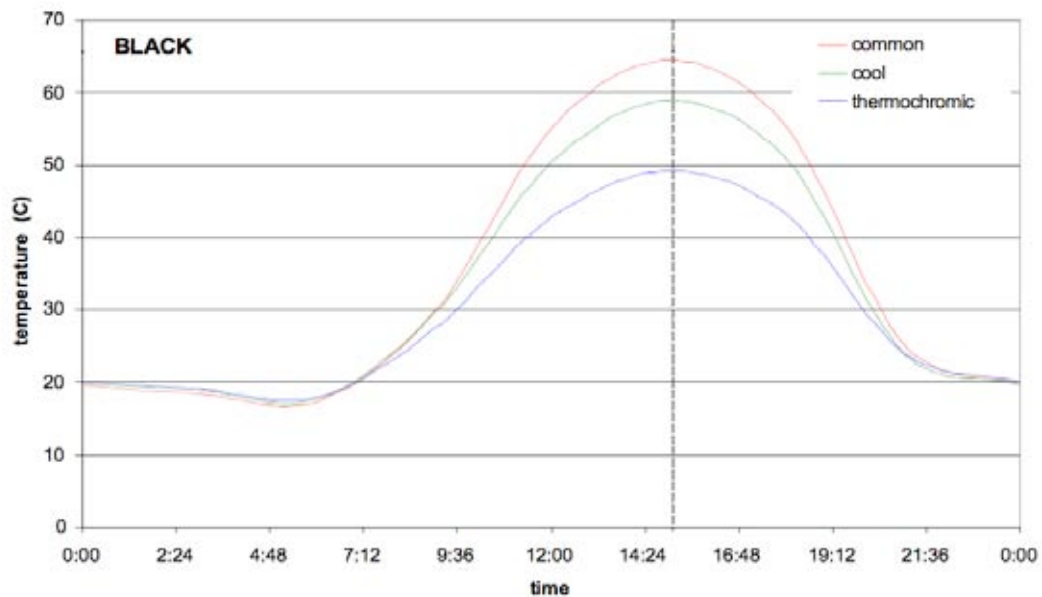
Figure 2.18: Daily temperature profiles of common (red), cool (green) and thermocromic black coatings (blue) (Karlessi 2009)

2.3.2 Vegetation

Vegetation on and around buildings naturally influences the outdoor and also the indoor comfort. Trees for example can mitigate UHIs by controlling the heat gain and the casting of shadows. They also cool through evapotranspiration and reduce air pollution through dry deposition. Reduced storm-water run-off is another benefit. The following section describes the effects of different vegetation options including single plant units, parks and green roofs and walls.

2.3.2.1 Effects of Trees and Vegetation

Trees are useful in shading pavements, streets and parking lots. They show especially beneficial effects in strategically chosen locations around buildings. Deciduous species at the south, southwest, east and southeast of a building shade it from the summer sun, but allow sunlight to pass in winter. Largest benefits are achieved by trees west and east of the building. Evergreen species in the north can block cold winter winds (Gartland 2008). Trees are not the only vegetation option, vines are also useful, especially when shade is needed fast because they grow

much faster than trees. Bushes and shrubs are advisable when there is not enough space for trees. Although often seen as an extra expense, trees and vegetation produce net monetary benefits over their lifetime (Gartland 2008).

Several studies concerning the effect of trees and vegetation on buildings have been carried out. Fahmy et al. (2009) use dual stage simulations to determine the effects of different trees on the indoor climate of a residential area in New Cairo, Egypt. The program ENVI-Met was used to generate three sets of data: one without trees, one using 20 m high Yellow Poinciana, and one using 15 m high Ficus Elastica. The trees first were numerically modeled to get the ten values of trees leaf area density that ENVI-Met plants database needs. The ENVI-Met simulation was situated at the middle height of the facade of the three storey apartment blocks at 4.5 m above ground level. Weather files from the Typical Meteorological Year, version 2 (TMY2) of the EnergyPlus file were used to write the ENVI-Met output in and modify the exact site coordinates. The generated data was a day in June from 10 am to 15 pm local solar time. The weather data was then used by Design Builder to simulate the indoor comfort. The results of each of the three cases were different, which shows the different foliage effects. The best results of indoor comfort levels were achieved with the 15 m high trees. Therefore, the choice of the right tree is important. Trees used to the local climate grow better and are less susceptible to diseases. Furthermore, the so-called Ozone Forming Potential (OFP) of trees is an interesting factor in the choice of the right tree. A species with low OFP should be chosen (Gartland 2008).

Yoshida et al. (2009) measured the energy balance of two single plant units to determine their contribution to mitigating UHIs. They measured a potted hibiscus outdoors, and measured and modeled a camphor tree. The results showed that the evaporation efficiency does not change with solar radiation and is relatively low for a single plant, but the plant also contributes to UHI mitigation through shading.

Simulation studies for California indicate that the effects of increased urban albedo are most of the time larger than those of increased canopy cover, although differences generally are small (Taha 2009).

2.3.2.2 Impacts of Parks

Studies show that urban parks can mitigate UHIs only at micro- or mesoscale because the air temperature around them is mainly influenced by other parameters such as building density, anthropogenic heat or shading. Hamada & Ohta (2010) noted that the cooling effect never exceeded 500 m in their study. The air temperature is reduced significantly inside the park, but only the neighboring buildings can benefit from that. Parks are still beneficial from a social and city planning point of view, but from a thermal point of view a number of small parks is more effective than a single large one (Alexandri 2008, Alexandri & Jones 2006). Larger parks have a potential to form stronger cool islands, but the park size is not the only factor of influence. The shape of the park and the land use inside the park are also important (Cao et al. 2010).

2.3.2.3 Green Roofs and Walls

Roofs and walls promise a large opportunity to add vegetation to the urban landscape. Green roofs include the simpler and lighter intensive roofs and the more expensive extensive roofs that are often designed for human access. While extensive roofs usually need special structural support to bear the garden even when it is wet, light intensive roofs can also be used to retrofit existing roofs and for slopes up to 30° (Gartland 2008).

Besides a lot of other positive effects from economic to social (see GRHC 2010, Gartland 2008), green roofs offer benefits in mitigating the UHI effect. Those benefits include community cost savings from increased stormwater retention and decreased cost of meeting greenhouse gas reduction. The UHI effect is moderated by temperature regulation through evaporation and evapotranspiration, and the air quality is improved through filtering the air moving across the roof. Better air and less ground level ozone also mean less need for health care services.

The exact requirement of green roof coverage in a city is difficult to determine. Researchers conducted a mesoscale atmospheric simulation for the city of Toronto (GRHC 2010). The city's vegetation reduced the UHI up to 1°C over approximately a quarter of the city. By using a green roof coverage of 50%, cooling was extended over a third of the city, increasing maximum cooling to 2°C. The assumed coverage

is high, but it is estimated that only 6% are fully irrigated, which suggests that the actual coverage to obtain these results could be much smaller.

In summer, the hottest areas are the roofs, but when they are vegetated, it is the streets. When only the roofs are green, the temperature inside the canyon is not mitigated. When there are only green walls, the temperature at the roof level stays about the same. So to lower the temperature at urban scale, green roofs are more effective, for lower temperatures at building scale, green walls are better. The best results are of course achieved with a combination of both. This was investigated for nine cities in nine different climatic zones. Figure 2.17 shows the maximum temperature decreases achieved and indicates that the hottest and driest climate shows the largest effect (Alexandri 2008). Alexandri and Jones (2006) found that for Athens, Greece, green walls and roofs together reduced air temperatures in the canyon by 6 to 8°C.
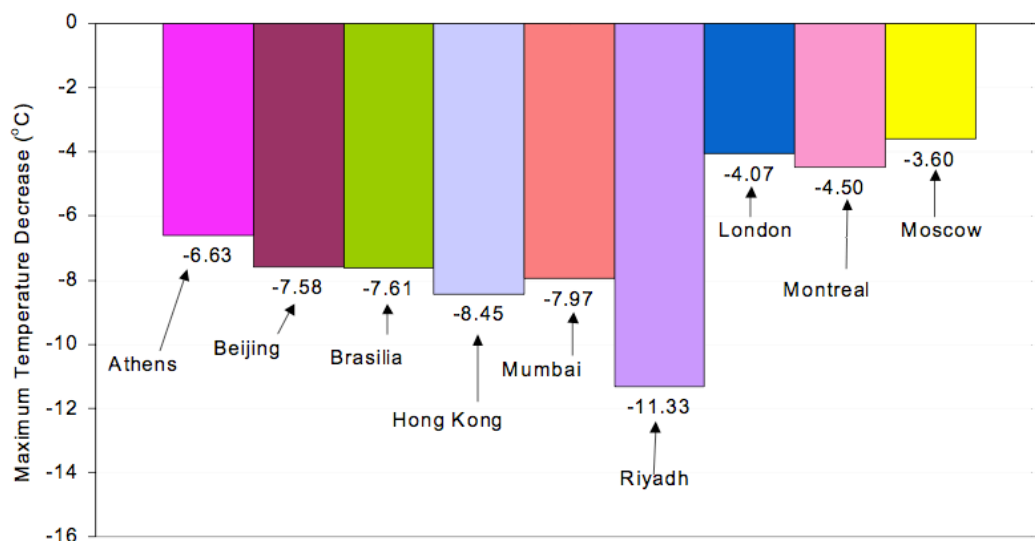
Figure 2.19: Effects of green roofs and walls (Alexandri 2008)

Figure 2.20 compares the modeled surface temperatures of four different roofs (concrete, white concrete, three-years old white concrete and a green roof) over a one-day period for the climate of Athens. Although hotter than new white concrete in the morning hours, green roofs are cooler in an overall view (Alexandri & Jones 2006).
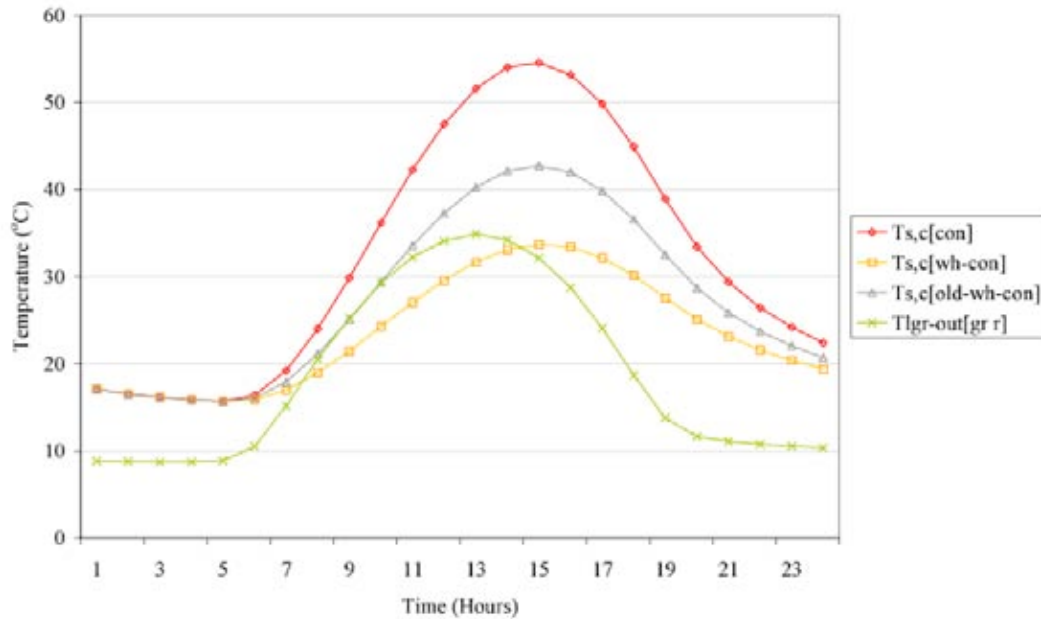
Figure 2.20: Surface temperatures of a concrete roof [con], a white concrete roof [wh-con], a three-years old white concrete roof [old-wh-con] and a green roof [gr r] (Alexandri & Jones 2006)

Alexandri & Jones (2006) also conducted a parametric simulation study for the following 4 cases for Athens: a no-green base case, a green roofs case, a green walls case and an all-green case. The cases were studied for three building height to building width ratios (H/W) and two orientations. All results showed that the all-green case was most effective in cooling air temperatures inside a street, although the temperature decrease is highest at roof level. An example of the results is shown in Figure 2.21. The effect of green roofs and walls gets smaller the wider the canyon is because then the street surface becomes more influential. The orientation of the canyon and its relation to the wind direction was found to play a less important role.

"*Green roof technology is spreading. […] In France, approximately 1 million m^2 of roofs are greened per annum. Similarly, approximately the same area was covered in 2009 in North America. Germany adds about 11 million m^2 of green roofs each year* (Worldgreenroof 2010)."
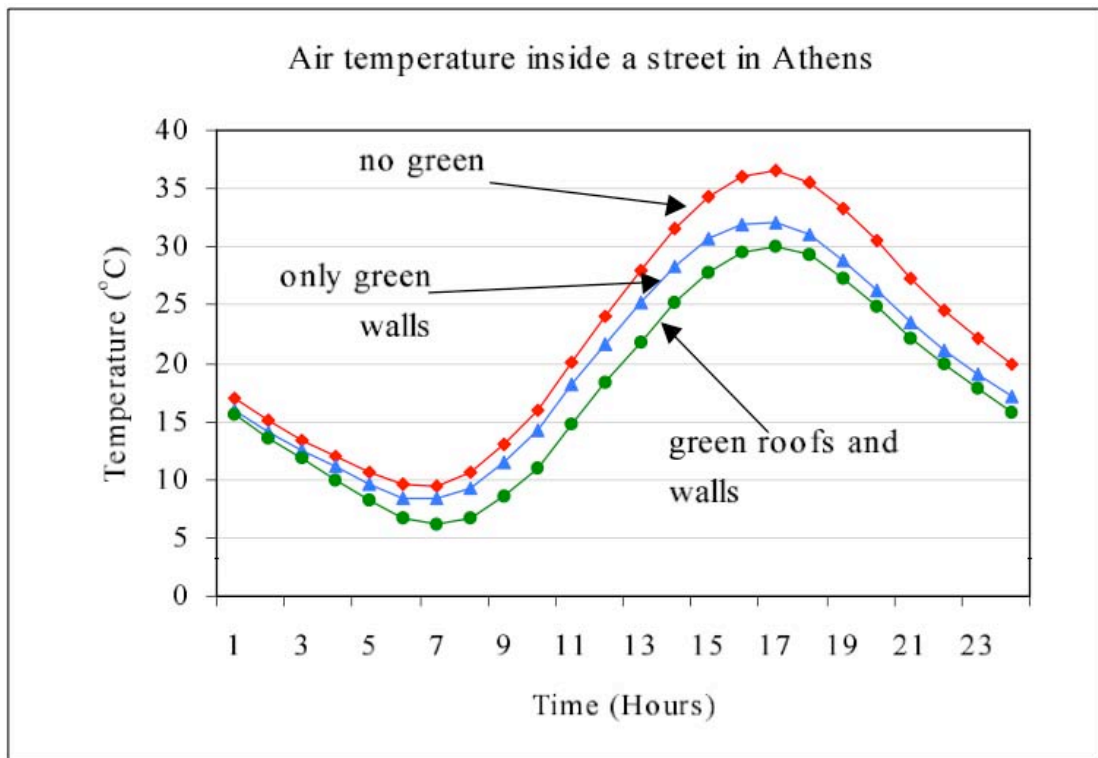
Figure 2.21: Averaged air temperatures for the no-green case, the green-walls case and the green roofs and walls case in an East-West orientated canyon with H/W= 0.50 (Alexandri & Jones 2006)

The rather poor understanding of green roofs in North America led to the foundation of Green Roofs for Healthy Cities North America in 1999 (GRHC 2010). The non-profit organization is dedicated to the development of a green roof and wall industry across North America and to the advancement of the development of the market for products and services. They develop best practices for design, installation and maintenance of green roofs and a training program for professionals to become accredited green roof professionals that can be found in an online database. GRHC also provides the Green Roofs Tree of Knowledge, a policy and research database on the internet. Recently, the VF-1 Fire Design Standard for Vegetative Roofs from GRHC was accepted as an American National Standard by the American National Standard Institute (ANSI). It provides design and installation references for roofing professionals to help eliminating the risk of fire on green roofs.

2.3.3 Urban Planning Measures

Unreasonable urban planning is one of the main causes for the formation of UHIs. In the following section, a description of urban planning measures to mitigate heat is given.

2.3.3.1 Cool Pavements

Pavement covers large percentages of urban areas and its surface temperature greatly influences the urban air temperature. The most commonly used materials for pavements are Asphalt Cement Concrete (ACC), commonly known as asphalt, and Portland Cement Concrete (PCC), known as concrete (Gartland 2008). Cool pavements offer a great opportunity of lowering air temperatures in cities, but not much effort was made in this direction so far and a lot of research is still needed. The following possibilities could make pavements cooler.

Asphalt is black or grey, impermeable and has a solar reflectance of 5 to 10% when new. During aging it gets lighter and achieves values of 10 to 20%. It can heat up to 65°C or higher and releases the stored energy in the evening and overnight (Gartland 2008). Due to its easy installation and low initial costs it is widely used. The use of light pigment or lighter colored aggregates can make it cooler by increasing its solar reflectance up to 30%. A solar reflectance of 25% and peak temperatures staying below 50°C are already considered as cool for pavements (Gartland 2008). Pavements can of course not be as light as cool roofs because of the risk of glare. Thermal emittance is not an important factor as pavement materials commonly have values of 80% or higher (Gartland 2008). During routine asphalt maintenance, emulsion seal coats and chip seals with lighter pigment and aggregates can be used on top of the existing pavement to make it cooler. Those can also be finished with brick ore stone-like textures to simulate other materials.

Concrete is light grey with a solar reflectance of 35 to 40 %, which is reduced to 25 to 35% due to dirt when it is aging. High-pressure washing can help preserving higher reflectance, but even dirty concrete pavement is cooler than ACC. Its temperature usually stays below 50°C (Gartland 2008). Concrete can also be cooled further by the use of lighter colored aggregates and cement binders. A method called white topping applies a thin layer of PCC over existing asphalt pavements. Ultra-thin white topping uses fiber reinforcement to strengthen the pavement. PCC lasts longer

than ACC and has lower maintenance and life cycle costs, but due to its higher initial costs it is used less often.

Besides the temperature reduction, lighter pavements also lead to less need for nighttime lightning as they reflect artificial light better. This results in less lightning energy use (Gartland 2008, Peyerl & Krispel 2008).

Another way of making pavements cooler, besides increasing their solar reflectance, is to make their surface permeable and allow water to drain, get stored in the soil beneath and cool through evaporation. Porous or permeable PCC (PCPC Portland Cement Pervious Concrete) and open-graded asphalt leave out the smallest particles in their mix, thus creating void space. When appropriately sized, those pores should remain free of dirt. Both materials have been successfully used on roads and parking lots in the US, but still need further research. They are also good for storm-water retention and the slightly rougher surface was found to decrease the noise of tires (Gartland 2008).

Other measures include colored coatings, resin-based pavements and block pavers. Resin-based pavements use clear tree resins as binders instead of petroleum-based binders, so they adopt the color of the aggregates used. Those can be taken straight from the construction site, making the road blend in with the environment. They are for example used in environmentally sensitive areas for hiking and biking paths (Gartland 2008). Block pavers are lattice blocks made of plastic, metal or concrete filled with rocks or plants. They are used successfully in low traffic areas. Colored coatings are achieved by mixing in special pigment additives to get shades of red, green, tan and grey. They are, for example, used to mark bike lanes. Zinc dioxide, titanium dioxide or the like could be added to make them lighter.

An interesting approach to cool pavements is presented by Mallik et al. (2009). They modeled a reduction of the urban heat island effect through the harvest of heat energy from asphalt pavements with water flowing through a piping system similar to solar collectors. They also built this as an experimental setup and measured the results. The effect depends on the location and spacing of the pipes combined with high-conductivity layers. Although much more research needs to be done and practical problems need to be solved, this is a promising option. The warmed water could be used further for other purposes.

Ping et al. (2009) studied the pavement material "PerfectCool" developed by NIPPO Corporation Co. Ltd., Japan, which consists of dark color pigments mixed with high infrared reflective pigments and fine hollow ceramic particles. The assembly of the coating is shown in Figure 2.22.
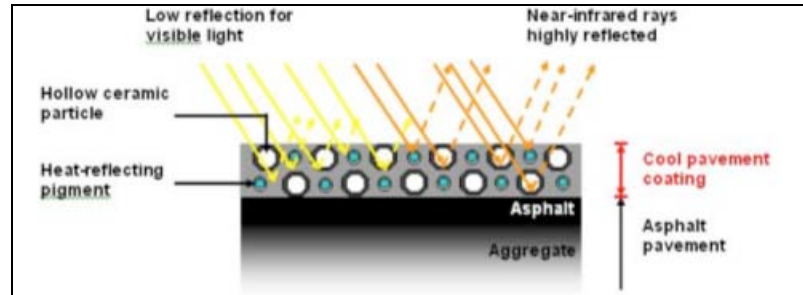
Figure 2.22: Principle of "PerfectCool" coating (Ping 2009)

Laboratory tests showed that the material has high NIR reflectivity, high emissivity and a lower surface temperature than common pavement materials, depending on the chosen color. On-site experiments led to surface temperature reductions to about 38°C, which was 17°C cooler than asphalt. Surveys revealed that most participants felt the temperature difference without knowing about the experiment. Simulations also indicated lower external wall surface temperatures and less energy consumption for a building surrounded by the material.

2.3.3.2 Ventilation Paths

In Tokyo, where the temperature has risen about 3°C over the past 100 years, a national research project about ventilation paths of cool sea breeze (so-called Kaze-no-michi) was introduced to mitigate UHI effects (Kagiya & Ashie 2009). Measurements showing the presence of a continuous wind flow were compared to CFD simulations on Japans supercomputer "the Earth Simulator" to determine the influence of high rise buildings, streets, parks and rivers on temperature and flow of the local wind and to find out how to make the best use of Kaze-no-michi. There are, for example, some skyscrapers along the coast, which form the so-called "Tokyo Wall" and block the sea breeze. For two areas, case studies with detailed 1:750 models in a wind tunnel were conducted. Redevelopment measures were also simulated and showed more wind and temperatures up to 2°C less. The results of all methods showed that the wind flow could effectively be used for city planning. Researchers classified the three types of Kaze-no-michi described in figure 2.23 and developed a PC software based on the models mentioned above to simulate the

effects of various measures such as greening, installation of water-retentive pavement and cool roofs.
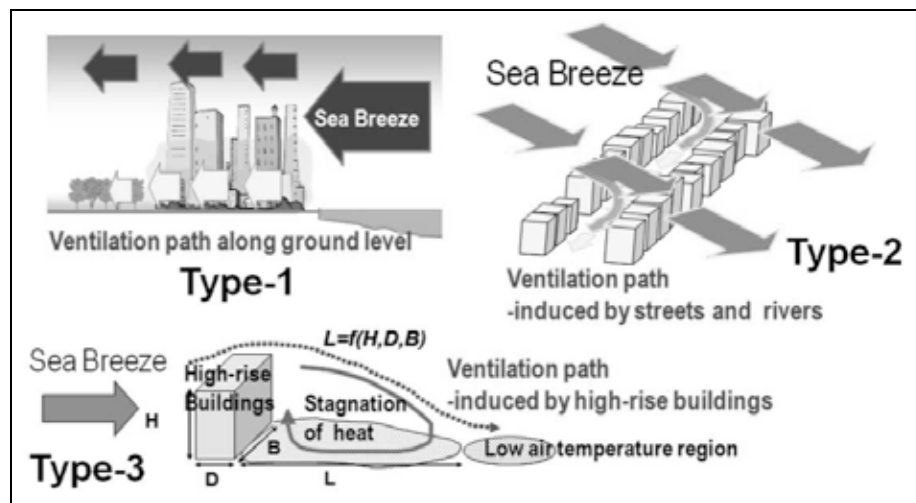
Figure 2.23: Types of Kaze-no-michi (Kagiya & Ashie 2009)

The Japanese researchers were inspired by the German ecological city planning approach used, for example, in Stuttgart, but their approach is three-dimensional in comparison to the German two-dimensional proposal as shown in figure 2.24 (Kagiya & Ashie 2009).
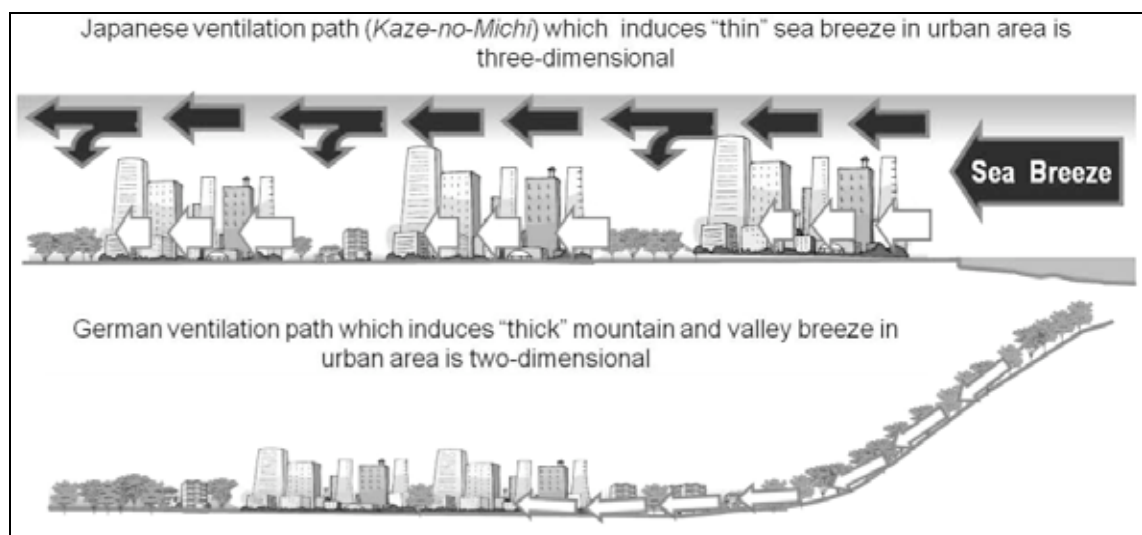
Figure 2.24: Japanese vs. German approach (Kagiya & Ashie 2009)

Wong et al. (2010) propose a method for designating urban ventilation corridors that can potentially be used to mitigate UHI using the "frontal area index". The index can simply be calculated from three-dimensional GIS building data.

2.3.3.3 Improved Land Use Plans

Moriyama & Tanaka (2009) suggest a "Compact Eco-City" model for Osaka with 30% of the area as green space (at present it is less than 10%) to mitigate UHI intensity. In Figure 2.25, the concept of their model is presented. It is described further in Table 2.1. Like in Tokyo, an arrangement that improves ventilation and uses Kaze-no-michi is suggested. The UHI boundary layer is divided by green belts or water surfaces around high-rise buildings. The use of cool roofs and cool pavements, good public transportation systems and a compact urban infrastructure are also important in the proposed concept.
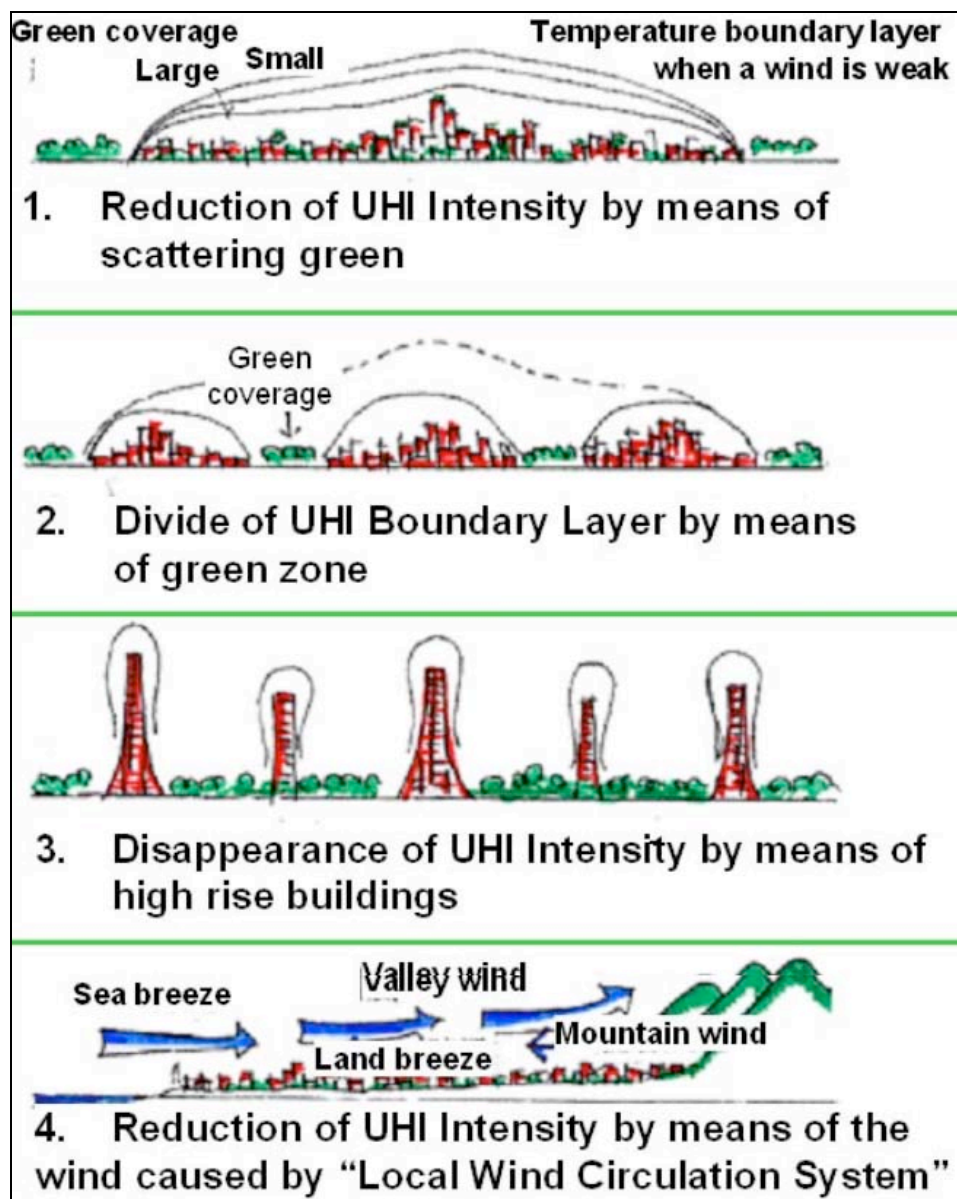
Figure 2.25: Concept of countermeasures (Moriyama & Tanaka 2009)

Table 2.1: Concept of countermeasures (Moriyama & Tanaka 2009)

measures viewpoint based on scale	Change of Land Cover (Especially, Green)	Reduction of Anthropogenic Heat (Buildings, Cars)	Wind Flow - Good Ventilation (Urban Form)
Urban Temp. Boundary Layer Regional scale 1:25000	· Green Area, Roof Garden, Cool Roof (High Reflection), Keeping Water Pave. , etc. · Introduce Large Green Area, Green Belt for Dividing	·Energy Saving ·Transportation ·District Heating and Cooling System Using Natural Energy	·Reduction of UBL by Local Wind such as Sea Breeze, Cold Air Drainage · Air Exchange between Upper Air and Earth Surface
Environmental Design of Outside Space District scale 1:2500	· Visual and Thermal Design for Health, Comfort ·Prevention of Thermal Storage by Road Surface ...	·Heat Release Method from Buildings (latent heat) and Cars, and its Location and Place	·Ventilation and Air Exchange by Form of Town, Arrangement of Buildings, Water Front, Open Spaces, Direction of Streets..

In Figure 2.26, the present situation with 10% green area is shown. The researchers now suggest an urban core with high-rise areas around the regularly located subway stations (indicated through circles) surrounded by a low-rise residential zone and a green zone as shown in Figure 2.27. The first step would be to install green belts between the terminal stations. The model has not yet been evaluated.

Figure 2.26: 10% case (Moriyama & Tanaka 2009)

Figure 2.27: 30% case (Moriyama & Tanaka 2009)

2.3.3.4 Pedestrian Ventilation System

Mirzaei & Haghighat (2009) propose the installation of a Pedestrian Ventilation System (PVS) to actively ventilate street canyons. The system allows controlling air movement, removing air pollution and improving pedestrian health and thermal comfort. The main principle is explained in Figure 2.28. It works with natural or forced convection via a vertical system of ventilation ducts that leads from the roofs to the street.
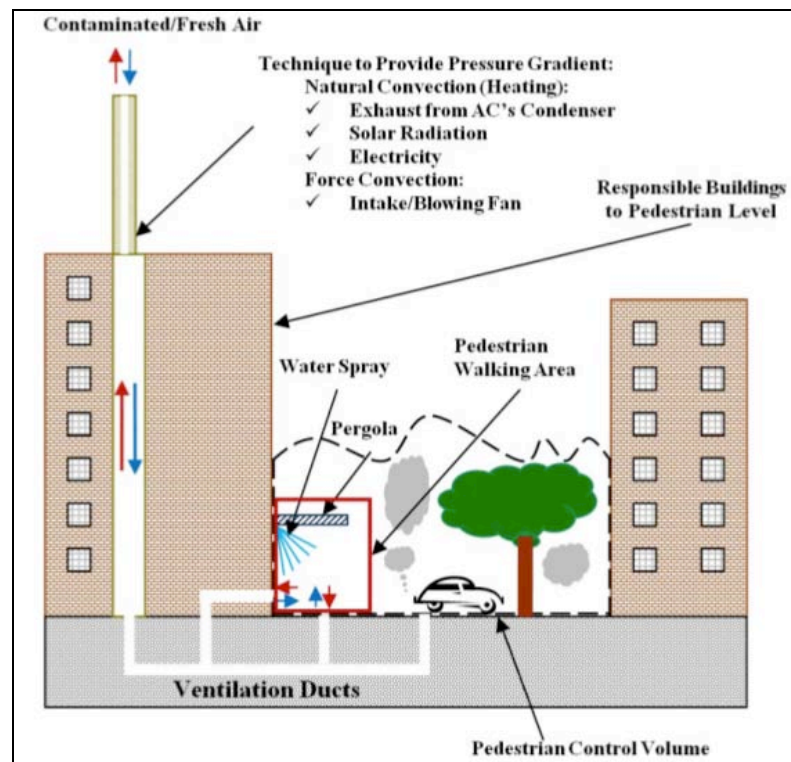
Figure 2.28: PVS (Mirzaei & Haghighat 2009)

For the four different strategies of the PVS proposed in Figure 2.29, case studies in CFD for stable and unstable weather conditions were conducted to get the air exchange rate and the pollution exchange rate and determine feasibility and performance. The results show a better air movement, but the temperature stays almost the same. However, more experiments and simulations are needed to test this approach.
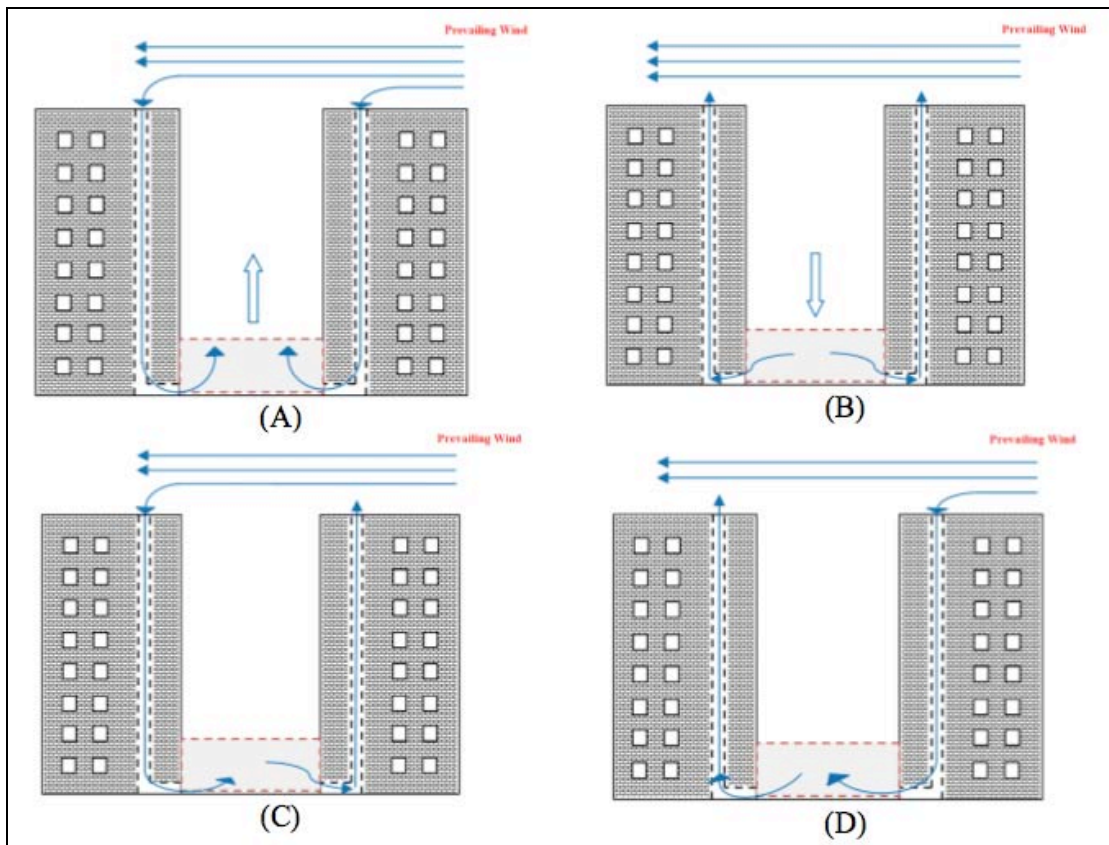
Figure 2.29: Strategies of the PVS (Mirzaei & Haghighat 2009)

3 METHOD

3.1 Overview

The objective of the conducted study was to analyze the heat island of a local area around the Vienna UT close to the Inner City of Vienna, Austria, for future implication of mitigation measures through simulation. Urban heat island studies for Vienna have so far concentrated on data from existing weather stations. For this study, the method of mobile traverses was chosen to collect more local data. With a mobile weather station mounted on a bike trailer, data was collected and compared to data from the weather station of the Department of Building Physics (BPI), which is located at the top of Vienna UT at Karlsplatz. For different locations, categories were defined and adequate stops in the area (border of 1., 3. and 4. district) were selected. The collected data was analyzed for a correlation between temperature and environment. The results are discussed in chapter 4.

3.2 Mobile Weather Station

The mobile weather station, as shown in Figure 3.1, was mounted on a bike trailer at a height of about 1.5 m, which is described by Gartland (2008) to be the ideal height to measure urban climate. It consists of a temperature and humidity sensor, a low power anemometer for wind speed (Vector Instruments Type A100L2) and a pyranometer for solar radiation (Skye Instruments), all connected to the same logger (Weatherstation DK-Stat1, Driesen + Kern GmbH). The trailer also carried a tripod for a camera with a compass attached to it. The bike pulling the trailer was furthermore equipped with two bags, which carried extra equipment. In the outmost net bags two Telaire 7001 CO_2 / temperature monitors connected to two Synotech onset HOBO data loggers were placed, one pair of them on each side of the bike to collect CO_2 data. The inner bags carried a Nikon Coolpix 8400 camera with 8.0 Mega pixels featuring a Nikon UR-E16 Fisheye Lens as well as a device for acoustic measurements (Brüel & Kjaer Type 2236).

Figure 3.1: Mobile weather station

The weather station was launched and read out using INFRALOG 301 Software. The measuring and recording intervals were set to 15 seconds. The loggers for the CO_2 measurement were also set to a 15 seconds interval. They were launched and read out using onset GREENLINE Software.

During some cool and rainy days between June 16 and June 21, 2010, the mobile weather station was placed on the roof of the Vienna UT close to the BPI weather station to test its accuracy. Figures 3.2 to 3.5 show the data of that time span compared to the BPI data for temperature, relative humidity, wind speed and solar radiation.

Figure 3.2 indicates that the temperature line of the mobile weather station follows closely the line of the BPI weather station. For relative humidity (Figure 3.3) the values of the mobile weather station tend to be lower sometimes. The biggest differences show the wind speed data pictured in Figure 3.4. The values are constantly lower for the mobile weather station. A possible reason for this is that the mobile weather station was standing at a slightly lower level than the BPI weather station and was surrounded by a rail, which kept some of the wind off. The lower stand is also a possible explanation for the solar radiation values, which follow the

BPI values closely, but are sometimes lower when the BPI weather station might have shaded the mobile weather station (see Figure 3.5). However, the BPI weather station and the mobile weather station generally displayed comparable values. No immense anomalies were found.
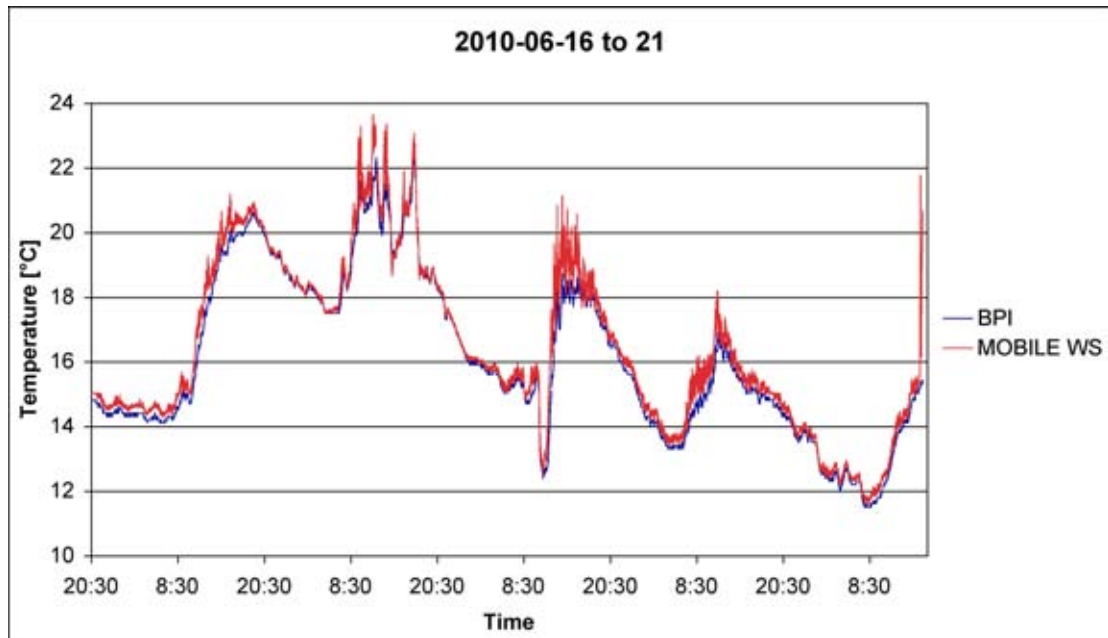
Figure 3.2: Accuracy of temperature measurements
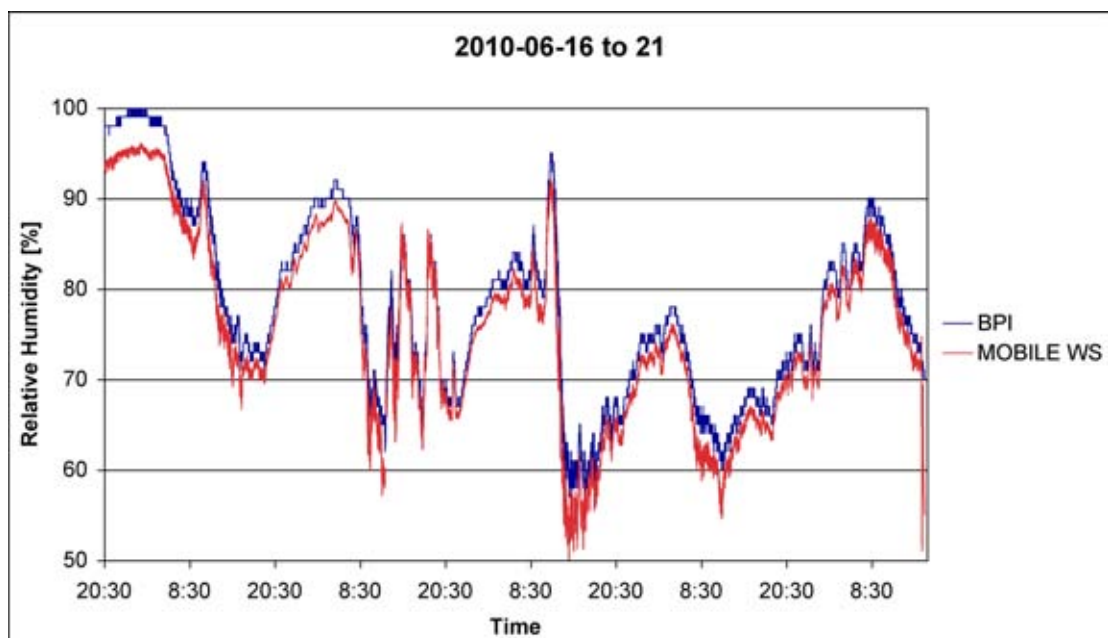
Figure 3.3: Accuracy of relative humidity measurements
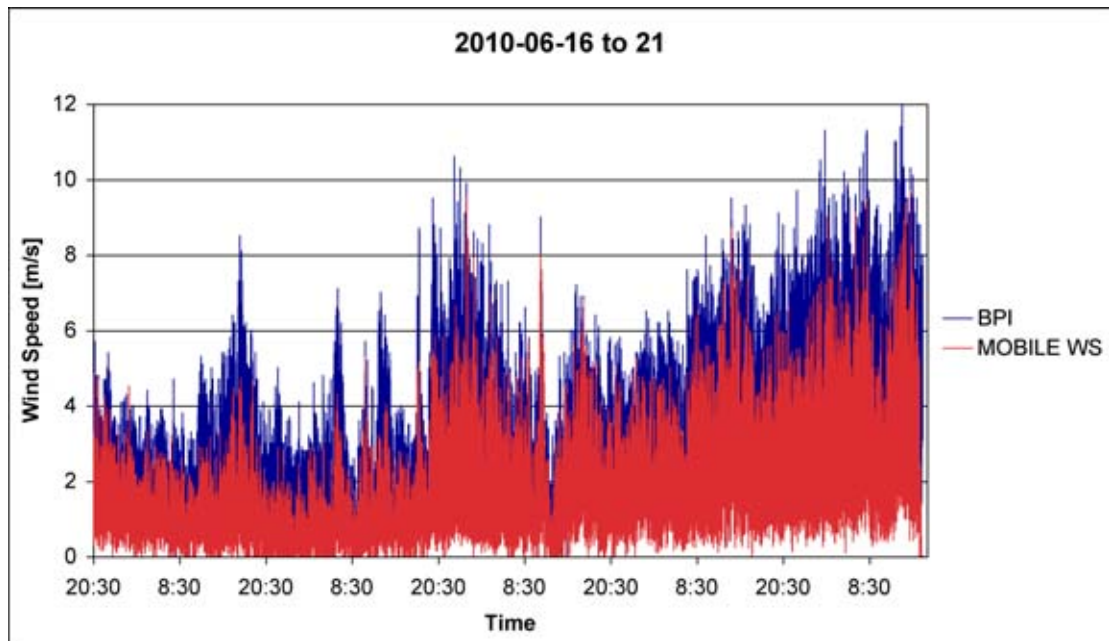
Figure 3.4: Accuracy of wind speed measurements
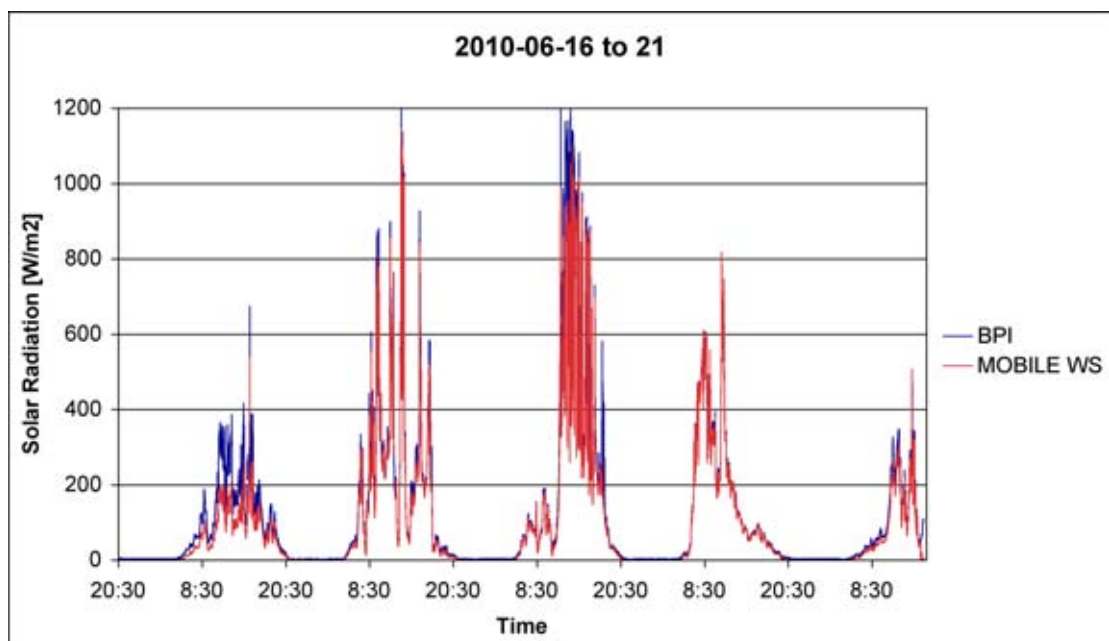
Figure 3.5: Accuracy of solar radiation measurements

3.3 Location Categories and Selected Stops

The categories and corresponding locations described in Table 3.1 were chosen for study. At the beginning the stop Karlsplatz 2 (KP2) was not scheduled, but soon was added to the list. Not every stop was included each time. Sometimes stops had to be left out due to different circumstances. The stop TU2 for example was once closed because of an event. One time measurements had to be stopped after rain set in and another time only half of the stops were done, but extended in time, because data from the BPI weather station was only available in 5-minute intervals for that day.

Table 3.1: Locations and categories

Category	Location	Code
Street without vegetation	Paniglgasse, 1040 Vienna	PAN
Yard without vegetation	Yard of Vienna UT, 1040 Vienna	TU1
Yard with vegetation	Yard of Vienna UT, 1040 Vienna	TU2
Place with vegetation	Karlsplatz, 1040 Vienna	KP1
Place close to water	Karlsplatz, 1040 Vienna	KP2
Place without vegetation	Schwarzenbergplatz, 1010 Vienna	SCH
Alley with heavy traffic	Schubertring, 1010 Vienna	RIN
Park	Stadtpark, 1010 Vienna	ST1
Park close to water	Stadtpark, 1010 Vienna	ST2
Broad street with heavy traffic	Am Heumarkt, 1030 Vienna	HEU
Reference station	Vienna UT, Karlsplatz, 1040 Vienna	BPI

Figure 3.6 shows a satellite image of the positions of the stops, which also gives a rough impression of the surrounding materials and vegetation.

The following Figures 3.7 to 3.16 show the locations and surroundings of the chosen stops.

Figure 3.6: Location of stops (http://wien.gv.at/stadtplan/, modified)

Paniglgasse (PAN) is a small road enclosed by buildings. There is no vegetation nearby. The construction work, which is indicated in Figure 3.7, caused a slight shift in the exact position of the weather station because it has not yet been there when measurements started.

TU1 is a yard of the Vienna UT. There is also no vegetation on-site and all surfaces are sealed (see Figure 3.8).

Figure 3.7: PAN (picture by A. Maleki)   Figure 3.8: TU1 (picture by A. Maleki)

TU2 is the yard next to TU1. It features some trees and not all surfaces are paved as can be seen in Figure 3.9.

Figure 3.9: TU2   Figure 3.10: KP1

Stop Karlsplatz 1 (KP1) at Karlsplatz near the Vienna UT is a mixture of paved surfaces and vegetation (see Figure 3.10). There are some high buildings nearby and at a small distance there is a street with heavy traffic.

Figure 3.11: KP2   Figure 3.12: SCH

KP2, some distance away from KP1, is also located at Karlsplatz in front of Karlskirche and near Vienna UT next to the water basin. Figure 3.11 shows that the surfaces are all paved and that there are some trees further away.

The stop on Schwarzenbergplatz (SCH) was chosen in the middle of the totally paved place next to busy roads and is surrounded by buildings (see Figure 3.12).

Figure 3.13: RIN   Figure 3.14: ST1

The stop RIN as shown in Figure 3.13 is located on Schubertring, a broad alley with heavy traffic enclosed by buildings, which is surrounding the Inner City of Vienna.

ST1 is placed inside Vienna Stadtpark on a paved path surrounded by grass and low vegetation. In some distance there are trees and a large building, which can partly be seen in Figure 3.14.

Figure 3.15: ST2   Figure 3.16: HEU

Location ST2 is situated close to the pond in Stadtpark. As shown in Figure 3.15, there is a small path surrounded by water, grass and trees.

Figure 3.16 pictures the stop on Heumarkt (HEU), a broad street with heavy traffic. In the background parts of Stadtpark can be seen.

3.4 Measurements

The measurements took place during some warm and some hot days in June and July 2010 at different times of the day. For the stops PAN, TU2 and KP1 also long-time measurements from about 2 p.m. to 2 a.m. were conducted. Table 8.1 in the appendix shows the exact times of measurements and stops at each location.

The duration of each stop needed to be at least six minutes as the weather station needed some time to adapt to the circumstances. Figures 3.17 to 3.20 show the delay of the mobile weather station for temperature, relative humidity, wind speed and solar radiation for the test run on June 9, 2010. The weather station was put outside at 19:33 and reached equilibrium with the outdoor values of temperature and humidity about 5 minutes later. For wind speed and solar radiation there is no noticeable delay.
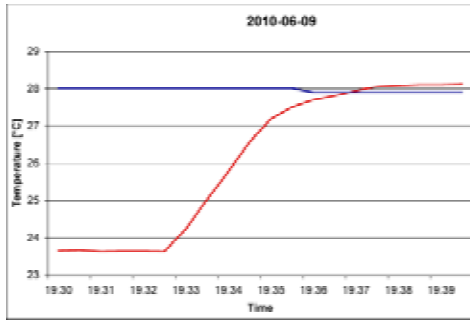
Figure 3.17: Delay temperature   Figure 3.18: Delay relative humidity
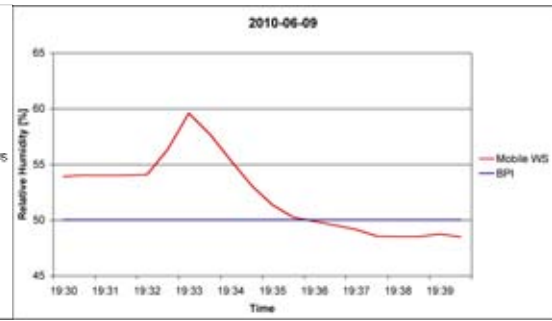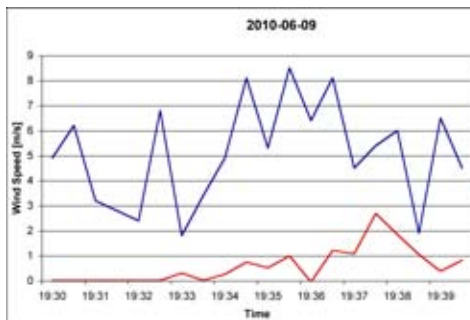
Figure 3.19: Delay wind speed   Figure 3.20: Delay solar radiation
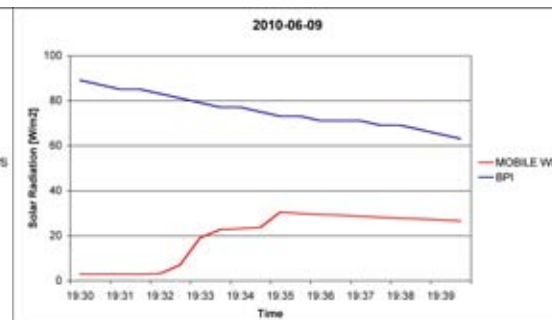
Besides the automatically logged values of temperature, relative humidity, wind speed, solar radiation and CO_2, extra measurements of the acoustic values Leq, L5, L95 and Lmax were carried out at each stop and the values noted in a protocol. Furthermore, a picture of the sky was taken close to the solar radiation measurement for further studies by computational analysis. The acoustic measurements and the computational analysis of the sky images for luminance values are not part of this diploma thesis.

3.5 Data Analysis

To analyze the collected data, the results were compared to the values of BPI weather station, which takes data every second. For the analysis, the values of every 15 seconds were taken, so that the amount of data for BPI weather station and mobile weather station is the same. The data of both stations was then averaged for every minute and the results analyzed and compared graphically. For temperature and relative humidity, the first 5 minutes of every stop were left out to account for the delay of the instruments. For the analysis of wind speed and solar radiation, the first and last minute of every stop were left out, as it is possible that the weather station was still moving.

The analyses include the relative deviation of the measured values from the BPI reference values. The relative deviation is calculated using equation 3.1:

$$D = (x-y) / y * 100 \ [\%] \tag{3.1}$$

D… relative deviation
x… measured value
y… reference value (corresponding BPI value)

Relative humidity and temperature values were used to calculate the absolute humidity. First, the saturation vapour pressure was calculated using equation 3.2:

$$E = 611.2 * exp \ (17.08085 * T / (234.175 + T)) \ [Pa] \tag{3.2}$$

E… saturation vapour pressure
T… temperature in °C

The results were then used to get the vapour pressure with the help of equation 3.3:

$$e = \varphi * E / 100 \ [Pa] \tag{3.3}$$

e… vapour pressure
φ… relative humidity
E… saturation vapour pressure

Finally, the vapour pressure was used to calculate the absolute humidity using equation 3.4:

$$p_w = e / (R * (273.15 + T)) \ [kg/m^3] \tag{3.4}$$

p_w… absolute humidity
e… vapour pressure
R… individual gas constant of water (R = 461.52 [J/kgK]
T… temperature in °C

The results for p_w were multiplied with 1,000 to get g/m^3 instead of kg/m^3.

4 RESULTS

4.1 Overview

This chapter summarizes the results of the data analysis. It is divided into the analysis of the short-time measurements and the analysis of the long-time measurements. Short-time measurements include measurements taking place over a time span of about 6 to 15 minutes for each stop. Long-time measurements were conducted for the stops TU2, KP1 and HEU for about 12 hours in a row. Further results can be found in the appendix.

4.2 Short-time Measurements

The following section shows the results of the mobile weather station compared to the data from the BPI weather station for short-time stops. The values were analyzed for relative deviation and regression. The chronological visualization of the values plotted against the BPI values is given in the appendix.

4.2.1 Relative Deviation

Figure 4.1 pictures the relative deviation of the temperature averaged for all short-time measurements. Zero equates the BPI weather station. In average all places show higher temperatures than the BPI weather station. The hottest locations of the study are the place without vegetation (SCH) and the park (ST1 and ST2), while the coolest places are a street without vegetation (PAN), and the yards TU1 and TU2.
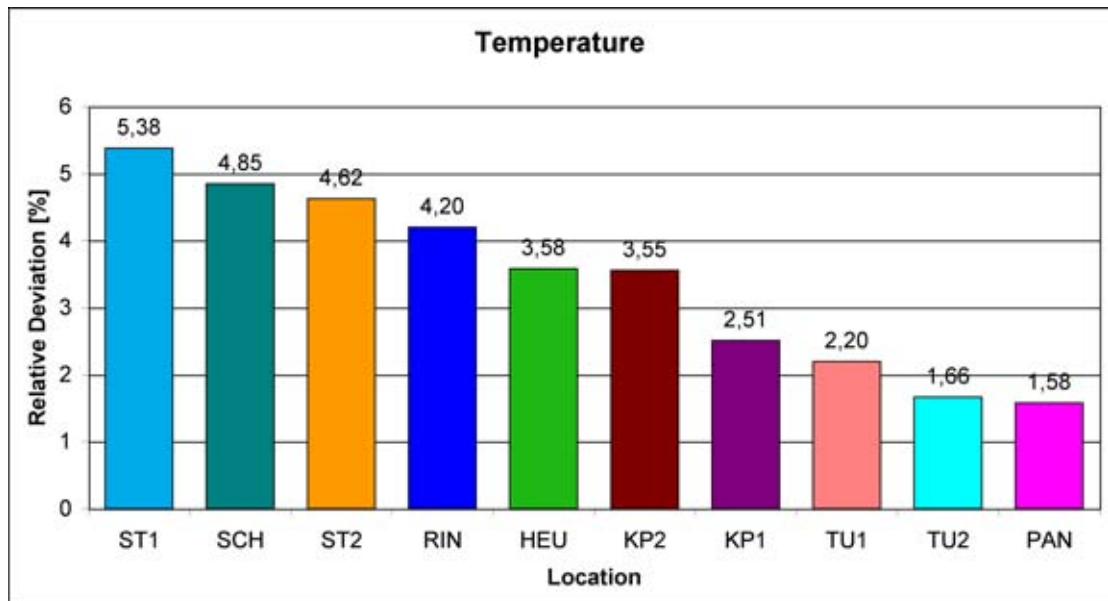
Figure 4.1: Relative deviation of temperature

Figure 4.2 shows the relative deviation of the solar radiation in the same way. All places show lower solar radiation than BPI. From left to right are the hottest to the coolest spots, following the order of Figure 4.1. The cooler locations all have especially low solar radiation values, while hotter locations have higher solar radiations with the exception of SCH and RIN, which will be discussed in chapter 5.
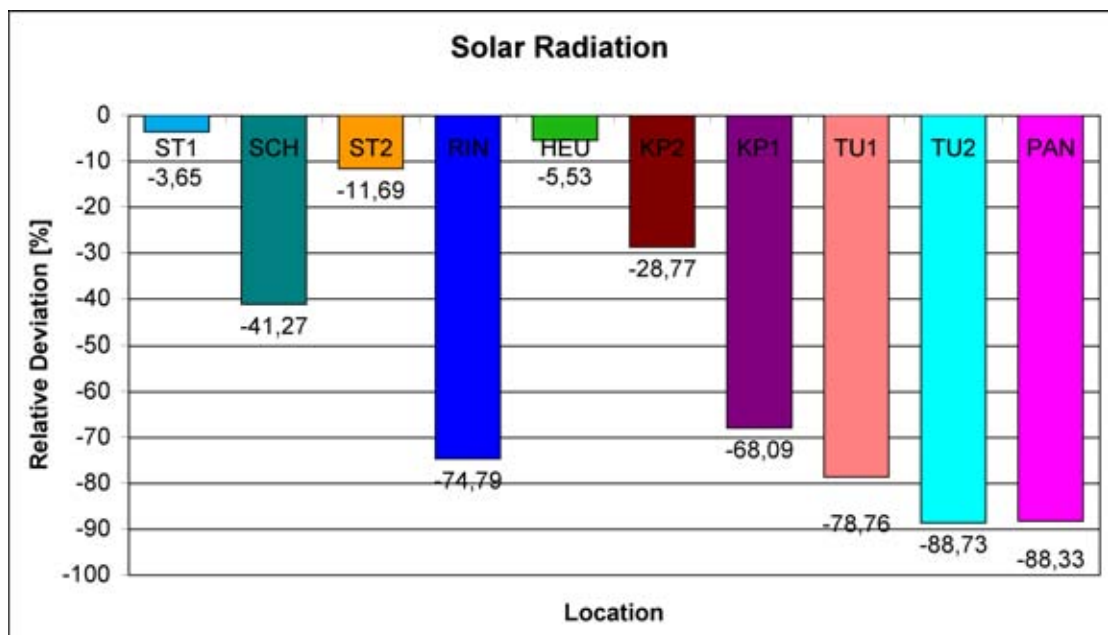
Figure 4.2: Relative deviation of solar radiation

Wind speed for all locations is obviously lower than BPI values as can be seen in Figure 4.3. The windiest spot is HEU, while the yards TU1 and TU2, which are

enclosed by buildings, show very low wind levels. Also the Stadtpark locations are not very windy.
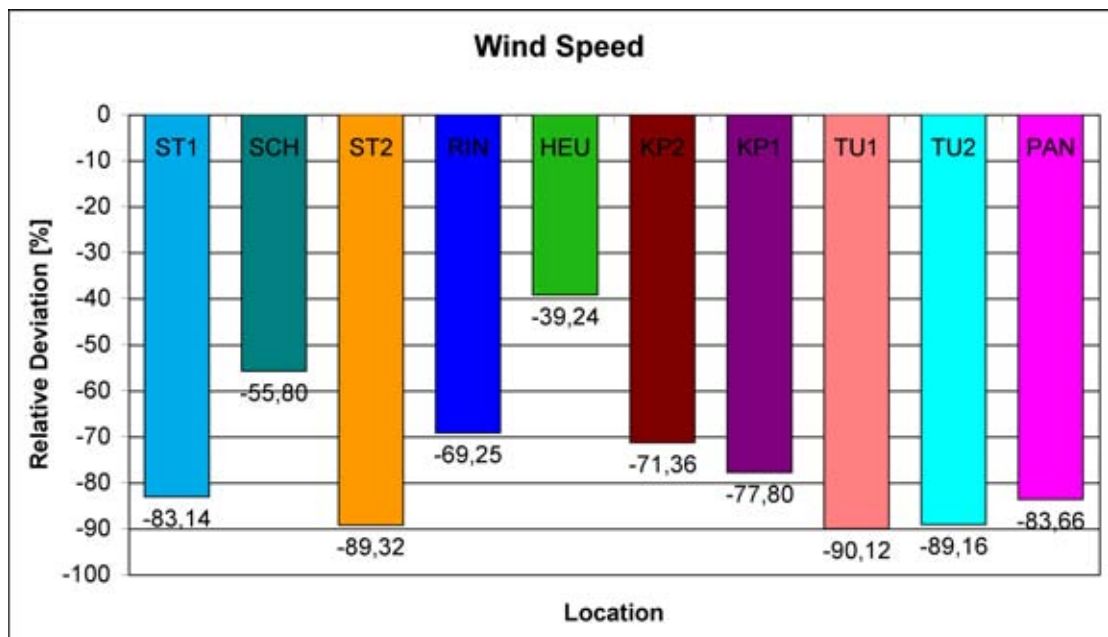
Figure 4.3: Relative deviation of wind speed

As expected, the absolute humidity is highest in places with more vegetation, namely ST1 and ST2 (see Figure 4.4). KP2 also shows higher humidity levels due to the water basin. All other values are lower than the BPI weather station.
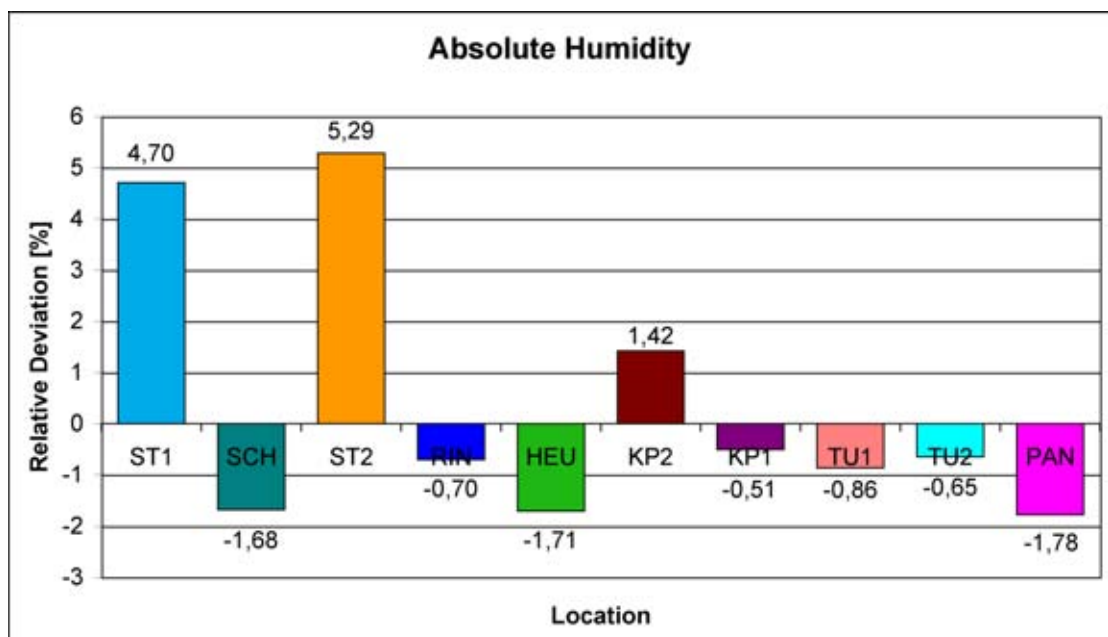
Figure 4.4: Relative deviation of absolute humidity

4.2.2 CO$_2$

Figure 4.5 displays the corresponding CO$_2$ levels for the locations, averaged for all short-time measurements. The streets with lots of traffic naturally have higher levels, while in the park there is less CO$_2$. Also TU1 shows rather high CO$_2$ values, but all in all the differences are not too large.
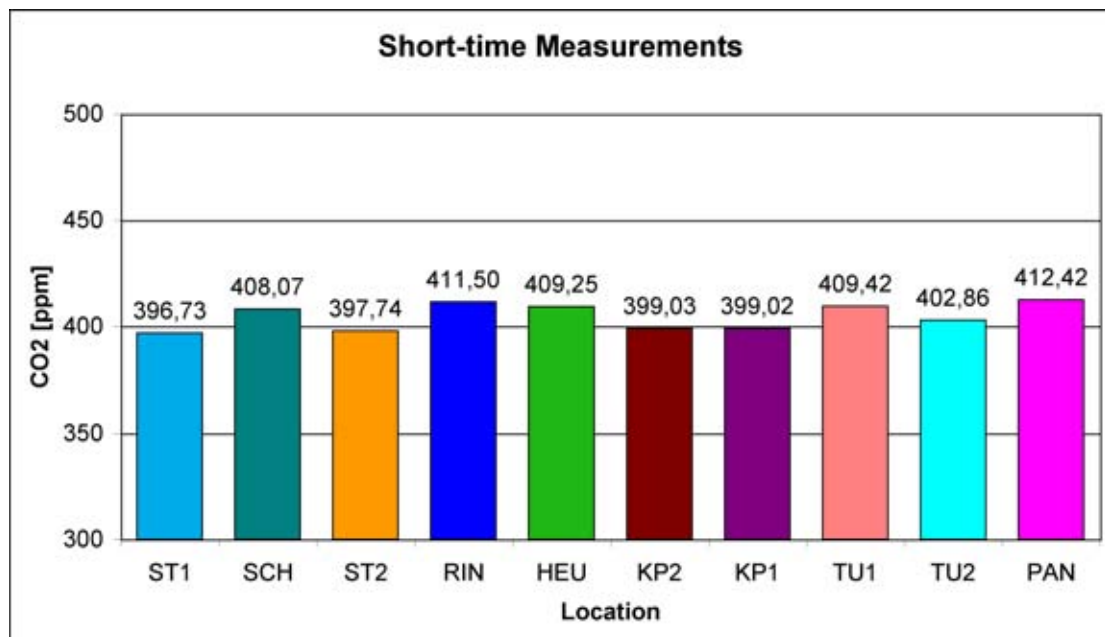
Figure 4.5: CO2 levels

4.2.3 Regression Analysis

The statistical method regression analysis was used to analyze temperature and solar radiation values. The diagrams show the regression line, its function (see equation 4.1) and its certainty.

$$y = k * x + d \tag{4.1}$$

4.2.3.1 Temperature

The regression analysis of the temperature values shows that the locations in general show higher temperatures than the BPI weather station most of the time (see Figures 4.1 to 4.10). Most locations show the same or a slightly lower deviation for higher temperatures while for KP2 the deviation gets higher when the

temperature increases. The locations PAN and TU2 show a tendency to be cooler than the BPI weather station at higher temperatures.
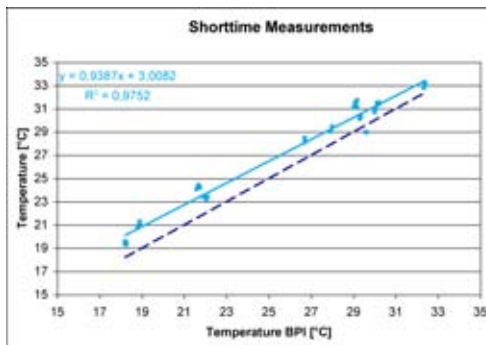
Figure 4.6: ST1
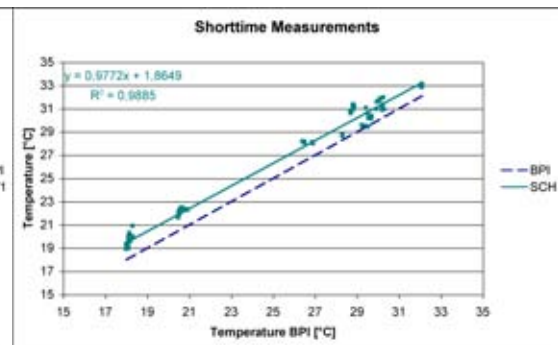
Figure 4.7: SCH
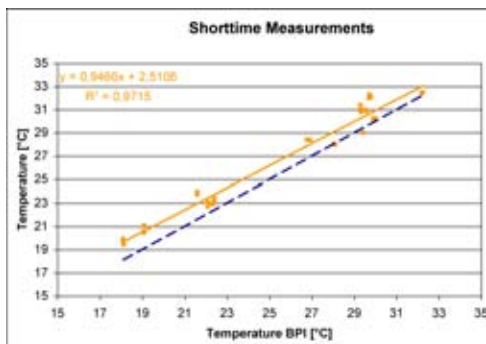
Figure 4.8: ST2
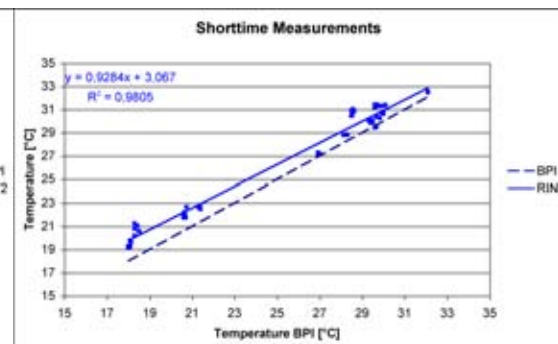
Figure 4.9: RIN
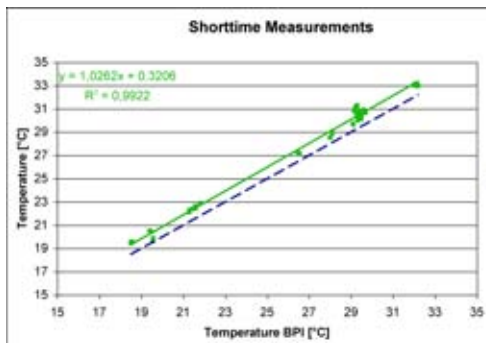
Figure 4.10: HEU
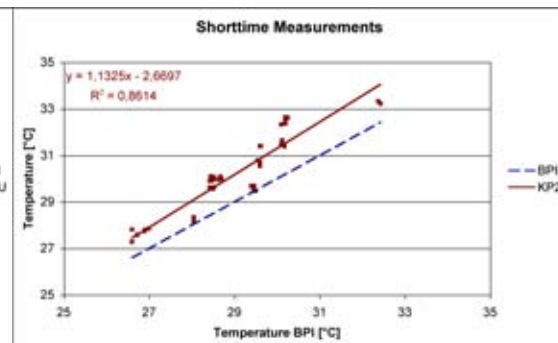
Figure 4.11: KP2
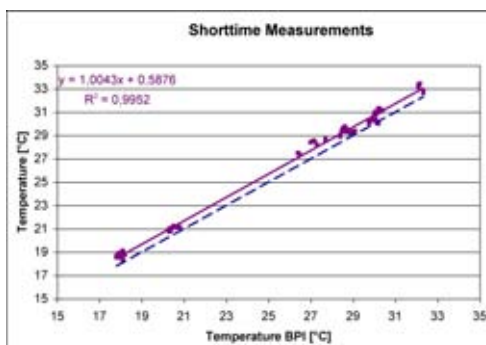
Figure 4.12: KP1
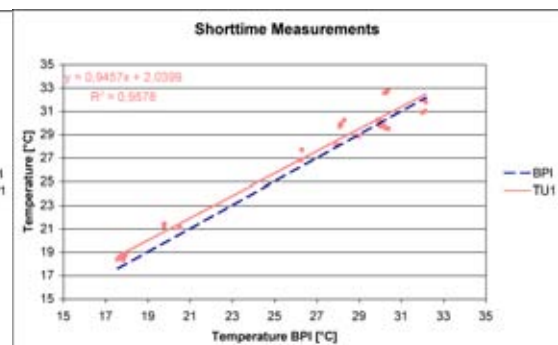
Figure 4.13: TU1
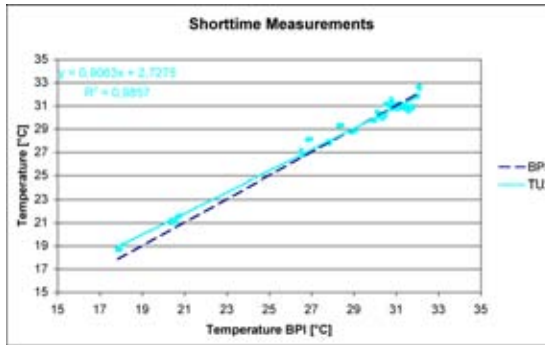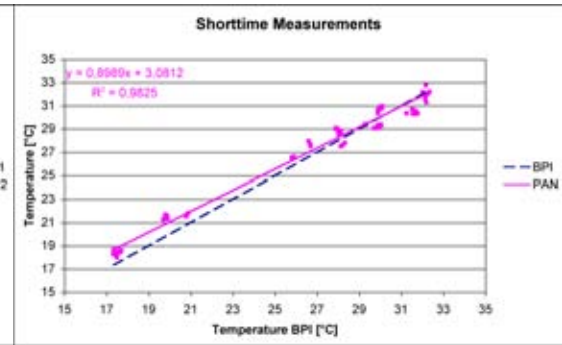
Figure 4.14: TU2   Figure 4.15: PAN

4.2.3.2 Solar Radiation

The solar radiation values of the different locations usually stay below the values of
the BPI weather station. The regression line for each location is shown in Figures
4.16 to 4.25. PAN and TU2 have the lowest values; they are also very low for high
BPI values. SCH and ST1 show a tendency to have higher values than the BPI
weather station for high solar radiation levels, while the HEU line follows the BPI line
quite closely.
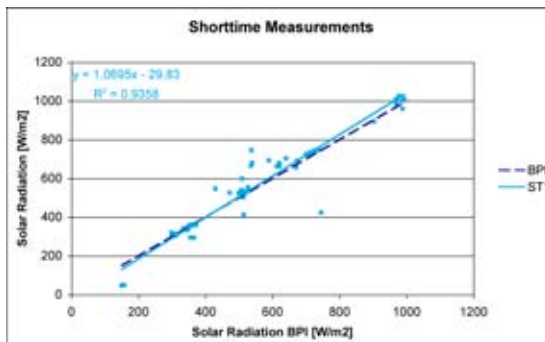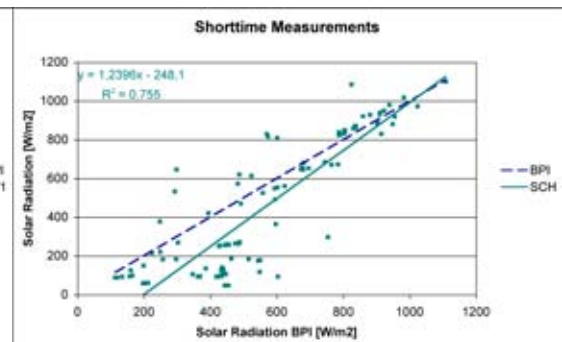
Figure 4.16: ST1   Figure 4.17: SCH
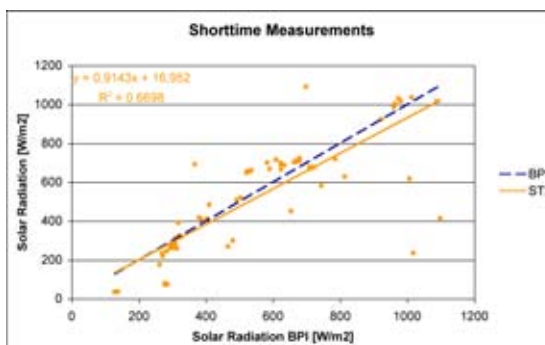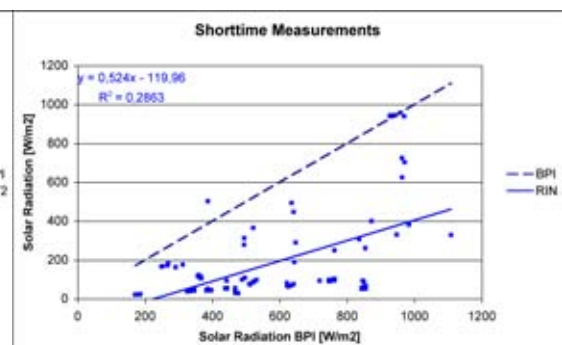
Figure 4.18: ST2   Figure 4.19: RIN
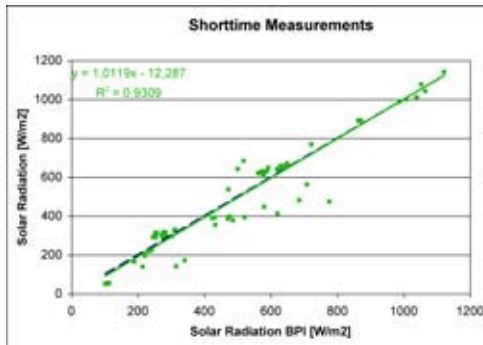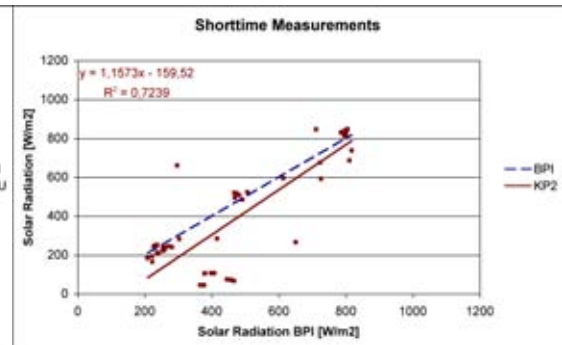
Figure 4.20: HEU   Figure 4.21: KP2
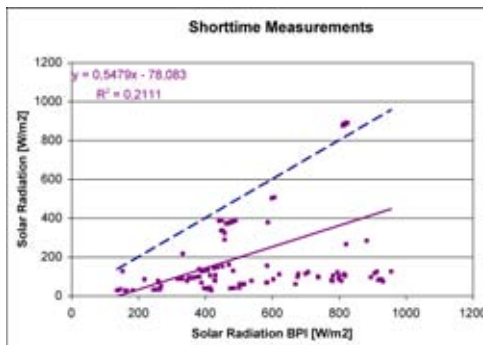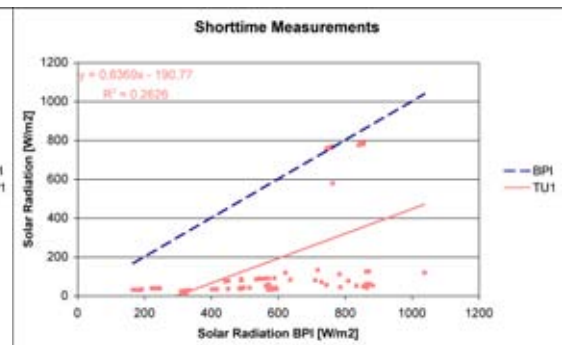
Figure 4.22: KP1   Figure 4.23: TU1
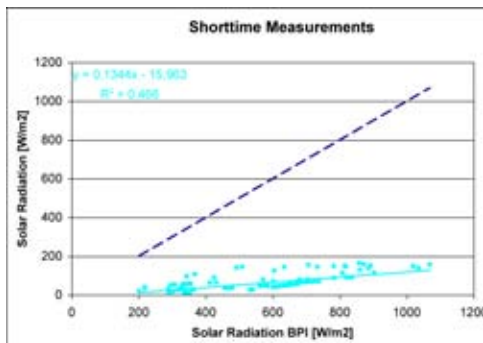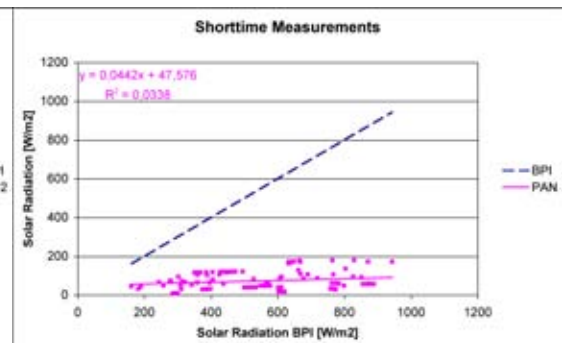
Figure 4.24: TU2   Figure 4.25: PAN

4.3 Long-time Measurements

Long-time measurements show the history of changes in the measured values over a longer time period. Temperature data is shown in Figures 4.26 to 4.29. Figure 4.28 indicates that the location TU2 is cooler during the day, but stays warmer during the night. Another long-time measurement between 7 p.m. and 2 a.m. at TU2 shows the same trend (see Figure 4.29). KP1 values (Figure 4.26) are sometimes slightly higher and sometimes a bit lower, but all in all quite similar to the BPI values, while HEU is obviously hotter all the time as can be seen in Figure 4.27.
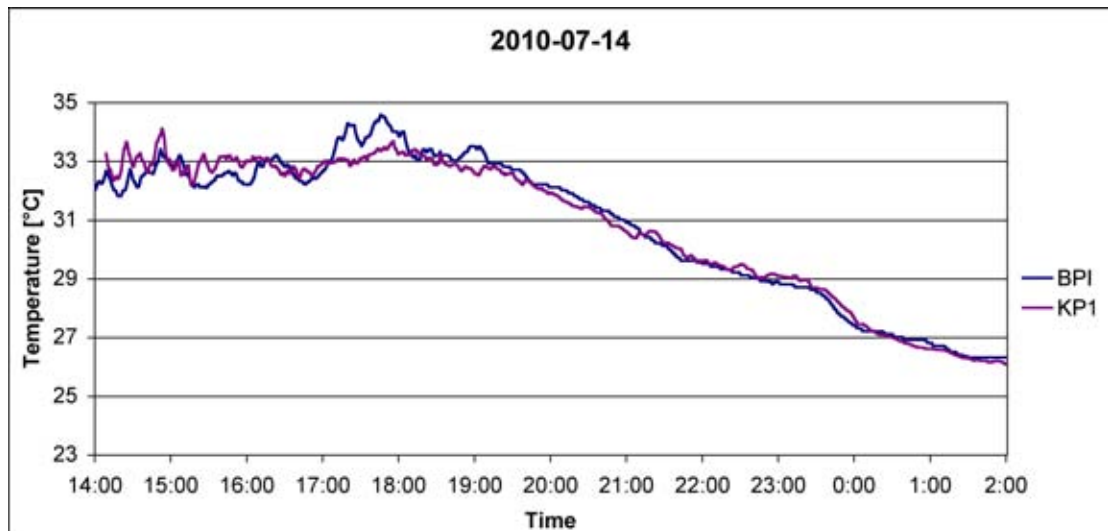
Figure 4.26: Long-time measurements KP1
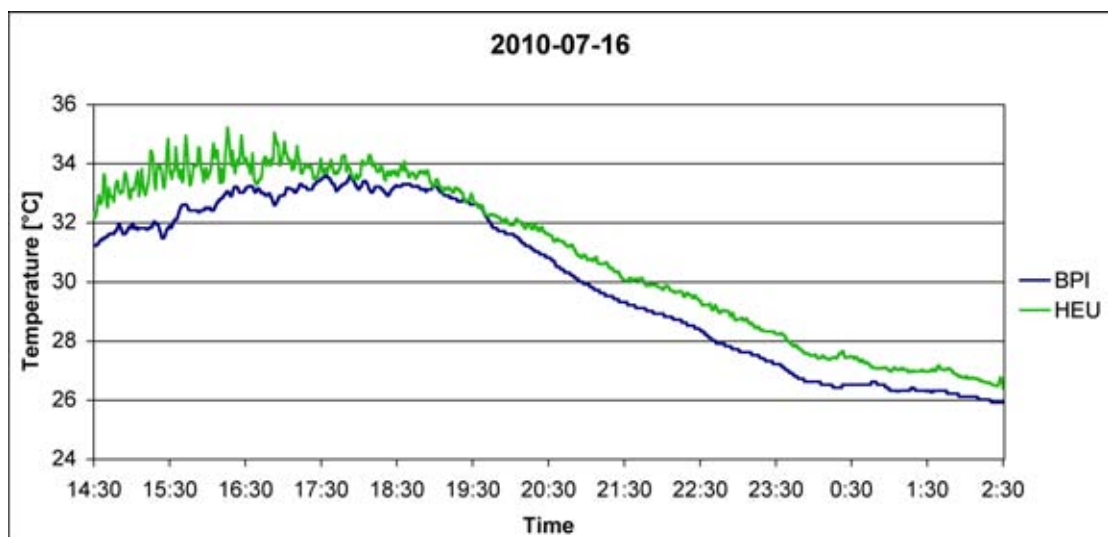
Figure 4.27: Long-time measurements HEU
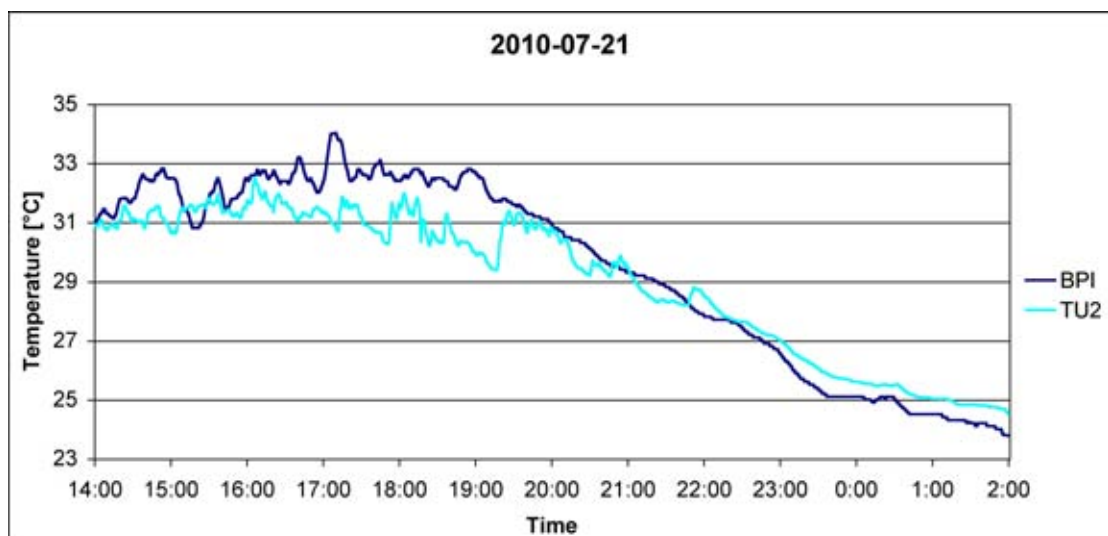
Figure 4.28: Long-time measurements TU2
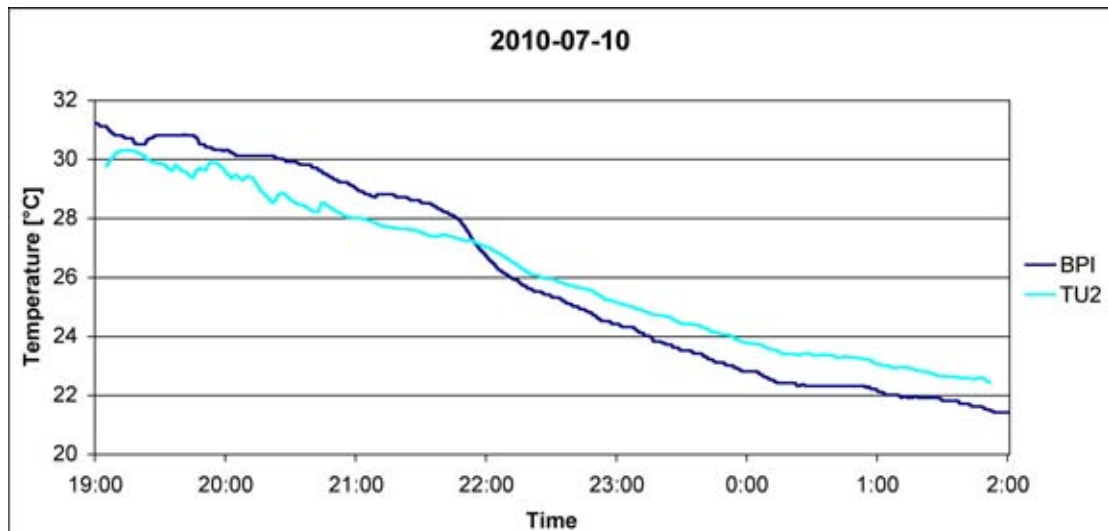
Figure 4.29: Long-time measurements TU2

4.3.1 Relative Deviation

Figure 4.30 combines the averaged relative deviation for temperature, solar radiation, wind speed and absolute humidity of the three long-time measurements in one diagram. It can be seen that the hottest stop (HEU) also has the highest solar radiation levels and wind speeds, while the coolest stop (TU2) has the lowest values.
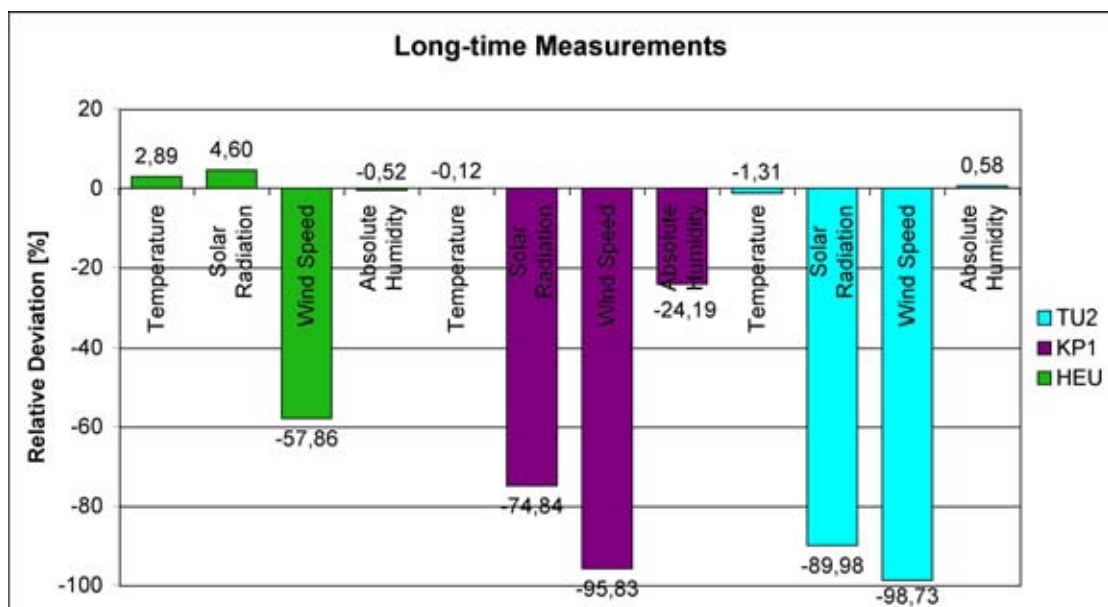
Figure 4.30: Relative deviation of long-time measurements

The variation of the deviation over time can be seen in Figure 4.31 for temperature values, in Figure 4.32 for solar radiation and in Figure 4.33 for wind speed. The

values have been averaged for intervals of 10 minutes. While all three locations show different heating during the day, they all are cooling slowly during the night.
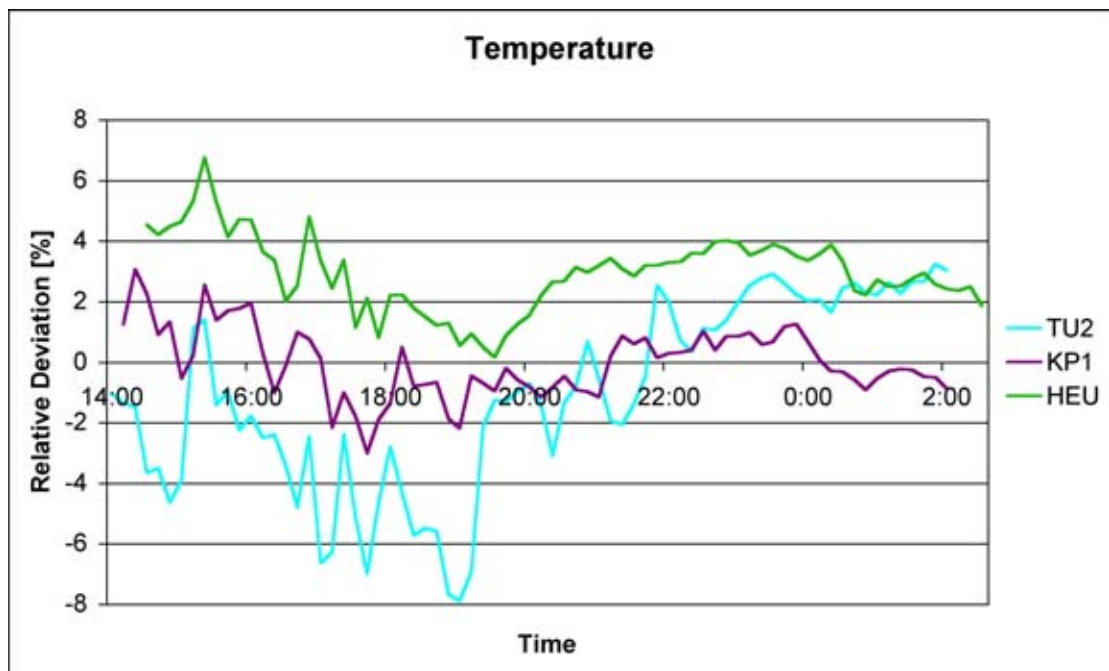
Figure 4.31: Relative deviation of temperature
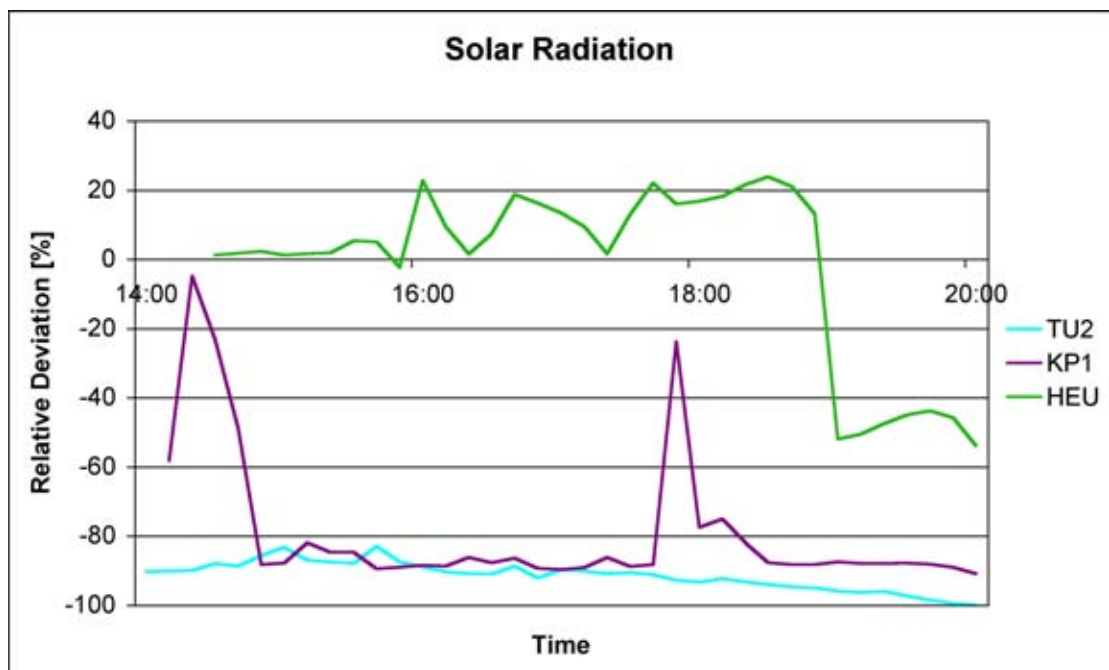
Figure 4.32: Relative deviation of solar radiation
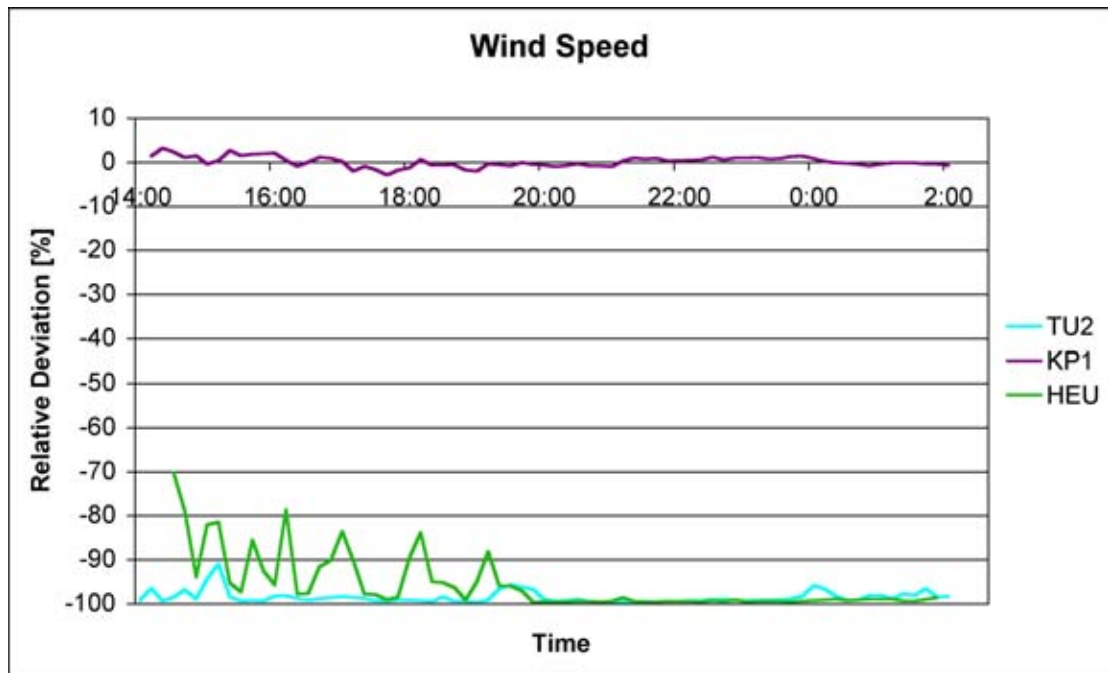
Figure 4.33: Relative deviation of wind speed

4.3.2 CO_2

The averaged CO_2 values shown in Figure 4.34 differ from the short-time measurements where HEU has a higher CO_2 level than KP1. While KP1 here is much higher, TU2 is much lower. HEU stays about the same.
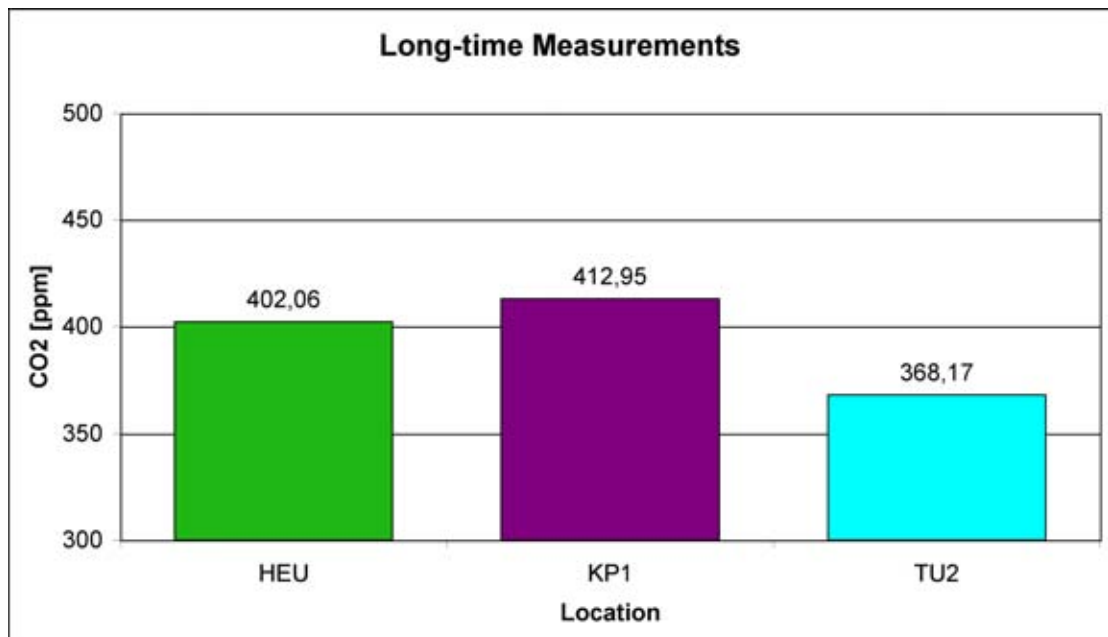
Figure 4.34: CO_2 values

4.3.3 Regression Analysis

The regression analysis for the long-time temperature measurements can be seen in Figures 4.35 to 4.37. It shows similar results as the regression analysis for the short-time measurements for the locations HEU and TU2. The latter also tends to be cooler at higher temperatures over a longer time period. Opposite to the short-time measurements, KP1 follows the BPI values closely and also shows a tendency to be cooler at higher temperatures.
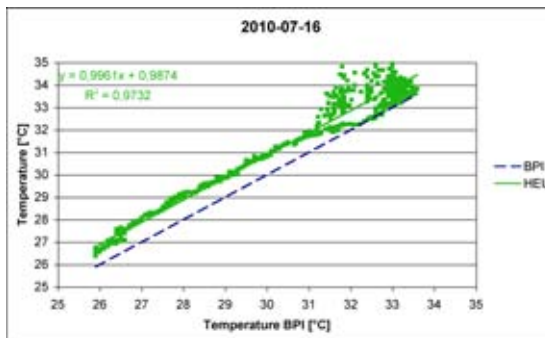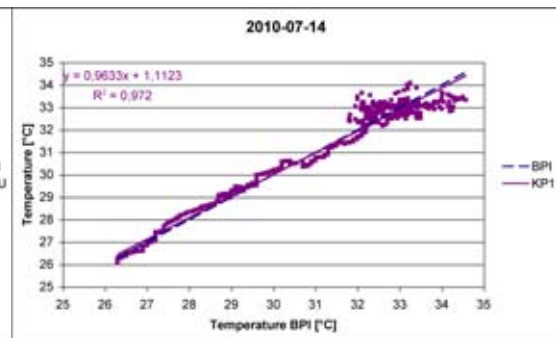
Figure 4.35: HEU   Figure 4.36: KP1
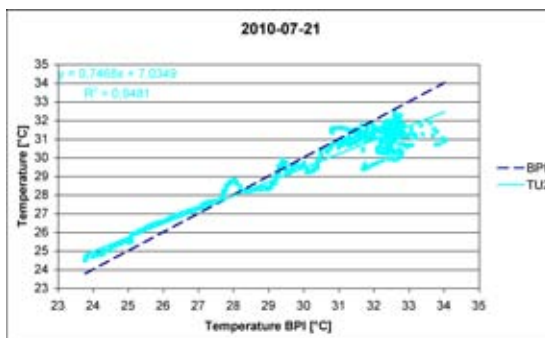
Figure 4.37: TU2

Figures 4.38 to 4.40 show that the results of the solar radiation analysis are similar to the corresponding analyses of short-time measurements.
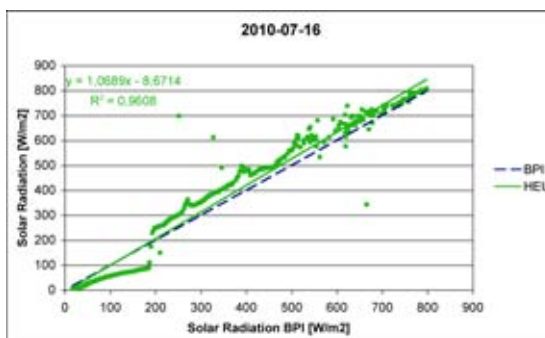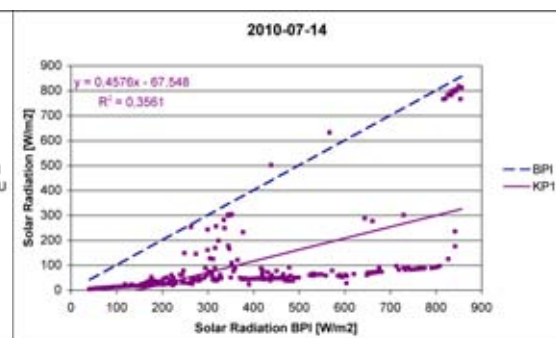
Figure 4.38: HEU   Figure 4.39: KP1
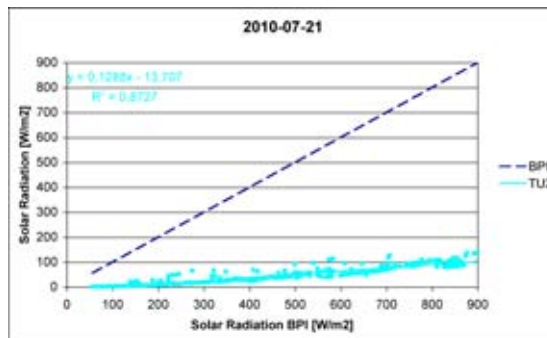
Figure 4.40: TU2

4.4 Analysis of Sky Images

For each location, a fisheye picture of the sky was analyzed manually for the percentage of built environment, vegetation and sky. Table 4.1 summarizes the results. The pictures used for the analysis are attached in the appendix.

Table 4.1: Percentage of built environment, vegetation and sky

Location	Sky [%]	Built environment [%]	Vegetation [%]
ST1	80	<1	20
SCH	75	25	0
ST2	60	<1	40
RIN	50	20	30
HEU	65	35	<1
KP2	85	10	5
KP1	30	20	50
TU1	25	75	0
TU2	25	55	20
PAN	35	65	<1

5 DISCUSSION

5.1 Overview

It is obvious from the results that urban heat islands can vary greatly in small-scale areas. Relative deviation of the temperatures for the locations studied range between minus 1.31 and plus 5.38 % (see Figures 4.1 and 4.30). The following section discusses the correlation of temperature with the local environment and the results for each category. The connection between surroundings and temperature cannot be doubted. The most interesting part in order to find possibilities for efficient UHI mitigation measures are the factors that influence the temperature. The relative deviation of the solar radiation values, displayed in Figure 4.2, shows the trend that more shading leads to lower temperatures, but two obvious exceptions indicate that solar radiation is not the only factor of importance here.

5.2 Park

The hottest overall temperatures during the measurements were recorded at ST1. Located in Stadtpark, expectations were that this is a cooler spot. The analysis of the measured values shows that this at the same time is the place with the highest solar radiation. Most likely the pavement heats up very much during the day and leads to the local high temperatures. Also grass can heat up significantly when it is dry. The high sky view factor is also a reason for the high solar radiation values and high temperatures, but it most likely also leads to faster cooling at night. Unfortunately, no long-time measurements were conducted in Stadtpark yet to prove this. The regression analysis shows a tendency that for higher temperatures the difference to BPI values is a little bit smaller, while solar radiation tends to be even higher at higher BPI values. Wind levels are low, the trees – although further away – seem to keep off some wind that could lead to cooling.

The somewhat cooler, but still high temperatures of ST2, which is closer to trees and sometimes a bit shaded, indicate that the temperature also depends on the type of vegetation nearby. Trees, for example, also cool through shading, while grass can heat up significantly when dry. Here also solar radiation values are quite high, but

show a tendency to be lower than BPI values. Wind speed is even lower than at ST1 and has no big influence on temperature.

As expected, absolute humidity values were high, especially at ST2 close to the pond, while CO_2 values in the park were the lowest.

5.3 Place without Vegetation

The second highest temperatures were measured at Schwarzenbergplatz (SCH), which was to be expected, as the whole place consists of sealed surfaces and is surrounded by buildings. Interesting is that the solar radiation values are quite low, indicating that the place is rather shaded, although its sky view factor is high. A reason for this can be found in the time: most measurements took place after 4 p.m. When looking at the measurements that took place before 4 p.m., solar radiation values are amongst the highest (see Figure 5.1). Later the place gets shaded, but is still hot because the materials on site stored the heat before. Wind speed is a little bit higher than at most other studied locations, but in general all wind speed levels are really low. CO_2 levels are higher here and might also influence temperature, but the differences measured are not so high for all stops.
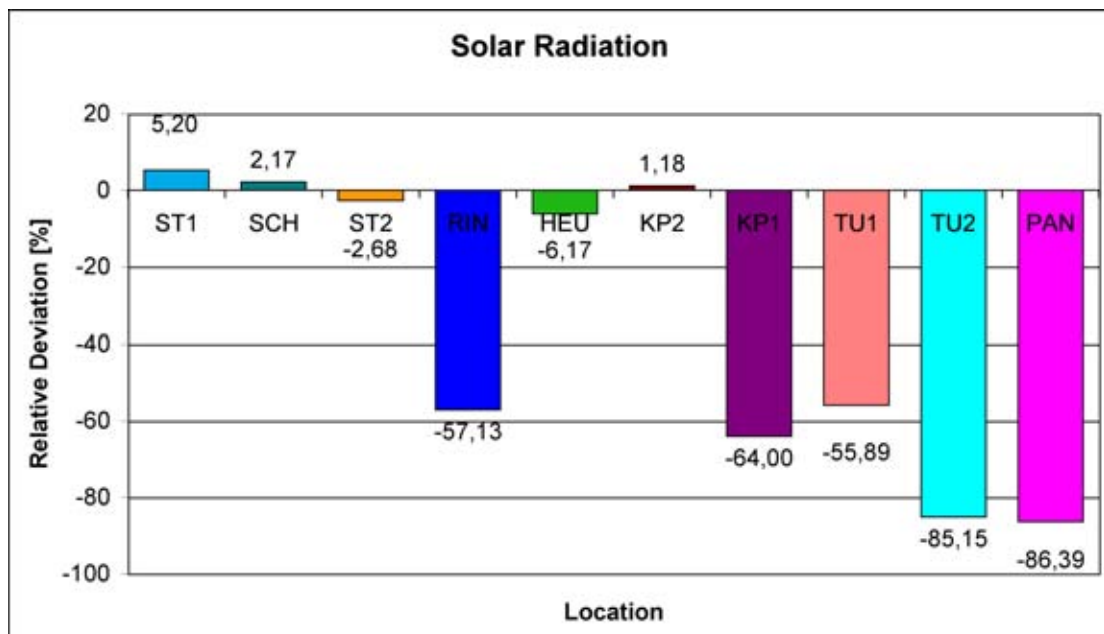
Figure 5.1: Solar radiation before 4 p.m.

5.4 Alley with Heavy Traffic

The stop RIN was also very hot. However, looking at the solar radiation levels, those were always rather low at any time of the day. For measurements before 4 p.m., as shown in Figure 5.1, they were slightly higher and looking at the measurements around midday they were again higher (see Figure 5.2). This suggests that they might be even higher much earlier and that, like at Schwarzenbergplatz, the heat gets stored and released later. Longtime measurements could help solving that question. Furthermore, wind speed levels are really low and the sky view factor is ranging in the middle field of all studied spots. Even though having vegetation this spot is hotter than the non-vegetated street with heavy traffic (HEU), which will be discussed next. CO_2 levels are amongst the highest and may be of influence here, while for HEU the wind plays an important role.
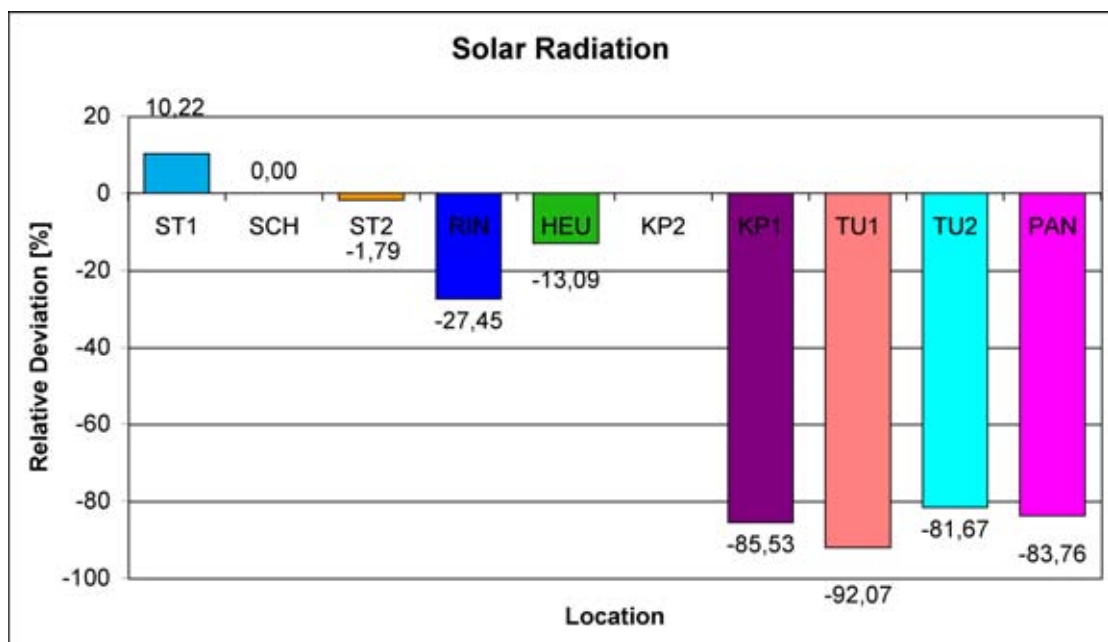
Figure 5.2: Solar radiation levels around midday

5.5 Broad Street with Heavy Traffic

Although having a high sky view factor and high solar radiation values, HEU was not as hot as expected. When looking at the measured values, the higher wind speed levels compared to all other stops are quite obvious. The wind keeps surfaces cooler through convection and most likely balances air temperatures at Heumarkt. Long-time measurements show that HEU still stays hotter than BPI all of the time.

5.6 Place with Vegetation

KP2 shows almost the same average temperature as HEU, but lower solar radiation values, which is also an effect of the times of the measurements. The much higher sky view factor and the sealed surfaces would suggest even higher temperatures, but the water basin is able to store a lot of heat during the day and has a balancing effect on temperatures. Due to the water basin, KP2 also is the only location besides the park that shows higher absolute humidity values than BPI.

5.7 Yards

TU1 and TU2 have about the same sky view factor, but TU1 gets some more solar radiation than TU2 and therefore is slightly hotter. Both tend to be cooler at higher temperatures. TU1 also has rather high CO_2 values potentially contributing to heating, which might be due to a spatial connection with Paniglgasse or emissions from the surrounding labs and bureaus.

Location TU2 turned out to be a cool island during the day, but long-time measurements show that it is a heat island at night. This might not be a problem for a university, but for similar yards in residential buildings as night cooling is an important factor for human comfort during sleep. The low sky view factor, which results in shading and cooler temperatures during the day, also leads to less heat loss at night. Also there is little wind to clear the release of heat.

5.8 Street without Vegetation

PAN indicates that street canyons can also be cool islands and suggests that this depends greatly on the orientation of the street and the urban geometry. Low solar radiation levels at all times indicate that the place is shaded most of the day and never heats up that much in the first place, therefore also not trapping the heat. The regression line shows that it is even cooler at higher temperatures. Unlike HEU it also does not work as a wind tunnel, the wind has almost no influence here.

6 CONCLUSIONS

6.1 Contribution

The study done in this diploma thesis describes first results of the analysis of a local heat island in Vienna, Austria, and the contribution of the local environment to its formation. It shows that there can be large temperature differences within a small area, which are not sufficiently represented by single weather stations. The differences can be attributed to the local environment conditions via several parameters. Most temperature levels can be explained looking at the solar radiation values and the sky view. This indicates that shading and the urban geometry are of great influence. Strong winds can also balance the UHI. CO_2 values showed only little differences, so their contribution was not clear and needs to be studied further. The study shows that it is essential to analyze the local conditions when wanting to implement mitigation measures and also shows tendencies for different categories. The influence of solar radiation and the importance of shading are clearly shown. This is especially interesting for planners facing climate change.

6.2 Future Research

The study will be continued by A. Maleki as part of a Ph.D. thesis at the Department of Building Physics and Building Ecology at the UT Vienna. More measurements will be conducted at different times of day and night and will be analyzed with further methods. The result will be used as a basis for simulation studies of heat island mitigation measures.

7 REFERENCES

7.1 Literature

Alexandri, E. 2008.
Green cities of tomorrow?
From SB07 Lisbon – Sustainable Construction, Materials and Practices: Challenge of the Industry for the New Millenium.
Available from http://www.baufachinformation.de/

Alexandri, E. & Jones, P. 2006.
Sustainable Urban Future in Southern Europe – What about the Heat Island Effect?
ERSA 2006, 46th Congress of European Regional Science Association – Enlargement, Southern Europe and the Mediterranean, Aug 30 – Sept 3 2006, Volos, Greece.

Arnfield, A. J. 2002.
Two decades of urban climate research: a review of turbulence, exchanges of energy and water, and the urban heat island.
International Journal of Climatology, Volume 23, 2003, Pages 1-26.

Auer, I., Böhm R. & Mohnl, H. 1989.
Klima von Wien. Eine anwendungsorientierte Klimatographie.
Magistrat der Stadt Wien, Vienna, Austria.

Brandt, K. 2005.
Mikroklima. Meteorologie in der Nähe des Erdbodens.
Brandt-Verlag, Bonn, Germany.

Cao, X. et al. 2010.
Quantifying the cool island intensity of urban parks using ASTER and IKONOS data.
Landscape and Urban Planning, Volume 96, 2010, Pages 224-231.

Capon, R. & Hacker, J. 2009.
Modelling climate change adaptation measures to reduce overheating risk in existing dwellings.
Building Simulation 2009, Eleventh International IBPSA Conference, July 27-30, 2009, Glasgow, Scotland.

Chai, Y., Ye, J. & Wang, F. 2009.

Modelling technical and economical benefits of three low energy techniques applied to a commercial office building.

Building Simulation 2009, Eleventh International IBPSA Conference, July 27-30, 2009, Glasgow, Scotland.

Crawley, D. B. 2007.

Creating weather files for climate change and urbanization impacts analysis.

Building Simulation 2007, Tenth International IBPSA Conference, September 03-06, 2007, Beijing, China.

Dénes-Béjat, T., Bozonnet, E. & Calmet, I. 2009.

Modelling the global warming effect on indoor temperature peaks and cooling systems consumption.

Building Simulation 2009, Eleventh International IBPSA Conference, July 27-30, 2009, Glasgow, Scotland.

Fahmy, M., Sharples, St. & Eltrapolsi, A. 2009.

Dual stage simulations to study the microclimatic effects of trees on thermal comfort in a residential building, Cairo, Egypt.

Building Simulation 2009, Eleventh International IBPSA Conference, July 27-30, 2009, Glasgow, Scotland.

Gartland, L. 2008.

Heat Islands. Understanding and Mitigating Heat in Urban Areas.

Earthscan, London, Great Britain.

Hamada, S. & Ohta, T. 2010.

Seasonal variations in the cooling effect of urban green areas on surrounding urban areas.

Urban Forestry &Urban Greening, Volume 9, 2010, Pages 15-24.

Hogan, A. W. & Ferrick, M. G. 1998.

Observations in Nonurban Heat Islands.

Journal of Applied Meteorology, Volume 37, Issue 2, February 1998, Pages 232-236.

Kagiya, K. & Ashie, Y. 2009.

National Research Project on Kaze-no-michi for City Planning: Creation of Ventilation Paths of Cool Sea Breeze in Tokyo.

SICCUHI, September 21-23, 2009, Berkeley, California.

Available from http://heatisland2009.lbl.gov/papers.html

Kandya, A. et al. 2009.
An Experimental Study of Mitigating the Urban Heat Island Effect by Novel Applications of Bamboo as a Construction Material.
SICCUHI, September 21-23, 2009, Berkeley, California.
Available from http://heatisland2009.lbl.gov/papers.html

Karlessi, T. et al. 2009.
Thermochromic energy efficient coatings for buildings and urban structures.
SICCUHI, September 21-23, 2009, Berkeley, California.
Available from http://heatisland2009.lbl.gov/papers.html

Kolokotroni, M. & Giridharan, R. 2008.
Urban heat island intensity in London: An investigation of the impact of physical characteristics on changes in outdoor air temperature during summer.
Solar Energy, Volume 82, Issue 11, November 2008, Pages 986-998.

Kolokotsa, D., Psomas, A. & Karapidakis, E. 2009.
Urban heat island in southern Europe: The case study of Hania, Crete.
Solar Energy, Volume 83, Issue 10, October 2009, Pages 1871-1883.

Kuttler, W. 2009.
Klimatologie.
Verlag Ferdinand Schöningh, Paderborn, Germany.

Leinich, V. 2008.
Der Einfluss mikroklimatischer Randbedingungen auf die Prognose der Energieperformance in der Architektur.
Diploma Thesis, Vienna UT, 2008.

Levinson, R. et al. 2009.
A novel technique for the production of cool colored roofing materials.
SICCUHI, September 21-23, 2009, Berkeley, California.
Available from http://heatisland2009.lbl.gov/papers.html

Li, K., Lin, B. & Jiang, D. 2009.
A New Urban Planning Approach for Heat Island Study at the Community Scale.
SICCUHI, September 21-23, 2009, Berkeley, California.
Available from http://heatisland2009.lbl.gov/papers.html

MA 22. 2003.

Stadtklimauntersuchung Wien.

Bearbeitet von Schwab, U. & Steinicke, W., MA 22, Magistrat der Stadt Wien, 2003.

Mallick, R. B., Chen, B.-L. & Bhowmick, S. 2009.

Reduction of Urban Heat Island Effect through Harvest of Heat Energy from Asphalt Pavements.

SICCUHI, September 21-23, 2009, Berkeley, California.

Available from http://heatisland2009.lbl.gov/papers.html

Mascha, Ch. 2006.

Comfort Engineering und der Wille zur Form – Wechselwirkung zwischen Technologie und Gestaltung am Beispiel Haus der Forschung.

From Expertenforum Beton 2006, Klimaddesign – Heizen und Kühlen mit Beton.

Miguet, F. & Groleau, D. 2008.

Urban bioclimatic indicators for urban planers with the software tool SOLENE.

From SB07 Lisbon – Sustainable Construction, Materials and Practices: Challenge of the Industry for the New Millenium.

Available from http://www.baufachinformation.de/

Mills, D. M. & Dr. Kalkstein L. 2009.

Estimating Reduced Heat-Attributable Mortality for an Urban Revegetation Project.

SICCUHI, September 21-23, 2009, Berkeley, California.

Available from http://heatisland2009.lbl.gov/papers.html

Mirzaei, P. A. & Haghighat, F. 2009.

Pedestrian Ventilation System: A Novel Approach to Mitigate Urban Heat Islands.

SICCUHI, September 21-23, 2009, Berkeley, California.

Available from http://heatisland2009.lbl.gov/papers.html

Mirzaei, P. A. & Haghighat, F. 2010.

Approaches to study Urban Heat Island – Abilities and limitations.

Building and Environment, Volume 45, 2010, Pages 2192-2201.

Moriyama, M. & Tanaka, T. 2009.

The Mitigation of UHI Intensity by the Improvement of Land Use Plans in the Urban Central Area: Application to Osaka City, Japan.

SICCUHI, September 21-23, 2009, Berkeley, California.

Available from http://heatisland2009.lbl.gov/papers.html

Nakao, M. et al. 2009.
Continuous Moving Measurement Method for Thermal Environmental Distributions in Streets.
SICCUHI, September 21-23, 2009, Berkeley, California.
Available from http://heatisland2009.lbl.gov/papers.html

Narumi, D., Shigematsu, K. & Shimoda, Y. 2009.
Effect of the Evaporative Cooling Techniques by Spraying Mist Water on Reducing Urban Heat Flux and Saving Energy in Apartment House.
SICCUHI, September 21-23, 2009, Berkeley, California.
Available from http://heatisland2009.lbl.gov/papers.html

Okeil, A. 2010.
A holistic approach to energy efficient building forms.
Energy and Buildings, Volume 42, 2010, Pages 1437-1444.

Peyerl, M. & Krispel, St. 2008.
Sommerliches Überhitzen städtischer Strukturen – helle Betonflächen regulieren.
Expertenforum Beton – hoch belastete Verkehrsflächen, November 2008, Pages 24-30.

Ping et al. 2009.
A Study on the Effictiveness of Heat Mitigating Pavement Coatings in Singapore.
SICCUHI, September 21-23, 2009, Berkeley, California.
Available from http://heatisland2009.lbl.gov/papers.html

Rasheed, A. & Robinson, D. 2009.
Multiscale modelling of urban climate.
Building Simulation 2009, Eleventh International IBPSA Conference, July 27-30, 2009, Glasgow, Scotland.

Rizwan, A.M.; Dennis, Y. C. L. & Liu, Ch. 2007.
A review of the generation, determination and mitigation of Urban Heat Island.
Journal of Environmental Sciences, Volume 20, 2008, Pages 120-128.

Sakai, H. et al. 2009.
Reduction of Reflected Heat of the Sun by Retroreflective Materials.
SICCUHI, September 21-23, 2009, Berkeley, California.
Available from http://heatisland2009.lbl.gov/papers.html

Synnefa, A., Santamouris, M. & Kolokotsa, D. 2009.

Promotion of Cool Roofs in the EU – The Cool Roofs Project.

SICCUHI, September 21-23, 2009, Berkeley, California.

Available from http://heatisland2009.lbl.gov/papers.html

Taha, H. 2009.

Mesoscale and Meso-Urban Meteorological and Photochemical Modeling of Heat Island Mitigation in California: Results and Regulatory Aspects.

SICCUHI, September 21-23, 2009, Berkeley, California.

Available from http://heatisland2009.lbl.gov/papers.html

White, A. & Holmes, M. 2009.

Advanced simulation applications using ROOM.

Building Simulation 2009, Eleventh International IBPSA Conference, July 27-30, 2009, Glasgow, Scotland.

Wong, M.S. et al. 2010.

A simple method for designation of urban ventilation corridors and ist application to urban heat island analysis.

Building and Environment, Volume 45, 2010, Pages 1880-1889.

Yoshida, A. et al. 2009.

Field Measurement on Energy Budget of Isolated Plant Unit.

SICCUHI, September 21-23, 2009, Berkeley, California.

Available from http://heatisland2009.lbl.gov/papers.html

7.2 Internet

Autodesk 2010.   http://www.autodesk.com/ (last visited 08/2010)

ATMET 2010.   http://bridge.atmet.org/users/software.php (last visited 08/2010)

CITYgreen 2010.   http://www.americanforests.org/productsandpubs/citygreen/
                         (last visited 08/2010)

DesignBuilder 2010.   http://www.designbuilder.co.uk/ (last visited 08/2010)

EDSL 2010.   http://www.edsl.net/main/ (last visited 08/2010)

ENVI-met 2010.   http://www.envi-met.com/ (last visited 04/2010)

eQUEST 2010.   http://www.doe2.com/equest/ (last visited 08/2010)

EPFL 2010.   http://leso.epfl.ch/e/research_urbdev_multiscale.html
(last visited 04/2010)

EC 2010.   http://ec.europa.eu/ (last visited 04/2010)

EU-CRC 2010.   http://coolroofs-eu-crc.eu/ (last visited 04/2010)

GRHC 2010.   http://www.greenroofs.org/ (last visited 04/2010)

Heat Island Group 2010. http://eetd.lbl.gov/HeatIsland/ (last visited 04/2010)

HISTALP 2010.   http://www.zamg.ac.at/histalp/ (last visited 04/2010)

IPCC 2010.   http://www.ipcc.ch/ (last visited 04/2010)

i-Tree 2010.   http://www.itreetools.org/ (last visited 08/2010)

MIST 2010.   http://heatislandmitigationtool.com/ (last visited 08/2010)

MM5 2010.   http://www.mmm.ucar.edu/mm5/ (last visited 08/2010)

ORNL 2010.   http://www.ornl.gov/sci/roofs+walls/calculators/index.html
(last visited 08/2010)

RSC 2010.   http://www.roofcalc.com/ (last visited 08/2010)

SBIC 2010.   http://www.sbicouncil.org/displaycommon.cfm?an=
1&subarticlenbr=112 (last visited 08/2010)

SMUD 2010.   https://usage.smud.or/treebenefit/default.aspx
(last visited 08/2010)

SUNtool 2010.   http://www.suntool.net/ (last visited 04/2010)

TRNSYS 2010.   http://sel.me.wisc.edu/trnsys/default.htm (last visited 08/2010)

UN WUP 2009.   http://esa.un.org/unpd/wup/index.htm (last visited 04/2010)

Vienna UT 2010.   http://www.bpi.tuwien.ac.at/ (last visited 08/2010)

WBCSD 2010.   http://www.wbcsd.org/ (last visited 04/2010)

Worldgreenroof 2010.   http://www.worldgreenroof.org/Statistics.html (last visited 08/2010)

7.3 Further information

American Meteorological Society (AMS) Journals online: http://journals.ametsoc.org/

Heat Island Group: http://eetd.lbl.gov/HeatIsland/

International Energy Agency (IEA): http://www.iea.org/

SICCUHI: http://heatisland2009.lbl.gov/papers.html

US EPA: http://www.epa.gov/index.htm

World Energy Outlook: http://www.worldenergyoutlook.org/

World Meteorological Information: http://www.wmo.int/pages/index_en.html

7.4 Tables

Table 2.1:   Concept of countermeasures (Moriyama & Tanaka 2009, p.2)

All other tables made by author.

7.5 Figures

Figure 1.1:   Megatrends to 2050 (WBCSD 2010)

Figure 2.1:   Sketch of an UHI profile (US EPA 2010)

Figure 2.2:   Typical daytime potential temperature profiles (Gartland 2008, p.33)

Figure 2.3:   Typical nighttime potential temperature profiles (Gartland 2008, p.34)

Figure 2.4:   Modification of the PBL by cities (Kuttler 2009, p.201)

Figure 2.5:   Summer and winter UHI trends in Melbourne, Australia (Gartland 2008, p.3)

Figure 2.6:   Temperature contour map of Minneapolis, Minnesota (Gartland 2008, p.5)

Figure 2.7:   Thermal image of Vienna (MA22, 2003, p.1)

Figure 2.8:   Shadows for a RSB optimized for latitude 48.00 in December (Okeil 2010, p. 1439)

Figure 2.9:   Rooftop spraying (Narumi et al. 2009, p.3)

Figure 2.10: Veranda spraying (Narumi et al. 2009, p.3)

Figure 2.11: Spraying to the AC unit (Narumi et al. 2009, p.4)

Figure 2.12: Thermal image of the rooftop (Narumi et al. 2009, p.4)

Figure 2.13: Effects of solar reflectance and thermal emittance (Gartland 2008, p.60)

All other pictures made by author.

8 APPENDIX

8.1 Abbreviations

ABL	Atmospheric Boundary Layer
AC	Air Conditioning
ACC	Asphalt Cement Concrete
ANSI	American National Standard Institute
ASCII	American Standard Code for Information Interchange
ASHRAE	American Society of Heating, Refrigerating and Air Conditioning Engineers
ATMET	ATmospheric, Meteorological, and Environmental Technologies
CAMx	Comprehensive Air quality Model with extensions
CFD	Computational Fluid Dynamics
CIBSE	Chartered Institution of Building Services Engineers
CO_2	Carbon dioxide
CRRC	Cool Roofs Rating Council
DI	Discomfort Index
EC	European Commission
EDSL	Environmental Design Solutions Limited
EPFL	Ecole Polytechnique Fédérale de Lausanne
EU-CRC	European Union Cool Roofs Council
FA	Free Atmosphere
GIS	Geographical Information System
GRHC	Green Roofs for Healthy Cities North America
GPS	Global Positioning System
HVAC	Heating, Ventilating and Air Conditioning
H/W	building height to building width ratio
IBPSA	International Building Performance Simulation Association
IPCC	Intergovernmental Panel on Climate Change
LBNL	Lawrence Berkeley National Laboratory
NIR	Near InfraRed
MIST	Mitigation Impact Screening Tool
ML	Mixing Layer
MM5	Mesoscale Meteorological Model 5
OFP	Ozone Forming Potential
ORNL	Oak Ridge National Laboratory
PBL	Planetary Boundary Layer
PCC	Portland Cement Concrete
PCPC	Portland Cement Pervious Concrete

PVC	PolyVinyl Chloride
PVS	Pedestrian Ventilation System
RAMS	Regional Atmospheric Modeling System
RSB	Residential Solar Block
RSC	Roof Savings Calculator
SBIC	Sustainable Buildings Industry Council
SICCUHI	Second International Conference on Countermeasures to Urban Heat Islands
SL	Surface Layer
SMUD	Sacramento Municipal Utility District
SRI	Solar Reflectance Index
SUN	Sustainable Urban Neighbourhoods
TiO_2	Titanium dioxide
TMY2	Typical Meteorological Year, version 2
TPO	Thermoplastic Polyolefin
TRNSYS	TraNsient Systems Simulation
UBL	Urban Boundary Layer
UCL	Urban Canopy Layer
UCM	Urban Canopy Model
UHI	Urban Heat Island
UML	Urban Mixing Layer
UN WUP	United Nations World Urbanization Prospects
URS	Urban Roughness Sublayer
US DOE	United States Department of Energy
US EPA	United States Environmental Protection Agency
US LEED	United States Leadership in Energy and Environmental Design
UT Vienna	University of Technology Vienna
WBCSD	World Business Council for Sustainable Development
WRF	Weather Research and Forecasting Model
ZAMG	Zentralanstalt für Meteorologie und Geodynamik

8.2 Measurements

Table 8.1 shows the exact dates and times of the measurements and stops at each location.

Table 8.1: Measurements

Date	Start	PAN	TU1	TU2	KP1	KP2	SCH	RIN	ST1	ST2	HEU	End
2010-06-10	16:05	16:09-16:26	16:29-16:42	16:44-16:54	17:00-17:12	×	17:19-17:28	17:34-17:42	17:48-17:57	18:00-18:09	18:18-18:26	18:42
2010-06-11	16:45	16:46-16:56	16:58-17:05	17:06-17:14	17:20-17:29	×	17:35-17:43	17:47-17:55	17:58-18:06	18:09-18:16	18:23-18:32	18:46
2010-06-15	12:28	12:29-12:41	12:43-12:50	12:52-12:59	13:06-13:15	×	13:29-13:42	13:49-13:59	14:05-14:12	14:16-14:26	14:37-14:46	15:02
2010-06-22	10:26	10:27-10:38	10:41-10:47	10:49-10:54	11:02-11:10	×	11:19-11:40	11:44-11:55	12:00-12:08	12:11-12:18	12:28-12:35	12:50
2010-06-23	10:02	10:06-10:17	10:20-10:31	10:32-10:42	10:50-11:03	×	11:14-11:24	11:31-11:42	11:48-11:55	11:59-12:09	12:17-12:25	12:40
2010-06-23	16:00	16:01-16:08	16:10-16:16	16:17-16:25	16:30-16:40	×	16:45-16:52	16:55-17:02	17:04-17:11	17:13-17:19	17:26-17:32	17:44
2010-06-28	16:45	16:46-16:52	16:53-16:59	17:00-17:06	17:10-17:17	17:20-17:27	17:31-17:38	17:42-17:49	17:54-18:00	18:03-18:09	18:16-18:22	18:32
2010-06-29	17:15	17:16-17:23	17:24-17:30	17:31-17:37	17:43-17:54	17:56-18:03	18:07-18:13	18:15-18:22	18:25-18:31	18:33-18:39	18:45-18:52	19:02
2010-06-30	14:00	14:02-14:16	14:18-14:27	14:28-14:37	14:43-14:55	14:58-15:13	15:18-15:30	15:32-15:43	15:46-15:56	15:59-16:08	16:15-16:28	16:45
2010-07-01	16:44	16:45-16:54	16:55-17:01	×	17:06-17:12	17:14-17:20	17:25-17:33	17:37-17:44	17:48-17:54	17:56-18:02	18:0-18:14	18:21
2010-07-02	18:07	18:08-18:15	18:18-18:24	18:24-18:30	18:36-18:44	18:46-18:53	18:56-19:03	19:06-19:13	19:16-19:22	19:25-19:31	19:37-19:44	19:55
2010-07-05	15:37	15:38-15:45	15:47-15:54	15:55-16:02	16:07-16:15	16:17-16:24	16:29-16:35	×	×	×	×	16:42
2010-07-09	16:41	18:31-18:38	18:22-18:28	18:13-18:21	17:51-17:59	18:02-18:10	17:36-17:44	17:27-17:33	17:13-17:20	17:02-17:10	16:48-16:55	18:39
2010-07-10	13:37	15:08-15:18	15:21-15:31	15:32-16:42	14:34-14:50	14:53-15:05	14:20-14:30	14:02-14:16	×	×	13:47-13:56	16:44
2010-07-10	18:56	×	×	19:00-01:52	×	×	×	×	×	×	×	2:00
2010-07-12	16:54	16:56-17:11	17:13-17:28	17:30-17:45	17:51-18:06	18:09-18:24	×	×	×	×	×	18:28
2010-07-14	13:58	×	×	×	14:04-2:00	×	×	×	×	×	×	2:10
2010-07-16	14:16	×	×	×	×	×	×	×	×	×	14:24-02:30	2:45
2010-07-21	11:02	×	×	13:42-02:30	×	×	×	×	×	×	×	2:40

8.2.1 Short-time Measurements

8.2.1.1 Temperature

Figures 8.1 to 8.15 show the measured temperatures for each stop on the different days, compared to the continuous lines of the BPI weather station.
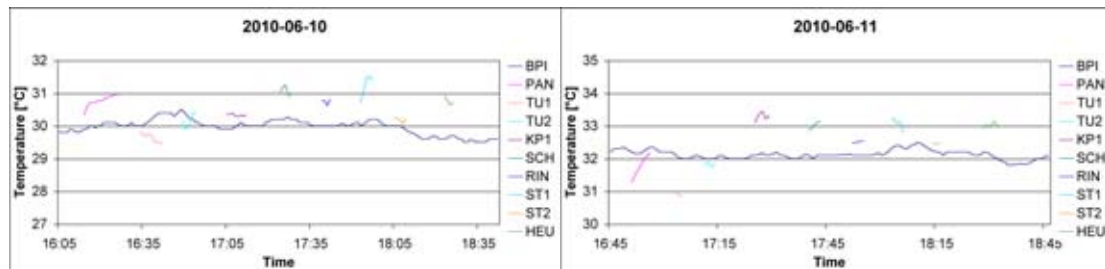
Figure 8.1: Temperature 2010-06-10

Figure 8.2: Temperature 2010-06-11
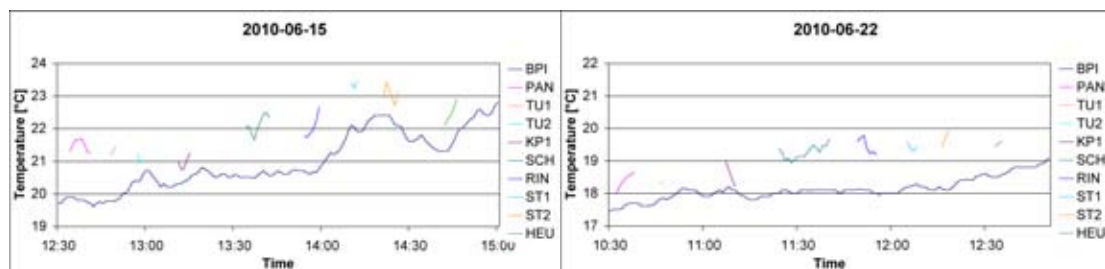
Figure 8.3: Temperature 2010-06-15

Figure 8.4: Temperature 2010-06-22
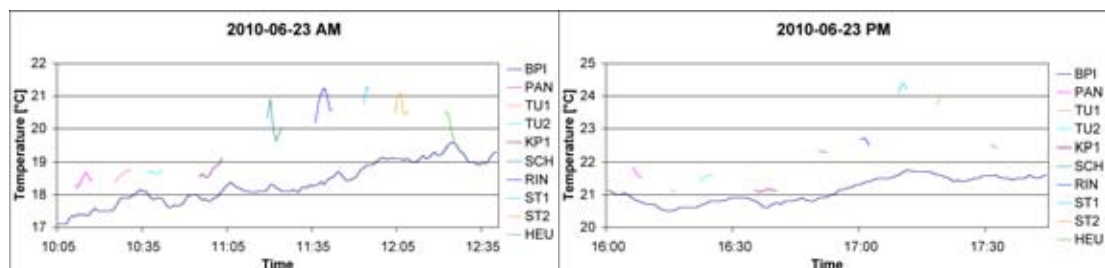
Figure 8.5: Temperature 2010-06-23 a.m.

Figure 8.6: Temperature 2010-06-23 p.m.
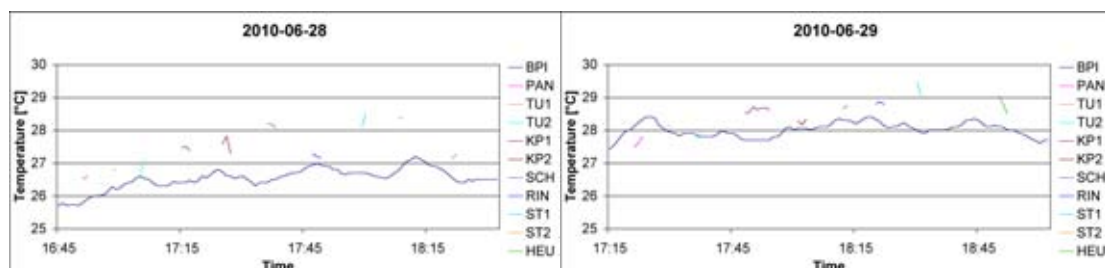
Figure 8.7: Temperature 2010-06-28

Figure 8.8: Temperature 2010-06-29
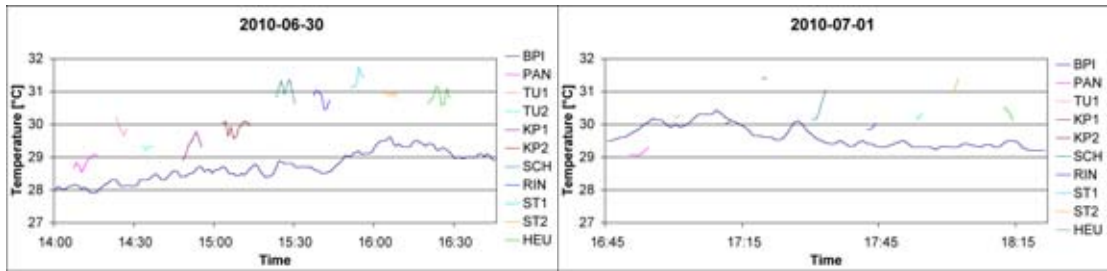
Figure 8.9: Temperature 2010-06-30

Figure 8.10: Temperature 2010-07-01
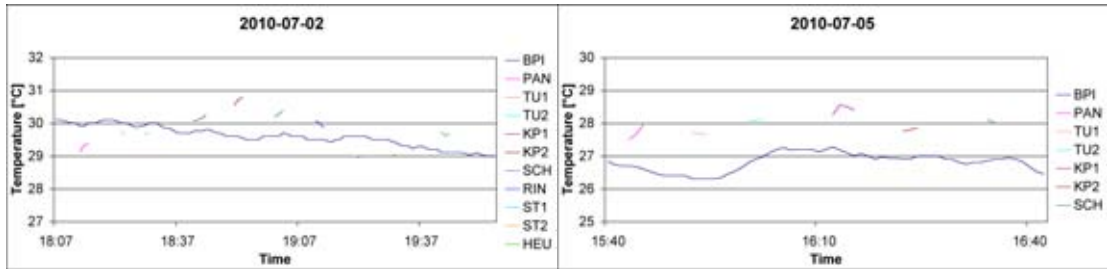
Figure 8.11: Temperature 2010-07-02

Figure 8.12: Temperature 2010-07-05
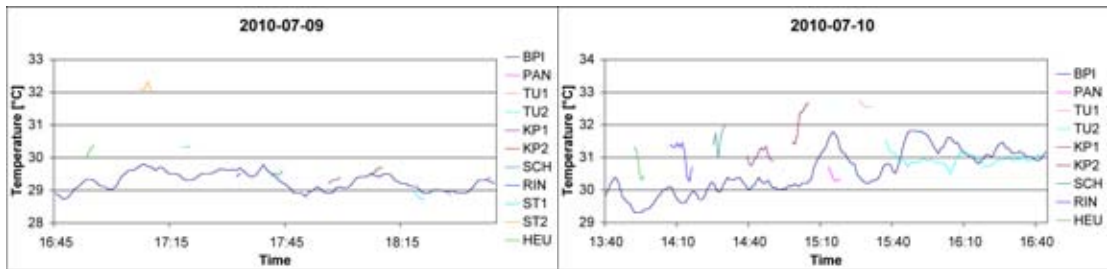
Figure 8.13: Temperature 2010-07-09

Figure 8.14: Temperature 2010-07-10
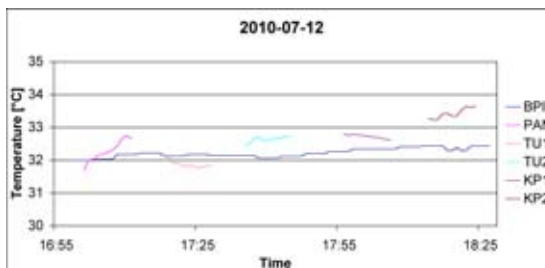
Figure 8.15: Temperature 2010-07-12

8.2.1.2 Solar Radiation

Figures 8.16 to 8.30 show the measured solar radiation values for each stop on the different days, compared to the continuous lines of the BPI weather station.
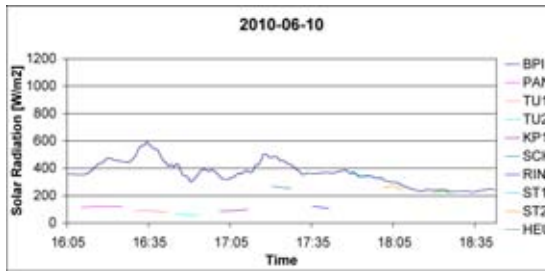
Figure 8.16: Solar radiation 2010-06-10
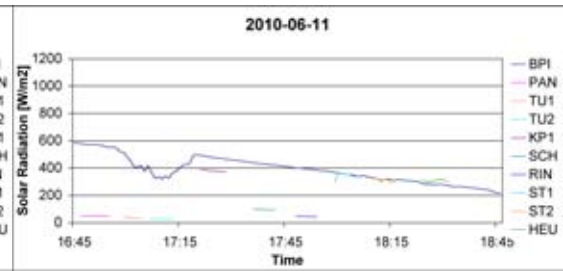
Figure 8.17: Solar radiation 2010-06-11
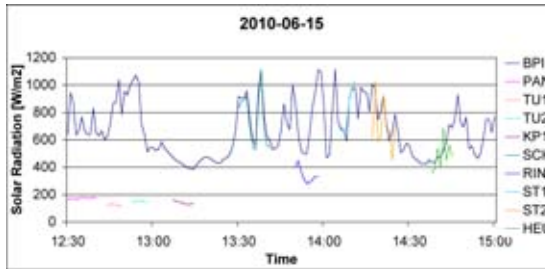
Figure 8.18: Solar radiation 2010-06-15
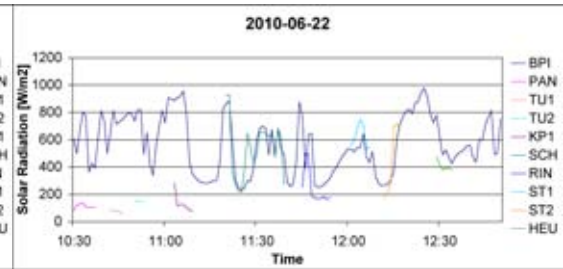
Figure 8.19: Solar radiation 2010-06-22
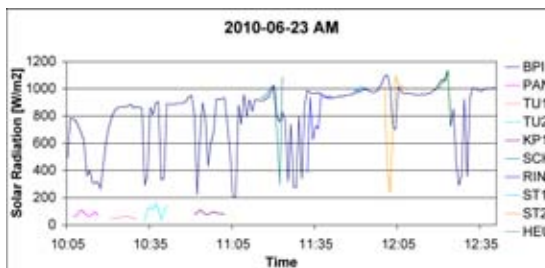
Figure 8.20: Solar radiation 2010-06-23 a.m.
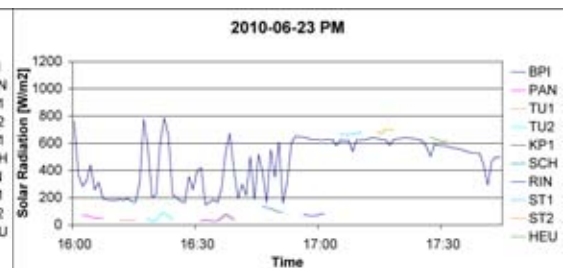
Figure 8.21: Solar radiation 2010-06-23 p.m.
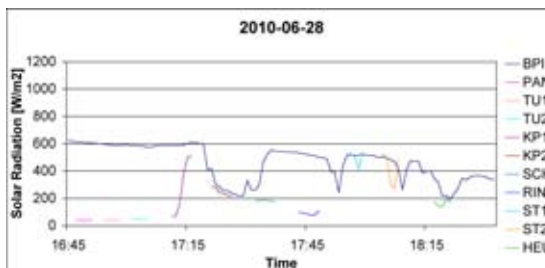
Figure 8.22: Solar radiation 2010-06-28
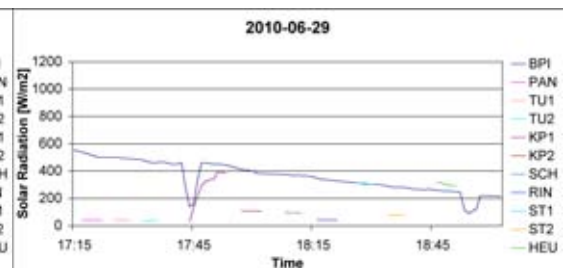
Figure 8.23: Solar radiation 2010-06-29
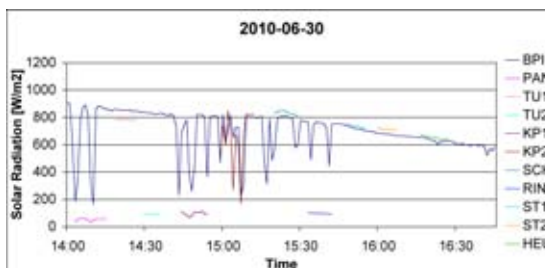
Figure 8.24: Solar radiation 2010-06-30
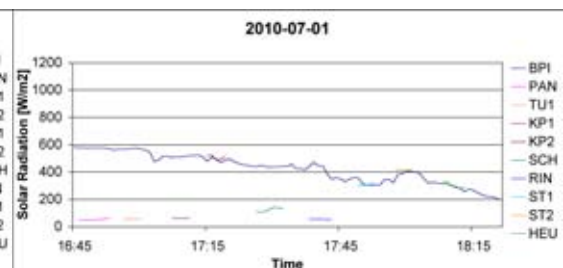
Figure 8.25: Solar radiation 2010-07-01
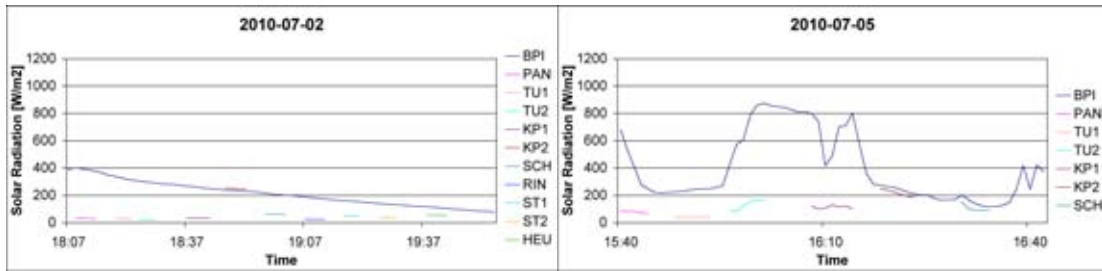
Figure 8.26: Solar radiation 2010-07-02

Figure 8.27: Solar radiation 2010-07-05
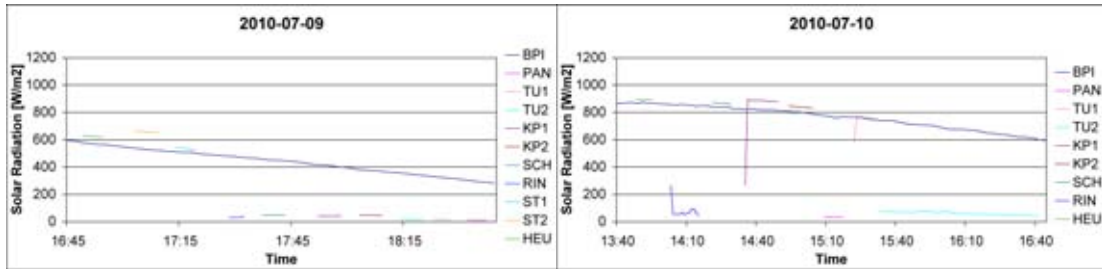
Figure 8.28: Solar radiation 2010-07-09

Figure 8.29: Solar radiation 2010-07-10
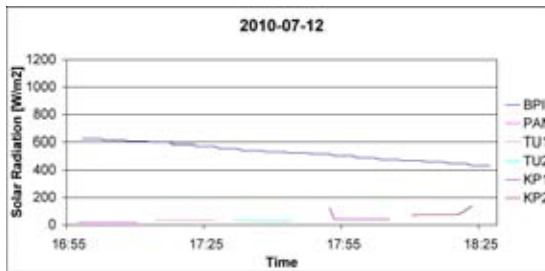
Figure 8.30: Solar radiation 2010-07-12

8.2.1.3 Wind Speed

Figures 8.31 to 8.45 show the measured wind speed for each stop on the different days, compared to the continuous lines of the BPI weather station.
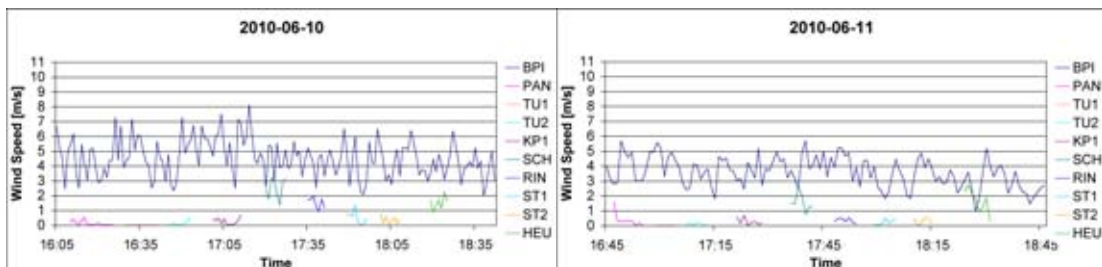
Figure 8.31: Wind speed 2010-06-10
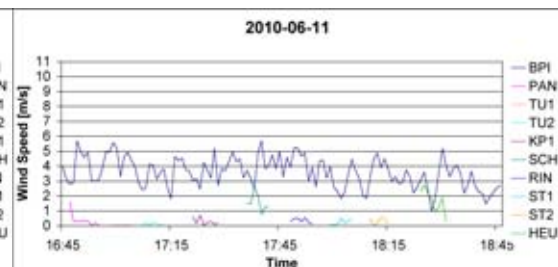
Figure 8.32: Wind speed 2010-06-11
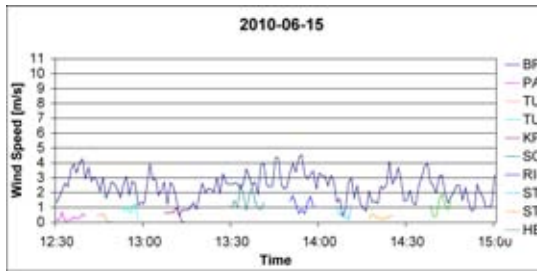
Figure 8.33: Wind speed 2010-06-15
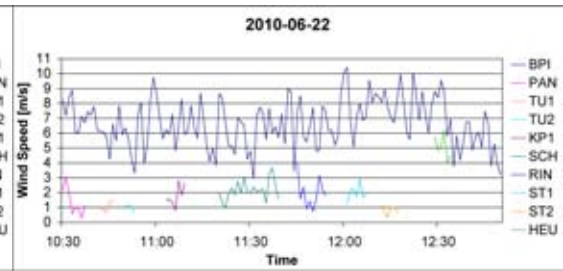
Figure 8.34: Wind speed 2010-06-22
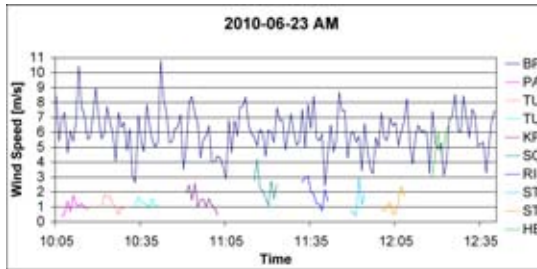
Figure 8.35: Wind speed 2010-06-23 a.m.
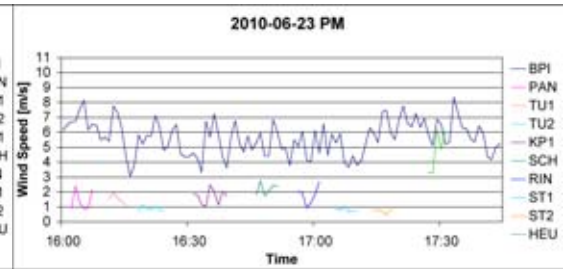
Figure 8.36: Wind speed 2010-06-23 p.m.
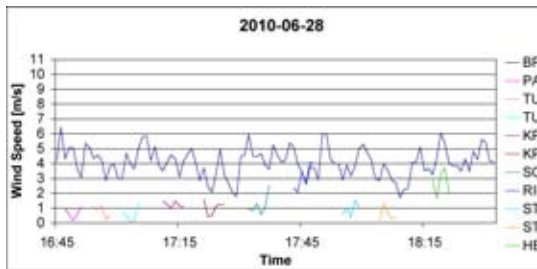
Figure 8.37: Wind speed 2010-06-28
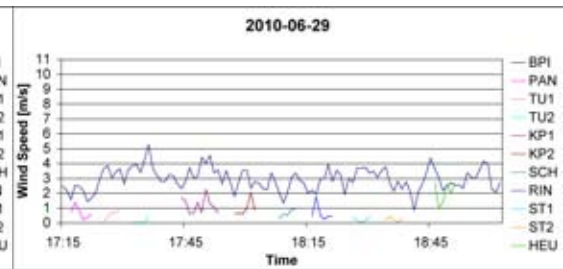
Figure 8.38: Wind speed 2010-06-29
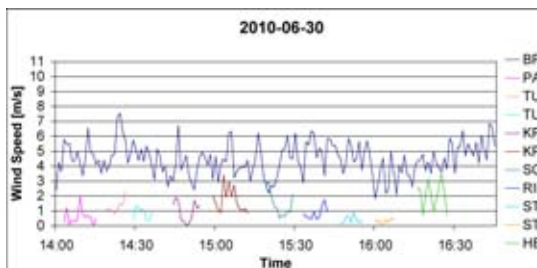
Figure 8.39: Wind speed 2010-06-30
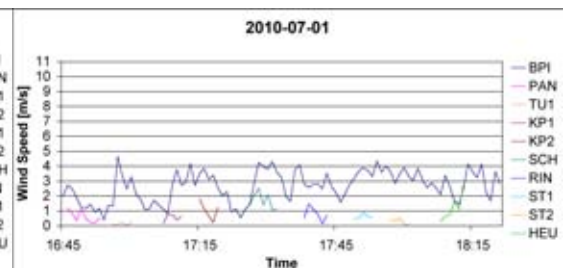
Figure 8.40: Wind speed 2010-07-01
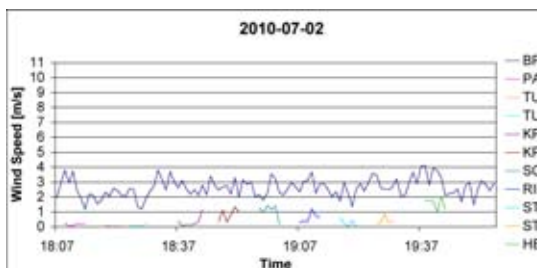
Figure 8.41: Wind speed 2010-07-02
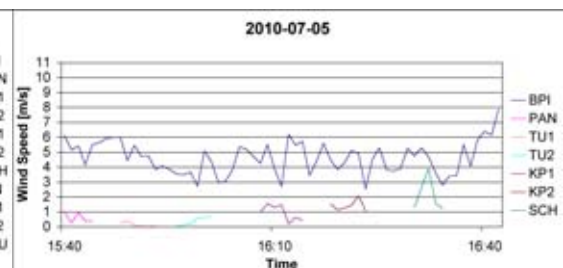
Figure 8.42: Wind speed 2010-07-05
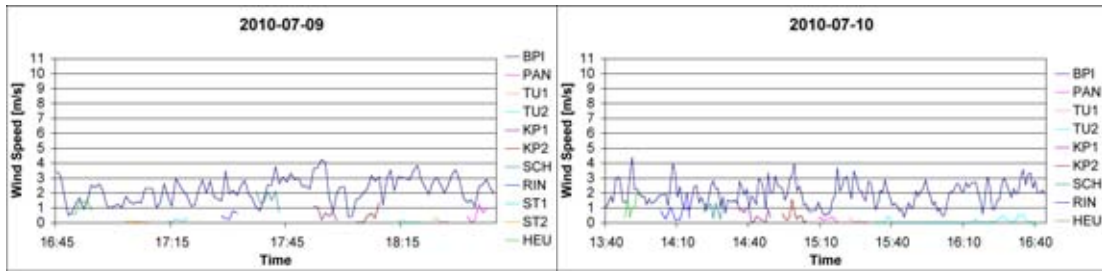
Figure 8.43: Wind speed 2010-07-09

Figure 8.44: Wind speed 2010-07-10
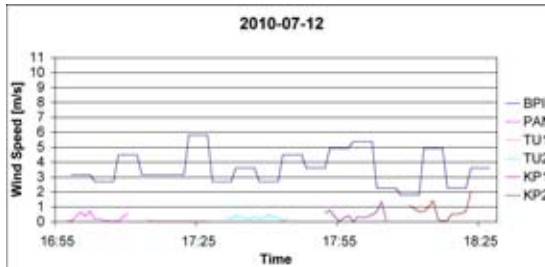
Figure 8.45: Wind speed 2010-07-12

8.2.1.4 Relative Humidity

Figures 8.46 to 8.60 show the measured relative humidity values for each stop on the different days, compared to the continuous lines of the BPI weather station. For analysis, the absolute humidity was calculated from these measured values and the corresponding temperature values.
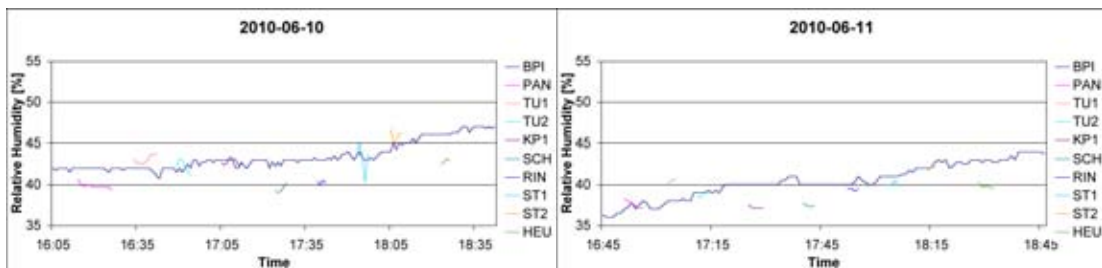
Figure 8.46: Relative humidity 2010-06-10

Figure 8.47: Relative humidity 2010-06-11
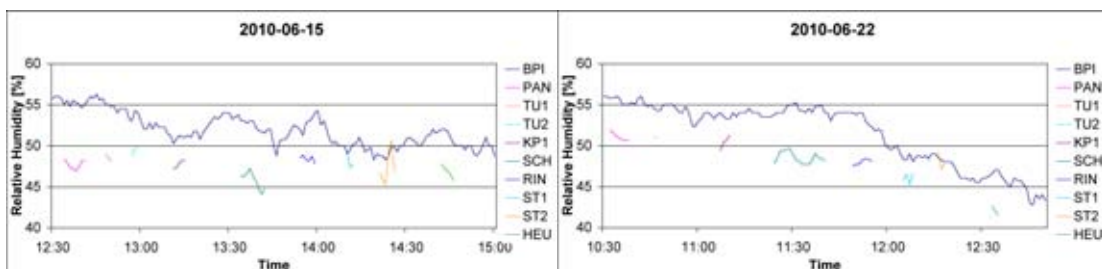
Figure 8.48: Relative humidity 2010-06-15

Figure 8.49: Relative humidity 2010-06-22
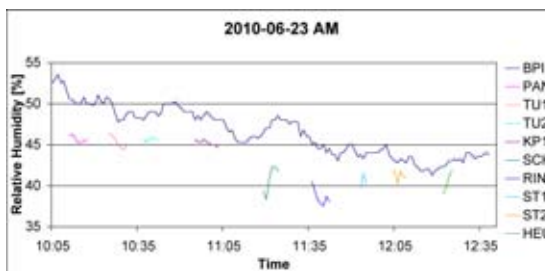
Figure 8.50: Relative humidity 2010-06-23 a.m.
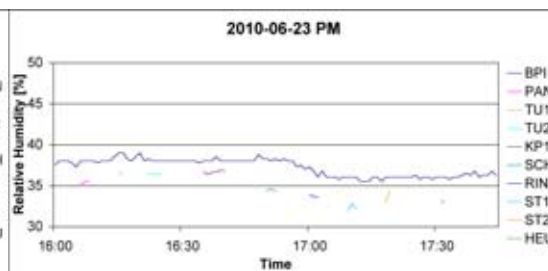
Figure 8.51: Relative humidity 2010-06-23 p.m.
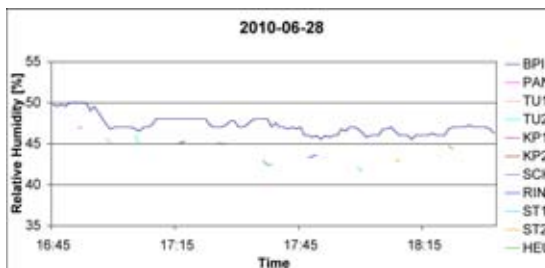
Figure 8.52: Relative humidity 2010-06-28
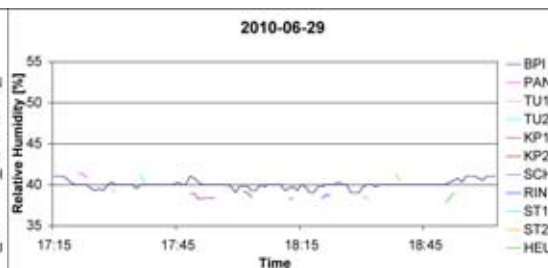
Figure 8.53: Relative humidity 2010-06-29
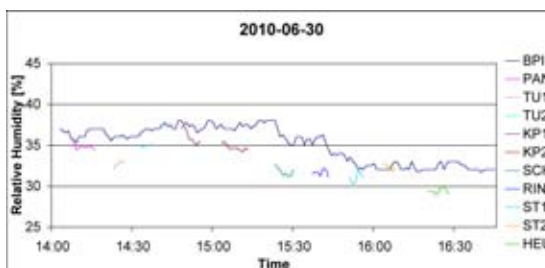
Figure 8.54: Relative humidity 2010-06-30
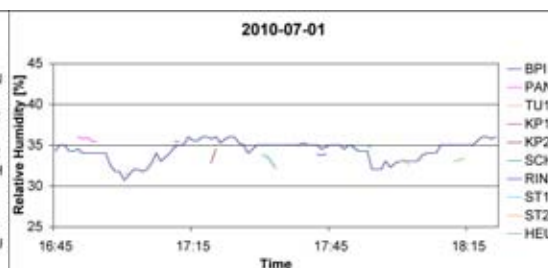
Figure 8.55: Relative humidity 2010-07-01
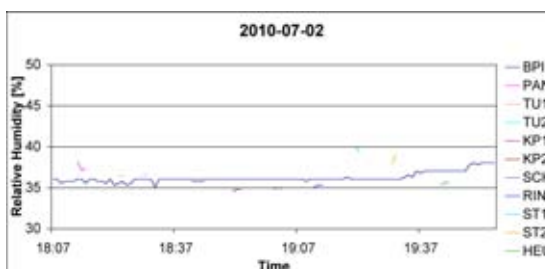
Figure 8.56: Relative humidity 2010-07-02
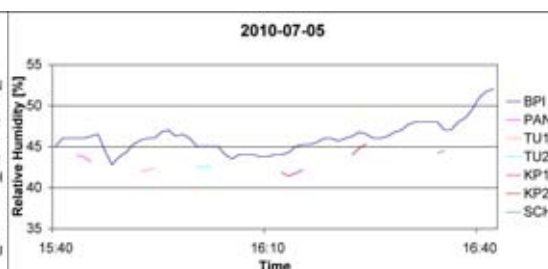
Figure 8.57: Relative humidity 2010-07-05
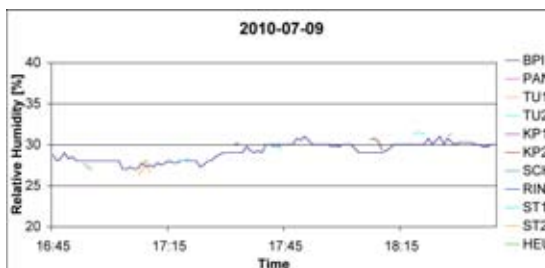
Figure 8.58: Relative humidity 2010-07-09
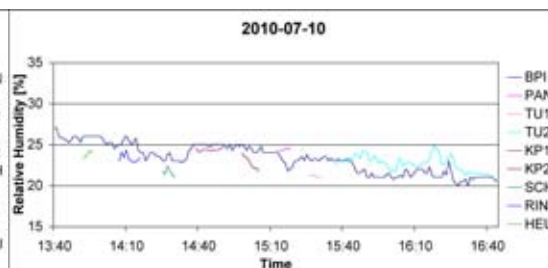
Figure 8.59: Relative humidity 2010-07-10
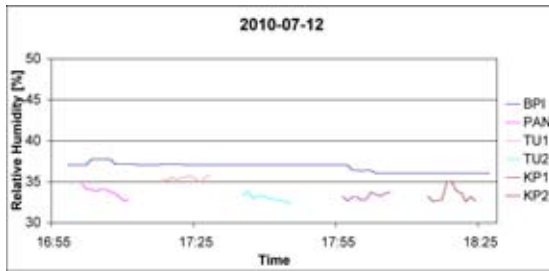
Figure 8.60: Relative humidity 2010-07-12

8.2.1.5 CO₂

Figures 8.61 to 8.75 show the measured CO_2 values for each measurement day. There were two measurement tools, called _201 and _202 here, to account for eventual measurement problems. Sometimes only one of them worked properly, which is the reason why there are not always two resulting lines.
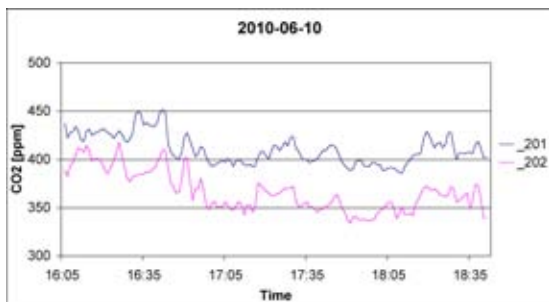
Figure 8.61: CO₂ 2010-06-10
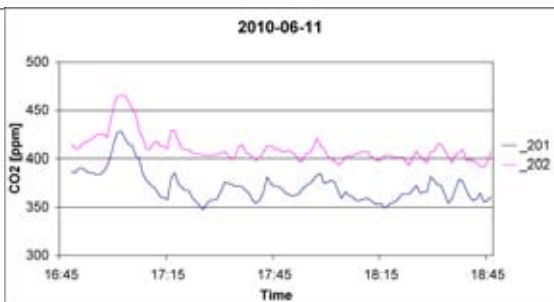
Figure 8.62: CO₂ 2010-06-11
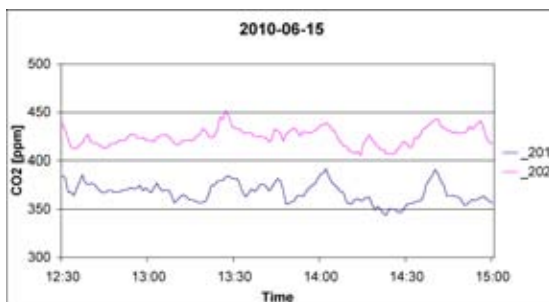
Figure 8.63: CO₂ 2010-06-15
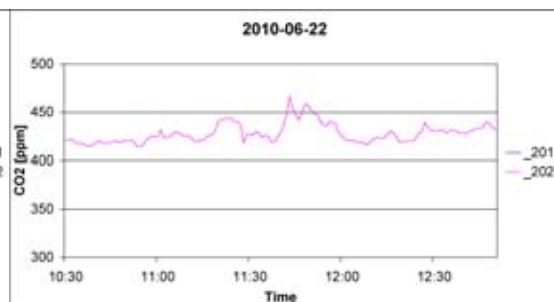
Figure 8.64: CO₂ 2010-06-22
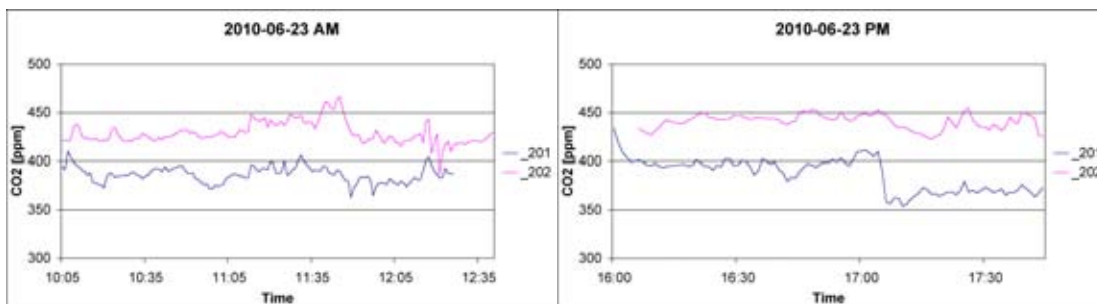
Figure 8.65: CO$_2$ 2010-06-23 a.m.

Figure 8.66: CO$_2$ 2010-06-23 p.m.
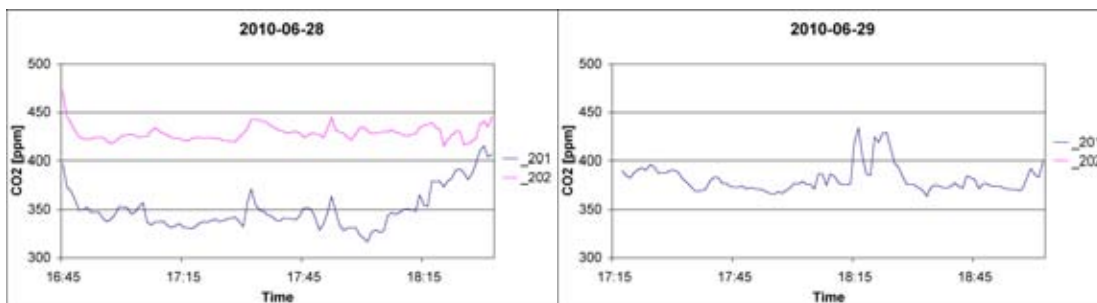
Figure 8.67: CO$_2$ 2010-06-28

Figure 8.68: CO$_2$ 2010-06-29
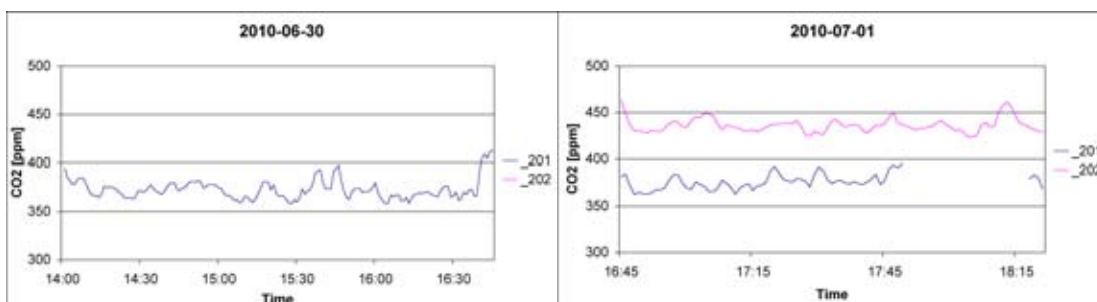
Figure 8.69: CO$_2$ 2010-06-30

Figure 8.70: CO$_2$ 2010-07-01
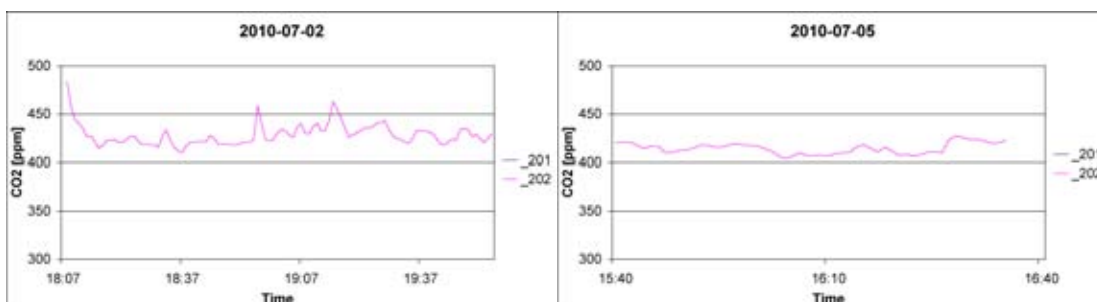
Figure 8.71: CO$_2$ 2010-07-02

Figure 8.72: CO$_2$ 2010-07-05

94
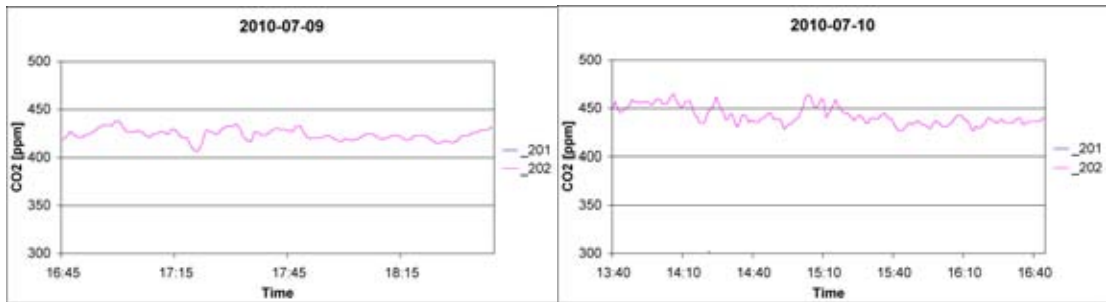
Figure 8.73: CO_2 2010-07-09

Figure 8.74: CO_2 2010-07-10
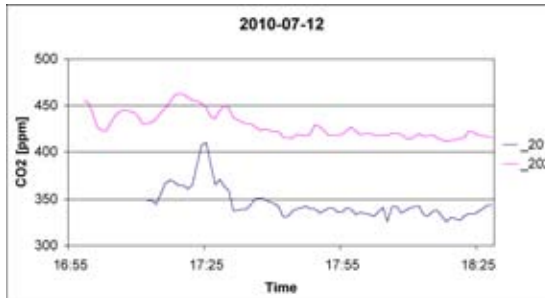
Figure 8.75: CO_2 2010-07-12

8.2.2 Long-time Measurements

8.2.2.1 Solar Radiation

Figures 8.76 to 8.79 show the results of the long-time solar radiation measurements. While TU2 and KP1 values are obviously lower than BPI values, only HEU values are higher.
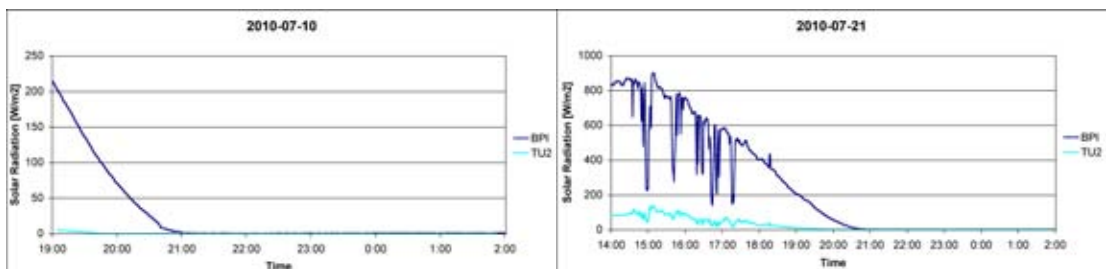
Figure 8.76: Solar radiation TU2 2010-07-10

Figure 8.77: Solar radiation TU2 2010-07-21
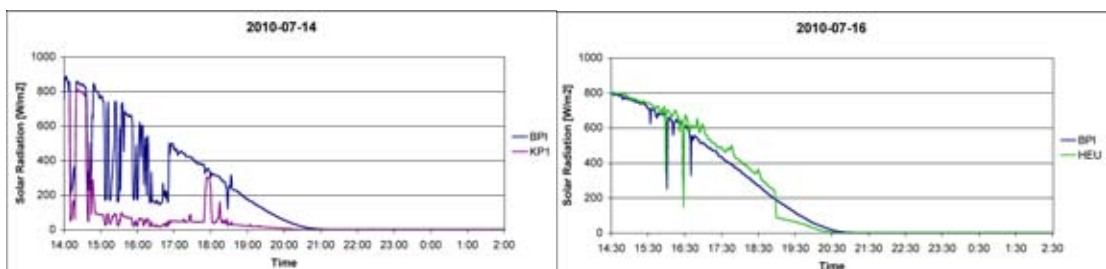
Figure 8.78: Solar radiation KP1 2010-07-14

Figure 8.79: Solar radiation HEU 2010-07-16

8.2.2.2 Wind Speed

Figures 8.80 to 8.83 show the results of the long-time wind speed measurements.
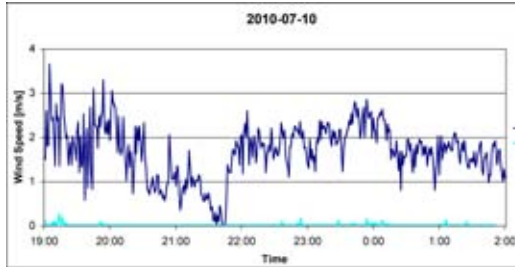
Figure 8.80: Wind speed TU2 2010-07-10   Figure 8.81: Wind speed TU2 2010-07-21
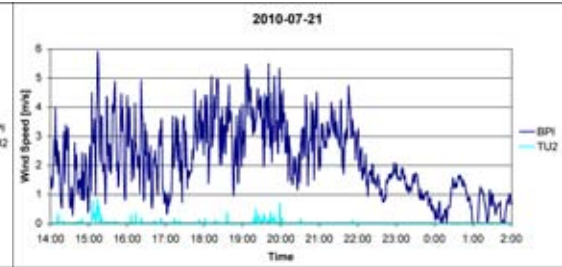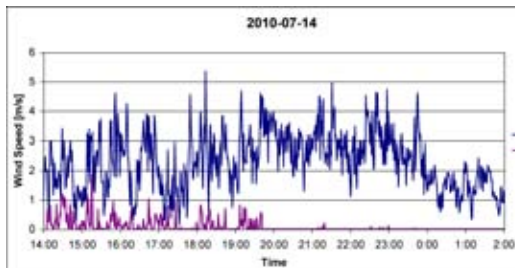
Figure 8.82: Wind speed KP1 2010-07-14   Figure 8.83: Wind speed HEU 2010-07-16
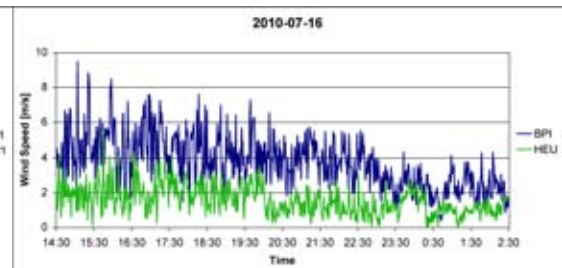
8.2.2.3 Relative Humidity

Figures 8.84 to 8.87 show the results of the long-time relative humidity measurements.
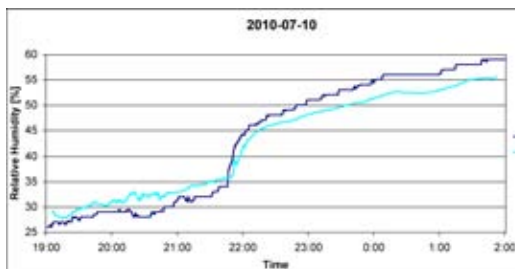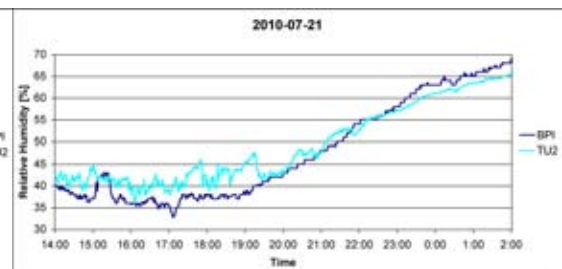

Figure 8.84: Relative humidity TU2 2010-07-10   Figure 8.85: Relative humidity TU2 2010-07-21
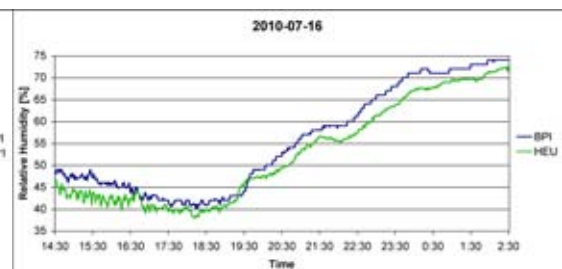

Figure 8.86: Relative humidity KP1 2010-07-14   Figure 8.87: Relative humidity HEU 2010-07-16

8.2.2.4 CO_2

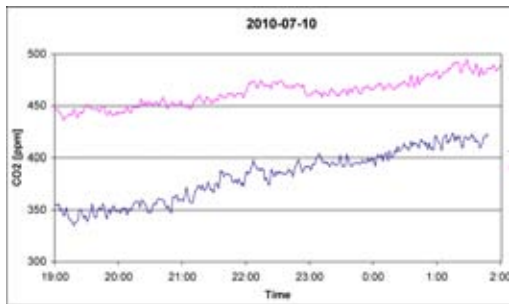Figures 8.88 to 8.91 show the results of the long-time CO_2 measurements.

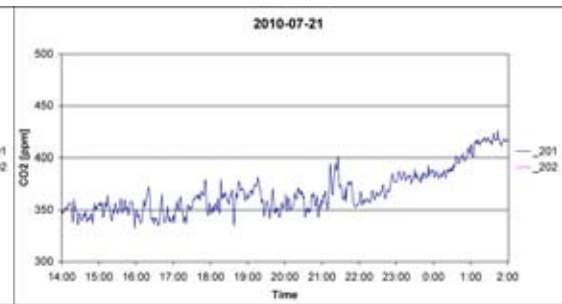Figure 8.88: CO_2 TU2 2010-07-10

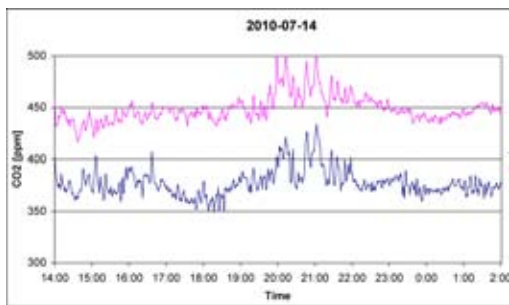Figure 8.89: CO_2 TU2 2010-07-21
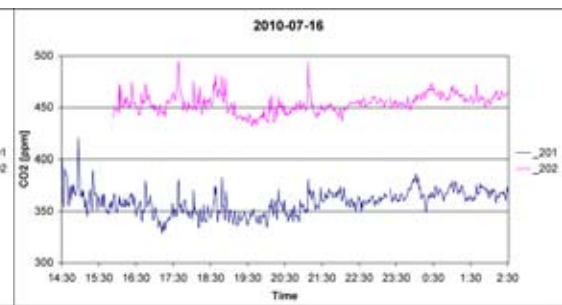

Figure 8.90: CO_2 KP1 2010-07-14

Figure 8.91: CO_2 HEU 2010-07-16

8.3 Fisheye Pictures

Figures 8.92 to 8.101 show the fisheye pictures of the locations that were analyzed for their parts of sky, vegetation and built environment.

Figure 8.92: PAN (picture by A. Maleki)

Figure 8.93: TU1(picture by A. Maleki)

Figure 8.94: TU2 (picture by A. Maleki)

Figure 8.95: KP1 (picture by A. Maleki)

Figure 8.96: KP2 (picture by A. Maleki)

Figure 8.97: SCH (picture by A. Maleki)

Figure 8.98: RIN (picture by A. Maleki)

Figure 8.99: ST1 (picture by A. Maleki)

Figure 8.100: ST2 (picture by A. Maleki)

Figure 8.101: HEU (picture by A. Maleki)